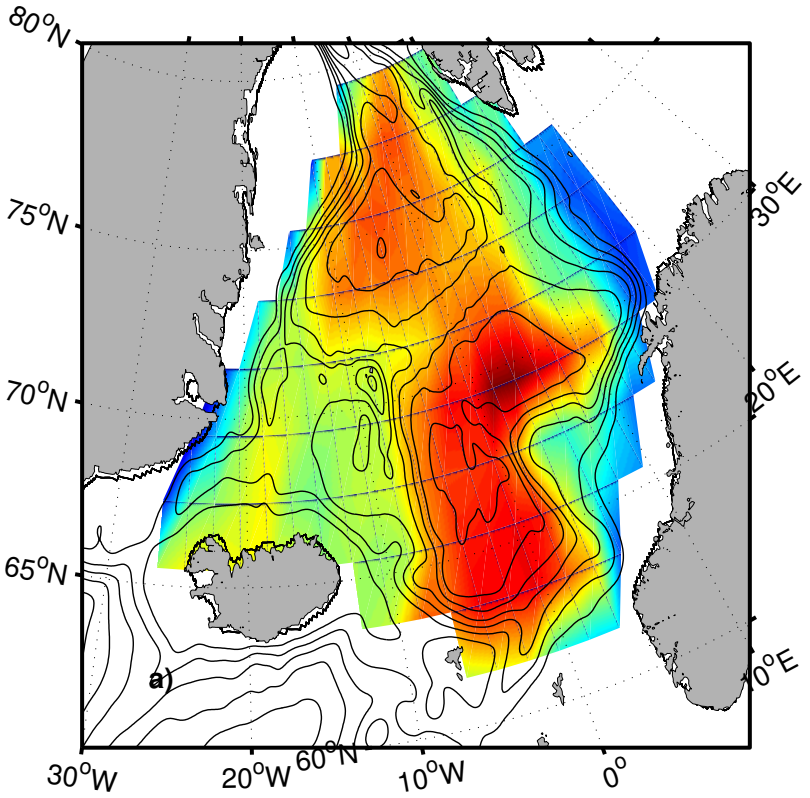

Geophysical Fluid Dynamics

J. H. LaCasce

Dept. of Geosciences
University of Oslo

LAST REVISED
November 29, 2017

Contents

Preface

The dynamics of the atmosphere and ocean are largely nonlinear. Nonlinearity is the reason these systems are chaotic and hence unpredictable. However much of what we understand about the systems comes from the study of the linear equations of motion. These are mathematically tractable (unlike, for the most part, their nonlinear counterparts), meaning we can derive solutions. These solutions include gravity waves, Rossby waves and storm formation—all of which are observed. So the linear dynamics informs our understanding of the actual systems.

These notes are intended as a one to two semester introduction to the dynamics of the atmosphere and ocean. The target audience is the advanced undergraduate or beginning graduate student. The philosophy is to obtain simplified equations and then use those to study specific atmospheric or oceanic flows. Some of the latter examples come from research done 50 years ago, but others are from much more recent work.

Thanks to the people in Oslo who over the years have suggested changes and improvements. Particular thanks to Jan Erik Weber, Pal Erik Isachsen, Lise Seland Graff, Anita Ager-Wick, Magnus Drivdal, Hanne Beatte Skattor, Sigmund Guttu, Rafael Escobar Lovdahl, Liv Denstad, Ada Gjermundsen and (others).

Chapter 1

Equations

The motion in the atmosphere and ocean is governed by a set of equations, the *Navier-Stokes* equations. These are used to produce our forecasts, both for the weather and ocean currents. While there are details about these equations which are uncertain (for example, how we represent processes smaller than the grid size of our models), they are for the most part accepted as fact. Let's consider how these equations come about.

1.1 Derivatives

A fundamental aspect is how various fields (temperature, wind, density) change in time and space. Thus we must first specify how to take derivatives.

Consider a scalar, ψ, which varies in both time and space, i.e. $\psi = \psi(x, y, z, t)$. This could be the wind speed in the east-west direction, or the ocean density. By the chain rule, the total change in the ψ is:

$$d\psi = \frac{\partial}{\partial t}\psi\, dt + \frac{\partial}{\partial x}\psi\, dx + \frac{\partial}{\partial y}\psi\, dy + \frac{\partial}{\partial z}\psi\, dz \tag{1.1}$$

so:

$$\frac{d\psi}{dt} = \frac{\partial}{\partial t}\psi + u\frac{\partial}{\partial x}\psi + v\frac{\partial}{\partial y}\psi + w\frac{\partial}{\partial z}\psi \tag{1.2}$$

or, in short form:

$$\frac{d\psi}{dt} = \frac{\partial}{\partial t}\psi + \vec{u}\cdot\nabla\psi \tag{1.3}$$

Here (u, v, w) are the components of the velocity in the (x, y, z) directions. On the left side, the derivative is a total derivative. That implies that ψ on the left side is only a function of time. This is the case when ψ is observed *following the flow*. If you measure temperature while riding in a balloon, moving with the winds, you would only record changes in time. We call this the *Lagrangian* formulation. The derivatives on the right side instead are partial derivatives. These are relevant for an observer at *a fixed location*. This person records temperature as a function of time, but her information also depends on her position. An observer at a different location will generally obtain a different result (depending on how far away she is). We call the right side the *Eulerian* formulation.

Most numerical models are based on the Eulerian formulation, albeit with some using Lagrangian or semi-Lagrangian representations of advection. But derivations are often simpler in the Lagrangian form. In particular, we will consider changes occuring to a fluid *parcel* moving with the flow. The parcel is an infinitesimal element. However, it nevertheless contains a large and fixed number of molecules. So it is small in the fluid sense, but large in the molecular sense. This permits us to think of the fluid as a continuum, rather than as a set of discrete molecules, as in a gas.

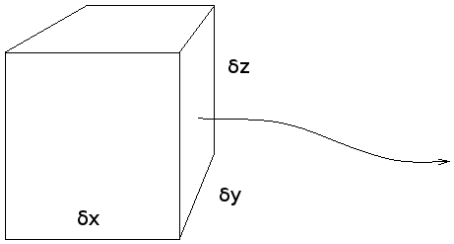

Figure 1.1: A infinitesimal element of fluid, with volume δV.

1.2 Continuity equation

Consider a fluid parcel, with a fixed number of molecules (Fig. 1.1). The parcel's mass is constant (because it has a fixed number of molecules) but its volume isn't. Mass conservation implies:

$$\frac{d}{dt}M = \frac{d}{dt}\rho\,\delta V = 0 \tag{1.4}$$

if M is the mass, ρ is the parcel's density and δV is its volume. Imagine the parcel is a cube, as in Fig. (1.1), with sides δx, δy and δz. Then we can write:

$$\frac{d}{dt}M = \delta x\delta y\delta z\,\frac{d}{dt}\rho + \rho\,\delta y\delta z\frac{d}{dt}\delta x + \rho\,\delta x\delta z\frac{d}{dt}\delta y + \rho\,\delta x\delta y\frac{d}{dt}\delta z \tag{1.5}$$

using the chain rule. Dividing through by M, we get:

$$\frac{1}{M}\frac{d}{dt}M = \frac{d}{dt}\rho + \frac{\rho}{\delta x}\frac{d}{dt}\delta x + \frac{\rho}{\delta y}\frac{d}{dt}\delta y + \frac{\rho}{\delta z}\frac{d}{dt}\delta z = 0 \tag{1.6}$$

The time derivatives can move through the δ terms so for example:

$$\frac{d}{dt}\delta x = \delta\frac{d}{dt}x = \delta u$$

Thus the relative change in mass is:

$$\frac{1}{M}\frac{d}{dt}M = \frac{d}{dt}\rho + \rho\frac{\delta u}{\delta x} + \rho\frac{\delta v}{\delta y} + \rho\frac{\delta w}{\delta z} = 0 \tag{1.7}$$

In the limit that $\delta \to 0$, this is:

$$\frac{1}{M}\frac{d}{dt}M = \frac{d}{dt}\rho + \rho\frac{\partial u}{\partial x} + \rho\frac{\partial v}{\partial y} + \rho\frac{\partial w}{\partial z} = 0 \tag{1.8}$$

So we have:

$$\frac{d\rho}{dt} + \rho(\nabla \cdot \vec{u}) = 0 \tag{1.9}$$

which is continuity equation in its Lagrangian form. This states the density of a parcel advected by the flow will change if the flow is divergent, i.e. if:

$$\nabla \cdot \vec{u} \neq 0 \tag{1.10}$$

The divergence determines whether the box shrinks or grows. If the box expands, the density must decrease to preserve the box's mass.

The continuity equation can also be written in its Eulerian form, using the definition of the Lagrangian derivative:

$$\frac{\partial \rho}{\partial t} + \vec{u} \cdot \nabla\rho + \rho(\nabla \cdot \vec{u}) = \frac{\partial \rho}{\partial t} + \nabla \cdot (\rho\vec{u}) = 0 \tag{1.11}$$

This pertains to a fixed volume, whose sides aren't changing. This states that the density of a fixed volume will change if there is a net density flux through the sides of the volume.

1.3 Momentum equations

The continuity equation pertains to mass. Now consider the fluid velocities. We can derive expressions for these using Newton's second law:

$$\vec{F} = m\vec{a} \tag{1.12}$$

The forces acting on our fluid parcel are:

- pressure gradients: $\frac{1}{\rho}\nabla p$
- gravity: $\vec{g}$
- friction: $\vec{F}$

Consider the pressure first. The force acting on the left side of the box (Fig. 1.1) is:

$$F_l = pA = p(x)\,\delta y\,\delta z$$

while the force on the right side is:

$$F_r = p(x+\delta x)\,\delta y\,\delta z$$

Thus the net force acting in the x-direction is:

$$F_l - F_r = [p(x) - p(x+\delta x)]\,\delta y\,\delta z$$

Since the parcel is small, we can expand the pressure on the right side in a Taylor series:

$$p(x+\delta x) = p(x) + \frac{\partial p}{\partial x}\delta x + ...$$

The higher order terms are small and we neglect them. Thus the net force is:

$$F_l - F_r = -\frac{\partial p}{\partial x}\,\delta x\,\delta y\,\delta z$$

So Newton's law states:

$$m\frac{du}{dt} = \rho(\delta x\,\delta y\,\delta z)\frac{du}{dt} = -\frac{\partial p}{\partial x}\,\delta x\,\delta y\,\delta z \tag{1.13}$$

Cancelling the volumes on both sides, we get:

$$\rho\frac{du}{dt} = -\frac{\partial p}{\partial x} \tag{1.14}$$

Pressure gradients in the other directions have the same effect, so we can write:

$$\frac{d\vec{u}}{dt} = -\frac{1}{\rho}\nabla p \tag{1.15}$$

Thus a pressure gradient produces an acceleration *down the gradient* (from high to low pressure). We'll examine this more closely later.

The gravitational force acts in the vertical direction:

$$m\frac{dw}{dt} = -mg \tag{1.16}$$

or just:

$$\frac{dw}{dt} = -g \tag{1.17}$$

We can combine this with the pressure gradient forced to produce a vector momentum equation:

$$\frac{d\vec{u}}{dt} = -\frac{1}{\rho}\nabla p - g\hat{k} \tag{1.18}$$

Note that this comprises three equations, for each velocity component (u, v, w).

Lastly there is the friction. At small scales, friction is due to molecular collisions, by which kinetic energy is converted to heat. At larger scales though, the friction is usually represented as due to the action of eddies which are unresolved in the flow. In much of what follows we neglect friction. Where it is important is in the vertical boundary layers, at the bottom of the atmosphere and ocean and at the surface of the ocean. We consider this further in section (4.5). We won't specify the friction yet, but just represent it as a vector, $\vec{F}$. Thus we have:

$$\frac{d}{dt}\vec{u} = -\frac{1}{\rho}\nabla p - g\hat{k} + \frac{1}{\rho}\vec{F} \tag{1.19}$$

This is the *momentum equation* in Lagrangian form. Under the influence of the forcing terms, the fluid parcel will accelerate.

This equation pertains to motion in a non-rotating (fixed) frame. There are additional acceleration terms which come about due to the earth's rotation. As opposed to the *real* forces shown in (1.19), rotation introduces *apparent* forces. A stationary parcel on the earth will rotate with the planet. From the perspective of an observer in space, the parcel is traveling in circles, completing a circuit once a day. Since circular motion represents an acceleration (the velocity is changing direction), there must be a corresponding force.

Consider such a stationary parcel, on a rotating sphere, represented by a vector, $\vec{A}$ (Fig. 1.2). During the time, δt, the vector rotates through an

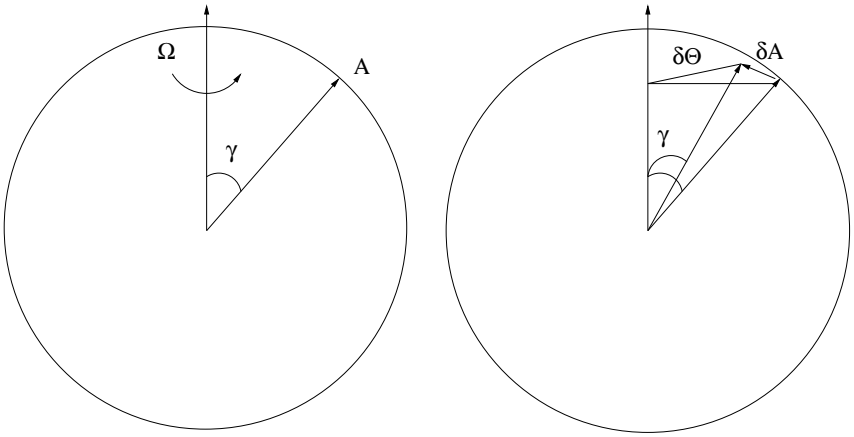

Figure 1.2: The effect of rotation on a vector, A, which is otherwise stationary. The vector rotates through an angle, $\delta\Theta$, in a time δt.

angle:

$$\delta\Theta = \Omega\delta t \tag{1.20}$$

where:

$$\Omega = \frac{2\pi}{86400}\ sec^{-1}$$

is the Earth's rotation rate (one day is 86,400 sec). The change in A is δA, the arc-length:

$$\delta\vec{A} = |\vec{A}|sin(\gamma)\delta\Theta = \Omega|\vec{A}|sin(\gamma)\delta t = (\vec{\Omega}\times\vec{A})\,\delta t \tag{1.21}$$

So we can write:

$$lim_{\delta\to 0}\ \frac{\delta\vec{A}}{\delta t} = \frac{d\vec{A}}{dt} = \vec{\Omega}\times\vec{A} \tag{1.22}$$

If $\vec{A}$ is not stationary but changing in the rotating frame, one can show that:

$$(\frac{d\vec{A}}{dt})_F = (\frac{d\vec{A}}{dt})_R + \vec{\Omega}\times\vec{A} \tag{1.23}$$

The F here refers to the fixed frame (space) and R to the rotating one (earth). If $\vec{A} = \vec{r}$, the position vector, then:

$$(\frac{d\vec{r}}{dt})_F \equiv \vec{u}_F = \vec{u}_R + \vec{\Omega} \times \vec{r} \tag{1.24}$$

So the velocity in the fixed frame is just that in the rotating frame plus the velocity associated with the rotation.

Now consider that $\vec{A}$ is velocity in the fixed frame, $\vec{u}_F$. Then:

$$(\frac{d\vec{u}_F}{dt})_F = (\frac{d\vec{u}_F}{dt})_R + \vec{\Omega} \times \vec{u}_F \tag{1.25}$$

Substituting in the previous expression for u_F, we get:

$$(\frac{d\vec{u}_F}{dt})_F = (\frac{d}{dt}[\vec{u}_R + \vec{\Omega} \times \vec{r}])_R + \vec{\Omega} \times [\vec{u}_R + \vec{\Omega} \times \vec{r}] \tag{1.26}$$

Collecting terms:

$$(\frac{d\vec{u}_F}{dt})_F = (\frac{d\vec{u}_R}{dt})_R + 2\vec{\Omega} \times \vec{u}_R + \vec{\Omega} \times \vec{\Omega} \times \vec{r} \tag{1.27}$$

We've picked up two additional terms: the *Coriolis* and *centrifugal* accelerations. These are the apparent forces which stem from the Earth's rotation. Both vanish if $\vec{\Omega} = 0$. Note that the centrifugal acceleration depends only on the position of the fluid parcel; the Coriolis term on the other hand depends on its *velocity*.

Plugging this expression into the momentum equation, we obtain:

$$(\frac{d\vec{u}_F}{dt})_F = (\frac{d\vec{u}_R}{dt})_R + 2\vec{\Omega} \times \vec{u}_R + \vec{\Omega} \times \vec{\Omega} \times \vec{r} = -\frac{1}{\rho}\nabla p + \vec{g} + \frac{1}{\rho}\vec{F} \tag{1.28}$$

This is the momentum equation for motion in a rotating frame.[1]

[1] In a frame with a constant rotation rate, to be specific. Allowing for variations in the rotation rate introduces an additional term.

The centrifugal acceleration acts perpendicular to the axis of rotation (Fig. 1.3). As such it projects onto both the radial and the N-S directions. This implies a parcel in the Northern Hemisphere would accelerate upward and southward. However these accelerations are balanced by gravity, which acts to pull the parcel toward the center *and* northward. The latter (which is not intuitive!) occurs because rotation changes the shape of the earth itself, making it ellipsoidal rather than spherical. The change in shape results in an exact cancellation of the N-S component of the centrifugal force.

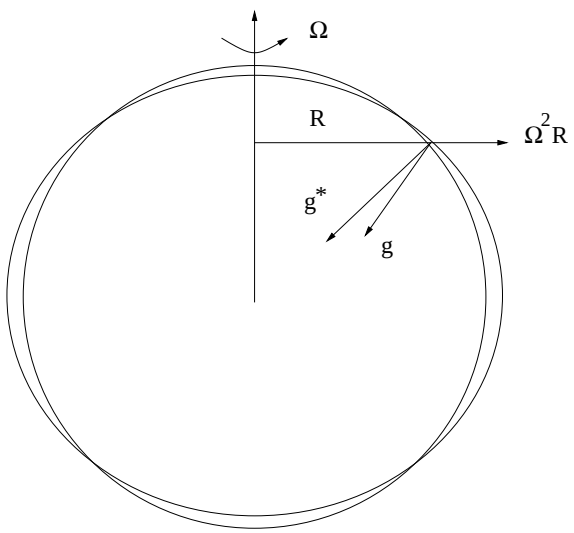

Figure 1.3: The centrifugal force and the deformed earth. Here is g is the gravitational vector for a spherical earth, and g^* is that for the actual earth. The latter is an *oblate spheroid*.

The radial acceleration too is overcome by gravity. If this weren't true, the atmosphere would fly off the earth. So the centrifugal force effectively *modifies gravity*, reducing it over what it would be if the earth were stationary. So the centrifugal acceleration causes no change in the velocity of a fluid parcel. As such, we can absorb it into gravity:

$$g' = g - \vec{\Omega} \times \vec{\Omega} \times \vec{r} \tag{1.29}$$

This correction is rather small (see the exercises), so we can ignore it. We will drop the prime on g hereafter.

Thus the momentum equation can be written:

$$(\frac{d\vec{u}_R}{dt})_R + 2\vec{\Omega} \times \vec{u}_R = -\frac{1}{\rho}\nabla p + \vec{g} + \frac{1}{\rho}\vec{F} \tag{1.30}$$

There is only one rotational term then, the Coriolis acceleration.

Hereafter we will focus on the dynamics in a region of the ocean or atmosphere. The proper coordinates for geophysical motion are spherical coordinates, but Cartesian coordinates simplify things greatly. So we imagine a fluid region in a plane, with the vertical coordinate parallel to the earth's radial coordinate and the (x, y) coordinates oriented east-west and north-south, respectively (Fig. 1.4). For now, we assume the plane is centered at a middle latitude, θ, for example 45 N.

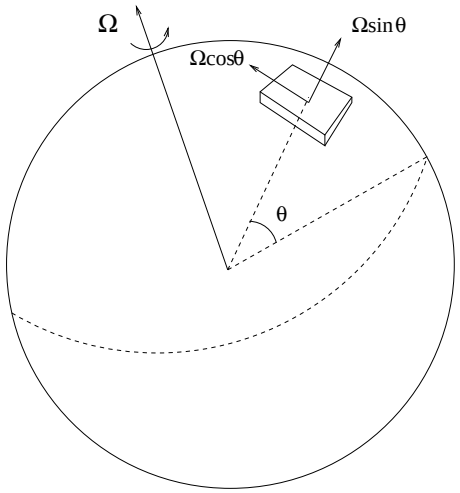

Figure 1.4: We examine the dynamics of a rectangular region of ocean or atmosphere centered at latitude θ.

There are three spatial directions and each has a corresponding momentum equation. We define the local coordinates (x, y, z) such that:

$$dx = R_e cos(\theta)\, d\phi, \quad dy = R_e\, d\theta, \quad dz = dr$$

where ϕ is the longitude, R_e is the earth's radius and r is the radial coordinate; x is the east-west coordinate, y the north-south coordinate and z the vertical coordinate. We define the corresponding velocities:

$$u \equiv \frac{dx}{dt}, \quad v \equiv \frac{dy}{dt}, \quad w \equiv \frac{dz}{dt}$$

The momentum equations determine the accelerations in (x,y,z).

The rotation vector $\vec{\Omega}$ projects onto both the y and z directions (Fig. 1.4). Thus the Coriolis acceleration is:

$$2\vec{\Omega} \times \vec{u} = (0, 2\Omega cos\theta, 2\Omega sin\theta) \times (u, v, w) =$$

$$2\Omega(w\, cos\theta - v\, sin\theta,\ u\, sin\theta, -u\, cos\theta) \tag{1.31}$$

So the Coriolis acceleration acts in all three directions.

An important point is that because the Coriolis forces acts perpendicular to the motion, it *does no work*—it doesn't change the speed of a fluid parcel, just its direction of motion. Despite this, the Coriolis force is one of the dominant terms at *synoptic* (weather) scales.

Collecting terms, we have:

$$\frac{du}{dt} + 2\Omega w\, cos\theta - 2\Omega v\, sin\theta = -\frac{1}{\rho}\frac{\partial p}{\partial x} + \frac{1}{\rho}F_x \quad (1.32)$$

$$\frac{dv}{dt} + 2\Omega u\, sin\theta = -\frac{1}{\rho}\frac{\partial p}{\partial y} + \frac{1}{\rho}F_y \quad (1.33)$$

$$\frac{dw}{dt} - 2\Omega u\, cos\theta = -\frac{1}{\rho}\frac{\partial p}{\partial z} - g + \frac{1}{\rho}F_z \quad (1.34)$$

These are the momentum equations in their Lagrangian form.[2]

1.4 Equations of state

With the continuity and momentum equations, we have four equations. But there are 6 unknowns— the pressure, the three components of the velocity, the density and the temperature. In fact there are additional variables as well: the humidity in the atmosphere and the salinity in the ocean. But even neglecting those, we require two additional equations to close the system.

One of these is an "equation of state" which relates the density to the temperature and, for the ocean, the salinity. In the atmosphere, the density and temperature are linked via the *Ideal Gas Law*:

$$p = \rho RT \quad (1.35)$$

where $R = 287\, Jkg^{-1}K^{-1}$ is the gas constant for dry air. The density and temperature of the gas thus determine its pressure. The Ideal Gas law is

[2] If we had used spherical coordinates instead, we would have several additional *curvature* terms. We'll see an example in sec. (2.2), when we examine the momentum equation in cylindrical coordinates.

applicable for a dry gas (one with zero humidity), but a similar equation applies in the presence of moisture if one replaces the temperature with the "virtual temperature".[3] For our purposes, it will suffice to consider a dry gas.

In the ocean, both salinity and temperature affect the density. The dependence is expressed:

$$\rho = \rho(T, S) = \rho_c(1 - \alpha_T(T - T_{ref}) + \alpha_S(S - S_{ref})) + h.o.t. \quad (1.36)$$

where ρ_c is a constant, T and S are the temperature and salinity (and T_{ref} and S_{ref} are reference values) and where $h.o.t.$ means "higher order terms". Increasing the temperature or decreasing the salinity reduces the water density. An important point is that the temperature and salinity corrections are much less than one, so that the density is dominated by the first term, ρ_c, a constant. We will exploit this later on.

1.5 Thermodynamic equations

The other equation we'll use is the *thermodynamic energy* equation, which expresses how the fluid responds to heating. The equation derives from the First Law of Thermodynamics, which states that the heat added to a volume minus the work done by the volume equals the change in its internal energy.

Consider the volume shown in Fig. (1.5). Gas is enclosed in a chamber to the left of a sliding piston. Heat is applied to the gas and it can then

[3] See, e.g. Holton, *An Introduction to Dynamic Meteorology*.

expand, pushing the piston.

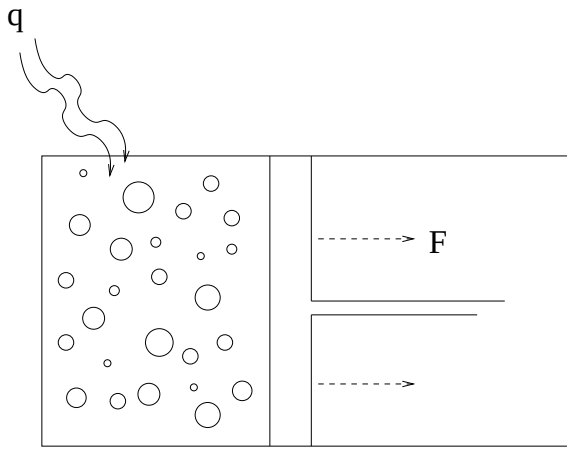

The heat added equals the change in the internal energy and of the gas plus the work done on the piston.

$$dq = de + dw \tag{1.37}$$

The work is the product of the force and the distance moved by the piston. For a small displacement, dx, this is:

$$dw = F dx = p\, A\, dx = p\, dV \tag{1.38}$$

If the volume increases, i.e. if $dV > 0$, the gas is doing the work; if the volume decreases, the gas is compressed and is being worked upon.

Let's assume the volume has a unit mass, so that:

$$\rho\, V = 1 \tag{1.39}$$

Then:

$$dV = d(\frac{1}{\rho}) \tag{1.40}$$

So we have:

$$dq = de + p\, d(\frac{1}{\rho}) \tag{1.41}$$

Now, if we add heat to the volume the gas' temperature will rise. If the volume is kept constant, the temperature increase is proportional to the heat added:

$$dq_v = c_v\, dT \tag{1.42}$$

where c_v is the *specific heat* at constant volume. One can determine c_v in the lab, by heating a gas in a fixed volume and measuring the temperature change. With a constant volume, the change in the gas' energy equals the heat added to it, so:

$$dq_v = de_v = c_v\, dT \tag{1.43}$$

What if the volume isn't constant? In fact, the internal energy still only depends on temperature (for an ideal gas). This is *Joule's Second Law*. So even if V changes, we have:

$$de = c_v\, dT \tag{1.44}$$

Thus we can write:

$$dq = c_v dT + p\, d\,(\frac{1}{\rho}) \tag{1.45}$$

If we divide through by dt, we obtain the theromdynamic energy equation:

$$\frac{dq}{dt} = c_v \frac{dT}{dt} + p\, \frac{d}{dt}(\frac{1}{\rho}) \tag{1.46}$$

Thus the rate of change of the temperature and density depend on the rate at which the gas is heated.

We can derive another version of the equation. Imagine instead we keep the *pressure* of the gas constant. That is, we allow the piston to move but in such a way that the force on the piston remains the same. If we add heat, the temperature will increase, but it does so at a different rate than if the volume is held constant. So we can write:

$$dq_p = c_p \, dT \tag{1.47}$$

where c_p is the specific heat at constant pressure. We expect that c_p should be greater than c_v because it requires more heat to raise the gas' temperature if the gas is also doing work on the piston.

We can rewrite the work term using the chain rule:

$$p \, d(\frac{1}{\rho}) = d(\frac{p}{\rho}) - \frac{1}{\rho} \, dp \tag{1.48}$$

So:

$$dq = c_v \, dT + d(\frac{p}{\rho}) - \frac{1}{\rho} \, dp \tag{1.49}$$

We can rewrite the second term on the RHS using the the ideal gas law:

$$d(\frac{p}{\rho}) = R \, dT \tag{1.50}$$

Substituting this in, we have:

$$dq = (c_v + R) \, dT - \frac{1}{\rho} dp \tag{1.51}$$

Now if the pressure is held constant, we have:

$$dq_p = (c_v + R)\, dT \tag{1.52}$$

So:

$$c_p = c_v + R$$

The specific heat at constant pressure is indeed larger than that at constant volume. For dry air, measurements yield:

$$c_v = 717\ Jkg^{-1}K^{-1}, \qquad c_p = 1004\ Jkg^{-1}K^{-1} \tag{1.53}$$

So:

$$R = 287\ Jkg^{-1}K^{-1} \tag{1.54}$$

as noted in sec. (1.4).

Therefore we can also write the thermodynamic equation as:

$$dq = c_p\, dT - \frac{1}{\rho} dp \tag{1.55}$$

Dividing by dt, we obtain the second version of the thermodynamic energy equation. So the two versions of the equation are:

$$c_v \frac{dT}{dt} + p \frac{d}{dt}(\frac{1}{\rho}) = \frac{dq}{dt} \tag{1.56}$$

$$c_p \frac{dT}{dt} - (\frac{1}{\rho}) \frac{dp}{dt} = \frac{dq}{dt} \tag{1.57}$$

Either one can be used, depending on the situation.

However, it will be convenient to use a *third* version of the equation. This pertains to the *potential temperature*. As one moves upward in atmosphere, both the temperature and pressure change. So if you are ascending in a balloon and taking measurements, you have to keep track of both the pressure and temperature. Put another way, it is not enough to label an air parcel by its temperature. A parcel with a temperature of 1C could be at the ground (at high latitudes) or at a great height (at low latitudes).

The potential temperature conveniently accounts for the change with temperature due to pressure. One can label a parcel by its potential temperature and that will suffice. Imagine we have a parcel of air at some height. We then move that parcel back to the surface– *without heating it*–and measure its temperature. This is its potential temperature.

From above, we have that:

$$c_p\, dT - \frac{1}{\rho}\, dp = dq \tag{1.58}$$

If there is zero heating, $dq = 0$, we have:

$$c_p\, dT - \frac{1}{\rho}\, dp = c_p\, dT - \frac{RT}{p}\, dp = 0 \tag{1.59}$$

again using the ideal gas law. We can rewrite this thus:

$$c_p\, dlnT - R\, dlnp = 0 \tag{1.60}$$

So:

$$c_p\, lnT - R\, lnp = const. \tag{1.61}$$

This implies:

$$c_p \, lnT - R \, lnp = c_p \, ln\theta - R \, lnp_s \tag{1.62}$$

where θ and p_s are the temperature and pressure at a chosen reference level, which we take to be the surface. Solving for θ we get:

$$\theta = T \, (\frac{p_s}{p})^{R/c_p} \tag{1.63}$$

This defines the potential temperature. It is linearly proportional to the actual temperature, but also depends on the pressure. The potential temperature increases with altitude, because the pressure decreases going up. In the ocean, the potential temperature increases from the bottom, because the pressure likewise decreases moving towards the sea surface.

An important point is that if there is no heating, an air parcel *conserves* its potential temperature. So without heating, the potential temperature is like a label for the parcel. In a similar vein, surfaces of constant potential temperature (also known as an *isentropic surface* or an *adiabat*) are of special interest. A parcel on an adiabat must remain there if there is no heating.

The advantage is that we can write the thermodynamic energy equation in terms of only one variable. Including heating, this is:

$$c_p \frac{d(ln\theta)}{dt} = \frac{1}{T} \frac{dq}{dt} \tag{1.64}$$

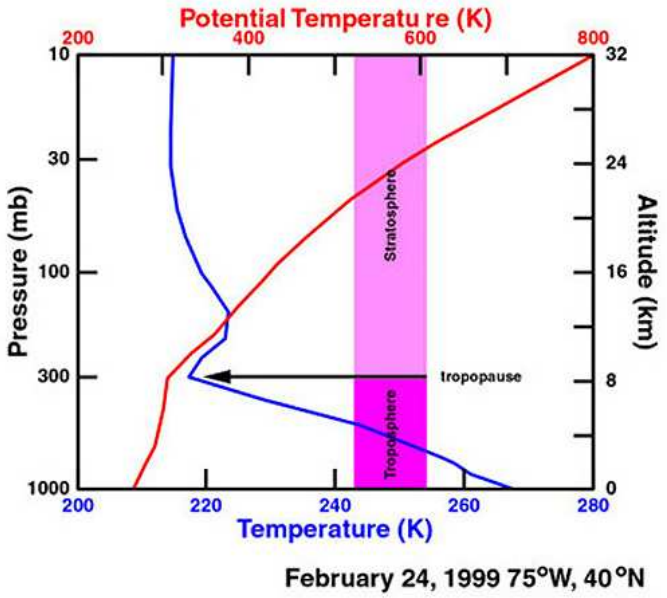

Figure 1.5: The potential temperature and temperature in the lower atmosphere. Courtesy of NASA/GSFC.

This is simpler than equations (1.56-1.57) because it doesn't involve the pressure.

The potential temperature and temperature in the atmosphere are plotted in Fig. (1.5). The temperature decreases almost linearly with height near the earth's surface, in the *troposphere*. At about 8 km, the temperature begins to rise again, in the *stratosphere*. In contrast, the potential temperature rises monotonically with height. This makes it a better variable for studying atmospheric motion.

The corresponding thermodynamic relation in the ocean is:

$$\frac{d}{dt}\sigma_\theta = J \tag{1.65}$$

where σ_θ is the *potential density* and J is the applied forcing. In analogy

to the potential temperature, the potential density is the density of a fluid parcel if raised adiabatically to a reference pressure (usually 100 kPa). As will be seen, the pressure increases with depth in the ocean, and this in turn increases the density on a parcel. The potential density corrects for this. In addition the forcing term, J, includes changes to either the temperature or the salinity. So J can also represent fresh water input, for example from melting ice.

A typical profile of potential density is shown in Fig. (1.6). The temperature (left panel) is warmest near the surface (although in this example, not very warm!). It decreases with depth until about 5000 m, but then increases again below that. The latter is due to the increase in pressure. The potential temperature on the other hand decreases monotonically with depth. The potential density, σ_θ (right panel), increases monotonically with depth.

For our purposes, it will suffice to assume that the density itself is conserved in the absence of thermodynamic forcing, i.e.:

$$\frac{d}{dt}\rho = 0 \tag{1.66}$$

1.6 *Exercises*

1.1. There are two observers, one at a weather station and another passing overhead in an airplane. The observer on the ground notices the temperature is falling at rate of 1^oC/day, while the air passenger observes the temperature *rising* at the same rate. If the plane is moving east at 10 m/sec, at constant height, what can you conclude about the temperature field?

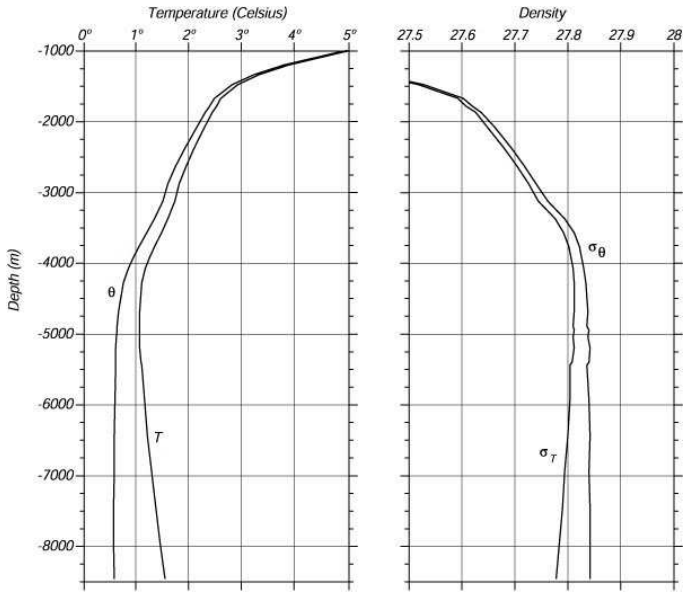

Figure 1.6: The temperature and potential temperature (left panel) and the potential density, σ_θ (right panel), plotted vs. depth. The additional density, σ_T, is an alternate form of the potential density. The data come from the Kermadec trench in the Pacific and are described by Warren (1973). Courtesy of Ocean World at Texas A&M University.

1.2. A car is driving eastward at 50 km/hr, at 60 N. What is the car's speed when viewed from space?

1.3. How much does rotation alter gravity? Calculate the centrifugal acceleration at the equator. How large is this compared to $g = 9.8$ m/sec^2?

1.4. Consider a train moving east at 50 km/hr in Oslo, Norway. What is the Coriolis acceleration acting on the train? Which direction is it pointing? How big is the acceleration compared to gravity? Now imagine the train is driving the same speed and direction, but in Wellington, New Zealand. What is the Coriolis acceleration?

1.5. A parcel of air has a temperature of 30C at the surface and rises adiabatically to the 200 hPa level. What is the density of the parcel there?

Assume the pressure at the surface is 1000 hPa.

1.6. Show that if the troposphere has a constant potential temperature, θ_0, the pressure decreases with height as:

$$p(z) = p_s(1 - \frac{gz}{c_p\theta_0})^{c_p/R}$$

Hint: use the hydrostatic relation together with the Ideal Gas Law, under the assumption that $\theta = \theta_0$. An atmosphere with constant potential temperature has an "adiabatic lapse rate".

Chapter 2

Basic balances

The equations of motion presented above can be used to model both winds and ocean currents. When we run numerical models for weather prediction, we are solving equations like these. But these are nonlinear partial differential equations, with no known analytical solutions, and as such, it can be difficult to uncover the wide range of flow phenomena encompassed by the equations. However, not all the terms in the equations are equally important at different scales. By neglecting the smaller terms, we can often greatly *simplify* the equations, in the best cases allowing us to obtain analytical solutions.

2.1 Hydrostatic balance

We can assess the sizes of the different terms by *scaling* the equations. We do this by estimating the size of the terms using typical values. We can illustrate this with the vertical momentum equation:

$$\frac{\partial}{\partial t}w + u\frac{\partial}{\partial x}w + v\frac{\partial}{\partial y}w + w\frac{\partial}{\partial z}w - 2\Omega u cos\theta = -\frac{1}{\rho}\frac{\partial}{\partial z}p - g \qquad (2.1)$$

$$\frac{W}{T} \quad \frac{UW}{L} \quad \frac{UW}{L} \quad \frac{W^2}{D} \quad 2\Omega U \quad \frac{\triangle_V P}{\rho D} \quad g$$

$$\frac{W}{gT} \quad \frac{UW}{gL} \quad \frac{UW}{gL} \quad \frac{W^2}{gD} \quad \frac{2\Omega U}{g} \quad \frac{\triangle_V P}{g\rho D} \quad 1$$

$$10^{-8} \quad 10^{-8} \quad 10^{-8} \quad 10^{-9} \quad 10^{-4} \quad 1 \quad 1$$

In the second line, we've estimated each term by a ratio of approximate values, for example $\frac{\partial}{\partial t}w$ by W/T, where w is a typical vertical velocity and T is a time scale.

For the scales, we'll use values typical of a weather system:

$$U \approx 10\, m/sec, \quad L \approx 10^6\, m, \quad D \approx 10^4\, m, \quad T = 1\, day \approx 10^5\, sec$$

$$2\Omega = \frac{2\pi}{86400\, sec} \approx 10^{-4}\, sec^{-1}, \quad \triangle_H P/\rho \approx 10^5\, m^2/sec^2$$

$$W \approx 1\, cm/sec \quad g \approx 10\, m^2/sec \qquad (2.2)$$

Notice that we use a single scale, L, for the two horizontal dimensions. This is because storm systems are quasi-circular, not drastically elliptical. However we use a different scale, D, for the depth of the troposphere, which is much less than L. Likewise we use the same scale, U, for the horizontal velocities, but a different one (W) for the vertical velocity. Also,

we assume we are at mid-latitudes, so that $cos(\theta)$ is of order one—this term would be smaller if we were near the equator (where $cos(\theta)$ vanishes).

In the third line of (2.1), we've divided through by g. This will turn out to be one of the dominant terms in the equation. Thus gravity has a scale of 1 in line 3. Doing this makes each term in the third line *dimensionless*. How each term compares to one will determine how important it is compared to gravity.

Putting the estimated values in these dimensionless ratios yields the values in the fourth line. We see that the first three terms are one hunded million times smaller than gravity! This implies these terms can be safely neglected in the equation. The fourth term is fully one billion times smaller and so is also unimportant. The Coriolis term is the largest of those on the left side of the equation, but it is nevertheless 4 orders of magnitude smaller than gravity. Thus the equation is dominated by the two terms on the right hand side:

$$\frac{\partial p}{\partial z} \approx -\rho g \tag{2.3}$$

This is the *hydrostatic balance*. This balance is remarkably accurate at the scales of weather systems. Furthermore, scaling using oceanic values produces the same result. So hydrostatic balance is an excellent approximation, in either system.

However, hydrostatic balance also applies if there is *no motion at all*. If we set $u = v = w = 0$ in the vertical momentum equation, we obtain the same balance. In fact, this is where the name comes from—"hydro"

meaning water and "static" meaning not moving. Neglecting friction, the momentum equations (1.32-1.34) reduce to:

$$\frac{\partial p}{\partial x} = \frac{\partial p}{\partial y} = 0$$

$$0 = -\frac{1}{\rho}\frac{\partial p}{\partial z} - g \tag{2.4}$$

Thus there are no pressure gradients in the horizontal direction, but in the vertical direction the pressure gradient is non-zero and is balanced by gravity.

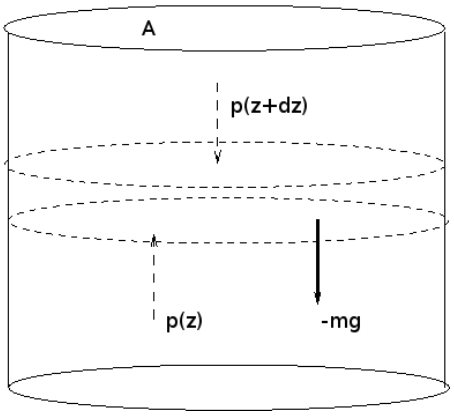

Figure 2.1: The hydrostatic balance.

Consider a layer of fluid at rest in a container (Fig. 2.1). The fluid is in a cylinder with area of A. The region indicated in the middle of the cylinder, with a thickness dz, has a mass:

$$m = \rho V = \rho A\, dz$$

and a weight, mg. The fluid underneath exerts a pressure upwards on the element, $p(z)$, while the fluid over exerts a pressure downwards, $p(z+dz)$.

The corresponding forces are the pressures times the area, A. Since the fluid is at rest, the forces must sum to zero:

$$p(z)A - p(z+dz)A - mg = 0$$

or

$$p(z+dz) - p(z) = -\frac{mg}{A} = -\rho g\, dz$$

Letting the height, dz, go to zero, we obtain (2.3). The hydrostatic balance thus expresses that the atmosphere doesn't collapse to a thin layer at the surface.

However, in reality there are horizontal pressure gradients and the velocities are non-zero. These are due to small deviations from hydrostatic state. But are the deviations themselves hydrostatic? To see, we separate the pressure and density into *static* and *dynamic* components:

$$p(x,y,z,t) = p_0(z) + p'(x,y,z,t)$$

$$\rho(x,y,z,t) = \rho_0(z) + \rho'(x,y,z,t) \tag{2.5}$$

The static components are only functions of z, so that they have no horizontal gradient. As such, they cannot cause acceleration in the horizontal velocities.

At synoptic scales, the dynamic components are generally much smaller than the static components:

$$|p'| \ll |p_0|, \quad |\rho'| \ll |\rho_0| \tag{2.6}$$

Thus we can write:

$$
\begin{aligned}
-\frac{1}{\rho}\frac{\partial}{\partial z}p - g &= -\frac{1}{\rho_0+\rho'}\frac{\partial}{\partial z}(p_0+p') - g \\
&\approx -\frac{1}{\rho_0}\left(1-\frac{\rho'}{\rho_0}\right)\left(\frac{\partial}{\partial z}p_0 + \frac{\partial}{\partial z}p'\right) - g \\
&= -\frac{1}{\rho_0}\left(1-\frac{\rho'}{\rho_0}\right)\left(-\rho_0 g + \frac{\partial}{\partial z}p'\right) - g \\
&= g - \frac{1}{\rho_0}\frac{\partial}{\partial z}p' - \frac{\rho'}{\rho_0}g + \frac{\rho'}{\rho_0^2}\frac{\partial}{\partial z}p' - g \\
&\approx -\frac{1}{\rho_0}\frac{\partial}{\partial z}p' - \frac{\rho'}{\rho_0}g
\end{aligned}
\tag{2.7}
$$

The static terms by definition obey the hydrostatic balance, so we substitute $-\rho_0 g$ for $-\frac{\partial}{\partial z}p_0$ in the third line. Also we neglect the term proportional to the *product* of the dynamical variables, $p'\rho'$, in the last line because this is much smaller than the other terms. These final two terms should replace the pressure gradient and gravity terms on the RHS of (2.1).

How do we scale these dynamical pressure terms? Measurements suggest the vertical variation of p' is such that:

$$\frac{1}{\rho_0}\frac{\partial}{\partial z}p' \approx 10^{-1}\ m/sec^2$$

The perturbation density, ρ', is roughly $1/100$ as large as the static density, so:

$$\frac{\rho'}{\rho_0}g \approx 10^{-1}\ m/sec^2$$

To scale these we again divide by g, so that both terms are of order 10^{-2}. Thus while they are smaller than the static terms, they are still *two orders of magnitude larger* than the next largest term in (2.1). Thus the approximate vertical momentum equation is still the hydrostatic balance, except now with the perturbation pressure and density:

$$\frac{\partial}{\partial z}p' = -\rho' g \tag{2.8}$$

The hydrostatic approximation is so accurate that it is used in most numerical models instead of the full vertical momentum equation. Models which use the latter are rarer and are called "non-hydrostatic" models. The only catch in adopting the hydrostatic balance is that we no longer have a prognostic equation for w. In hydrostatic models, w must be deduced in other ways.

In some texts, the following substitution is made:

$$-\frac{\rho'}{\rho_0}g \equiv b$$

where b is the *buoyancy*. However, we'll retain the density, and also drop the primes. But keep in mind that the pressure that we are focused on is the dynamic portion, linked to the motion.

2.2 Horizontal momentum balances

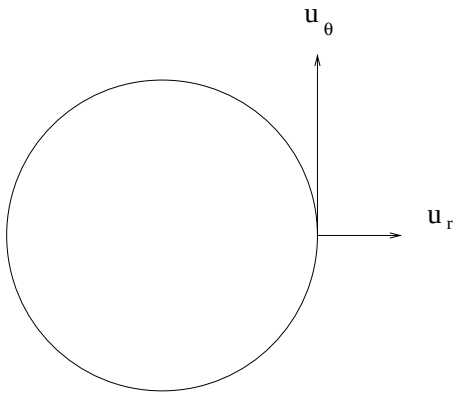

Figure 2.2: Circular flow.

Likewise in the horizontal momentum equations, not all the terms are

equally important. To illustrate this, we'll employ a perfectly circular flow, as shown in Fig. (2.2). Consider the momentum equation in cylindrical coordinates for the velocity in the radial direction:[1]

$$\frac{d}{dt}u_r - \frac{u_\theta^2}{r} + 2\Omega cos(\theta)w - 2\Omega sin(\theta)u_\theta = -\frac{1}{\rho}\frac{\partial}{\partial r}p \tag{2.9}$$

The term u_θ^2/r is called the *cyclostrophic* term. It is an additional term that arises in cylindrical coordinates (as also happens in spherical coordinates).

As the flow is purely circular, the radial velocity, u_r, is zero. So we have:

$$\frac{u_\theta^2}{r} + 2\Omega cos(\theta)w - 2\Omega sin(\theta)u_\theta = \frac{1}{\rho}\frac{\partial}{\partial r}p \tag{2.10}$$

$$\frac{U^2}{R} \quad 2\Omega W \quad 2\Omega U \quad \frac{\triangle p}{\rho R}$$

$$\frac{U}{2\Omega R} \quad \frac{W}{U} \quad 1 \quad \frac{\triangle p}{2\rho\Omega U R}$$

In the second line, we estimate each of the terms by scaling, as before. We assume again that we are at mid-latitudes, so that $cos(\theta)$ and $sin(\theta)$ are order one quantities. In the third line, we have divided through by the scale of the third term, the term with the vertical component of the Coriolis parameter.

The first point is that the second term is nearly always small in the atmosphere and ocean, where vertical velocities are much less than horizontal ones. Using the weather system values of $W \propto 1$ cm/sec and $U \propto 10$ m/sec, the ratio W/U is 10^{-3}. In the ocean, the horizontal velocities are typically of order 10 cm/sec, while the vertical velocities are measured

[1] See for example Batchelor, *Fluid Mechanics*.

in meters per day—roughly four orders of magnitude smaller. So we can neglect this term.

Notice that the terms involving the north-south component of the Coriolis vector, $2\Omega cos(\theta)$, have dropped out of all three momentum equations. It is only the vertical component which matters as synoptic scales. So we'll define:

$$f \equiv 2\Omega sin(\theta)$$

We'll use this hereafter.

That leaves the first and third terms on the LHS. Their relative sizes are dictated by the dimensionless parameter:

$$\epsilon \equiv \frac{U}{2\Omega R} = \frac{U}{fR}$$

This is an important non-dimensional quantity in geophysical fluid dynamics, and is known as the *Rossby number* (named after the Swedish meteorologist, C. G. Rossby). This gauges the relative importance of lateral advection and the Coriolis force. We often categorize flows in term of this parameter.

2.2.1 Geostrophic flow

If the Rossby number is small ($\epsilon \ll 1$), the cyclostrophic term is much smaller than the Coriolis term. Using synoptic scale values for the horizontal wind speed, the Coriolis parameter and the radius (sec. 2.1), the Rossby number is:

$$\epsilon = \frac{10}{10^{-4}(10^6)} = 0.1$$

In the ocean, the velocity scale is of order 10 cm/sec, while the length scale of ocean "storms", like Gulf Stream rings, is about 100 km. So the Rossby number is:

$$\epsilon = \frac{0.1}{10^{-4}(10^5)} = 0.01$$

Thus the Rossby number is small in both systems, at these scales.

If $\epsilon \ll 1$, the Coriolis term must be balanced by the pressure term on the RHS of (2.10). That implies that:

$$\frac{\triangle p}{\rho f U R} \approx 1$$

(If this weren't the case, there would be no flow). Thus we have:

$$f u_\theta = \frac{1}{\rho}\frac{\partial}{\partial r} p \tag{2.11}$$

This is known as *geostrophic balance*. This occurs at synoptic scales in both the atmosphere and ocean. Written in Cartesian coordinates, the balance is:

$$-f v = -\frac{1}{\rho}\frac{\partial}{\partial x} p \tag{2.12}$$

$$f u = -\frac{1}{\rho}\frac{\partial}{\partial y} p \tag{2.13}$$

This implies that if we know the pressure field, we can deduce the velocities.

Consider the flow in Fig. (2.3). The pressure is high to the south and low to the north. In the absence of rotation, this pressure difference would force the air to move north. But under the geostrophic balance, the air flows *parallel* to the pressure contours. Because $\frac{\partial}{\partial y} p < 0$, we have that $u > 0$

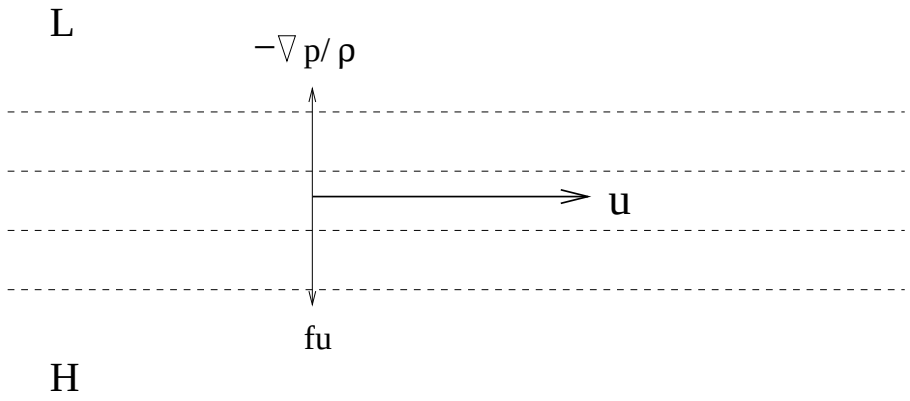

Figure 2.3: The geostrophic balance in the Northern Hemisphere.

(eastward), from (2.13). The Coriolis force is acting to the right of the motion, exactly balancing the pressure gradient force. And as the forces are balanced, the motion is constant in time (the flow is not accelerating).

If the pressure gradient changes in space, so will the geostrophic velocity. In Fig. (2.4), the flow accelerates into a region with more closely-packed pressure contours, then decelerates exiting the region.

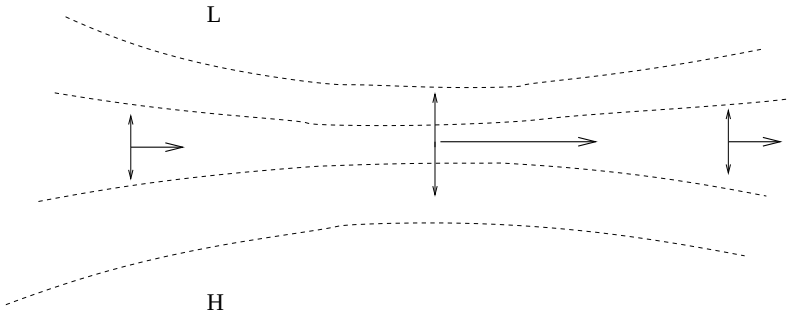

Figure 2.4: Geostrophic flow with non-constant pressure gradients.

As a result of the geostrophic relations, we can use pressure maps to estimate the winds, as in Fig. (2.5). This shows the surface pressure off the west coast of the US, with observed (green) and geostrophic (blue) wind vectors. First note that the geostrophic wind estimate agrees fairly well with the observed values. Note too that the wind is counter-clockwise

or *cyclonic* around the low pressure system. Had this been a high pressure system, we would have seen clockwise or *anti-cyclonic* flow.

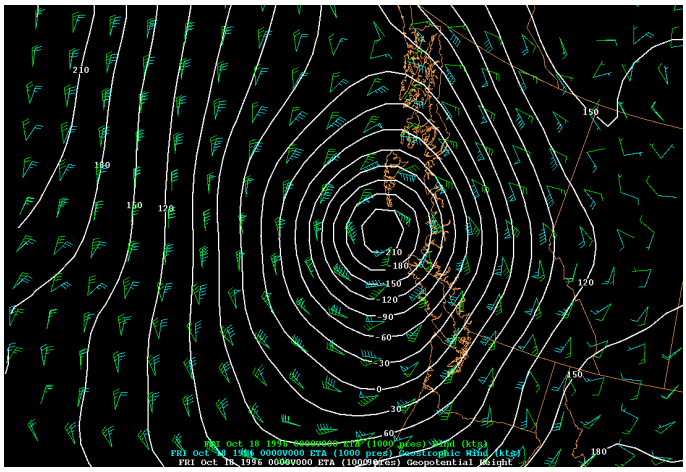

Figure 2.5: A low pressure system of the west coast of the United States. The green vectors are observed winds and the blue are geostrophic. Courtesy of the University of Washington.

Since $f = 2\Omega sin\theta$, the Coriolis force varies with latitude. It is strongest at high latitudes and weaker at low latitudes. Note too that it is *negative* in the southern hemisphere. Thus the flow in Fig. (2.3) would be westward, with the Coriolis force acting to the left. In addition, the Coriolis force is identically *zero* at the equator. In fact, the geostrophic balance cannot hold there and one must invoke other terms in the momentum equations.

2.2.2 Cyclostrophic flow

Now consider the case of a large Rossby number ($\epsilon \gg 1$). For example, a tornado (Fig. 2.6) at mid-latitudes has:

$$U \approx 30\, m/s, \quad f = 10^{-4}\, sec^{-1}, \quad R \approx 300\, m,$$

Thus $\epsilon = 1000$, implying the cyclostrophic term dominates over the Coriolis term. Indeed, instead divided the scaling parameters by $2\Omega U$, we might

Figure 2.6: A tornado in Oaklahoma in 2010. Courtesy of livescience.com.

have used U^2/R instead. Then we would have:

$$1 \quad \frac{2\Omega R}{U} \quad \frac{\triangle p}{\rho U^2}$$

Now the second term, which is just $1/\epsilon$, is very small (0.001 here). We would expect too that:

$$\frac{\triangle p}{\rho U^2} \approx 1$$

The result is *cyclostrophic balance*:

$$\frac{u_\theta^2}{r} = \frac{1}{\rho}\frac{\partial}{\partial r}p \tag{2.14}$$

This is a *non-rotating* balance, because f doesn't enter—we would have the same balance at the equator. The pressure gradient now is balanced by the centripetal acceleration.

We can solve for the velocity after multiplying by r and then taking the square root:

$$u_\theta = \pm\sqrt{\frac{r}{\rho}\frac{\partial}{\partial r}p} \tag{2.15}$$

There are two interesting points about this. One is that only low pressure systems are permitted, because we require $\frac{\partial}{\partial r}p > 0$ to have a real solution. However *either sign* of the circulation is allowed. So our tornado can have either *cyclonic* (counter-clockwise) or *anti-cyclonic* (clockwise) winds. Both cyclonic and anti-cyclonic tornadoes are in fact observed, but the former is much more common.

2.2.3 Inertial flow

There is a third possibility, that there is no radial pressure gradient at all. Then:

$$\frac{u_\theta^2}{r} + fu_\theta = 0 \quad \rightarrow \quad u_\theta = -fr \tag{2.16}$$

This is called *inertial flow*. It corresponds to circular motion in "solid body rotation" (with the velocity increasing linearly from the center, as it would with a DVD, for example). The velocity is negative, implying the rotation is clockwise (anti-cyclonic) in the Northern Hemisphere. The time for a parcel to complete a full circle is:

$$\frac{2\pi r}{u_\theta} = \frac{2\pi}{f} = \frac{0.5\ day}{|sin\theta|}\ , \tag{2.17}$$

This is known as the "inertial period".

"Inertial oscillations" are fairly rare in the atmosphere but are frequently seen at the ocean surface, being excited by the wind and other forcing. An example is shown in Fig. (2.7), of a pair of drifting buoys at the surface of the Gulf of Mexico. The pair is slowly separating, but simultaneously

executing large, anticyclonic loops. The inertial period at this latitude is nearly one day.

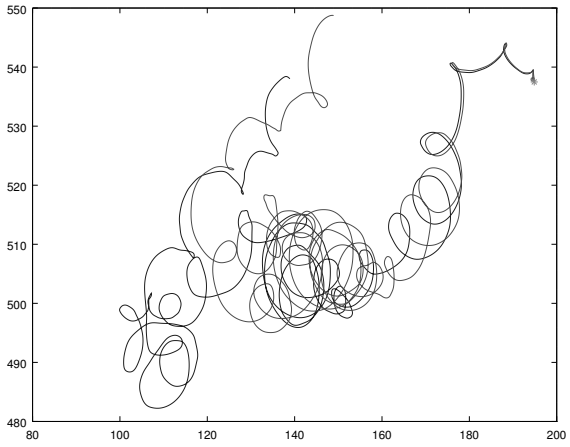

Figure 2.7: A pair of drifting buoys on the surface in the Gulf of Mexico, deployed as part of the GLAD experiment. The pair were deployed in the upper right corner of the figure. Courtesy of the University of Miami.

2.2.4 Gradient wind

The last possibility is that the Rossby number is order one ($\epsilon \approx 1$). Then all three terms in (2.10) are equally important. This is the *gradient wind balance*. We can then solve for u_θ using the quadratic formula:

$$u_\theta = -\frac{1}{2}fr \pm \frac{1}{2}(f^2r^2 + \frac{4r}{\rho}\frac{\partial}{\partial r}p)^{1/2} = -\frac{1}{2}fr \pm \frac{1}{2}fr(1 + \frac{4}{fr}\,u_g)^{1/2} \quad (2.18)$$

after using the definition of the geostrophic velocity.

The gradient wind solution actually contains all the previous solutions. If the pressure gradient is zero, the non-zero solution is $-fr$, as with inertial osciallations. If $u_g \ll fr$, then one of the roots is $u_\theta = u_g$. And if $f = 0$, the cyclostrophic solution is recovered.

Because the term in the square root must be positive, we must have:

$$f^2 r^2 + 4\, r\, f\, u_g \geq 0 \tag{2.19}$$

which implies:

$$u_g \geq -\frac{fr}{4} \tag{2.20}$$

Thus while there is no limit on how large u_g can be, it cannot be less than $-fr/4$. This means that anticyclones are limited in strength while cyclones aren't. So the strongest storms must be cyclonic under gradient wind.

The gradient wind balance, being a three-way balance of forces, has other implications. For a low pressure system, the gradient wind velocity is actually less than the geostrophic velocity, because there are two terms now balancing the same pressure gradient (left panel of Fig. 2.8). For a high pressure system on the other hand, the gradient wind velocity is greater than the geostrophic, because the Coriolis term now opposes the cyclostrophic term (right panel of Fig. 2.8). The asymmetry occurs because the cyclostrophic term always acts outward.

Likewise, the cyclostrophic term can actually oppose both the other terms, in the case of a low pressure system (Fig. 2.9). This implies that the winds are *anti-cyclonic*, so that the Coriolis acceleration is toward the center of the storm. Such clockwise low pressure systems, called *anomalous lows*, are fairly rare but occur occasionally at lower latitudes.

The gradient wind estimate thus differs from the geostrophic estimate. The difference is typically small for weather systems, about 10 % at mid-latitudes. To see this, we rewrite (2.10) thus:

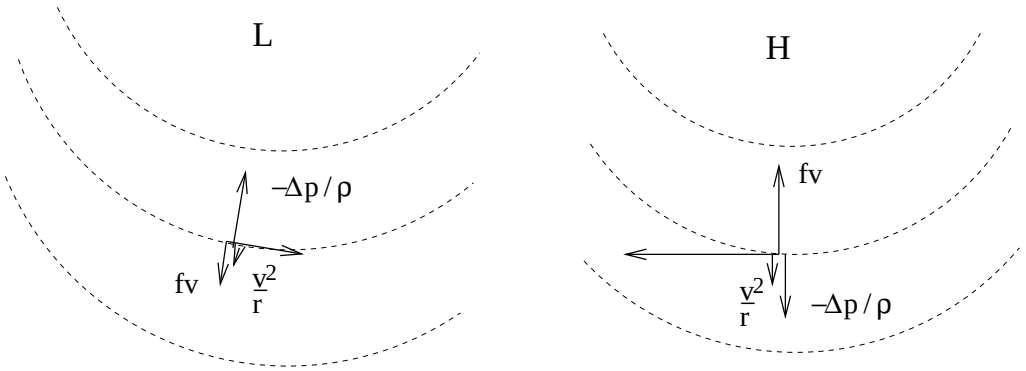

Figure 2.8: The balance of terms under the gradient wind approximation for a low (left) and high (right) pressure system.

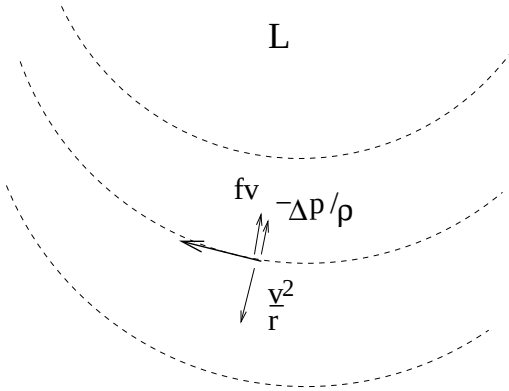

Figure 2.9: An anomalous low pressure system.

$$\frac{u_\theta^2}{r} + f u_\theta = \frac{1}{\rho}\frac{\partial}{\partial r} p = f u_g \tag{2.21}$$

Then:

$$\frac{u_g}{u_\theta} = 1 + \frac{u_\theta}{fr} = 1 + \epsilon \tag{2.22}$$

Thus if $\epsilon = 0.1$, the gradient wind estimate differs from the geostrophic value by 10 %. This is why the geostrophic winds in Fig. (2.5) differ slightly from the observed winds. At low latitudes, where ϵ can be 1-10, the gradient wind estimate is more accurate.

2.3 The f-plane and β-plane approximations

Another simplification is needed. The momentum equations are in Cartesian coordinates, but the Coriolis term, f, is in spherical coordinates. We could write it as a sinusoidal function of y, but this complicates the solutions. A better approach is to linearize f about a chosen latitude, θ_0. This is shown in Fig. (2.10). The linear function is much easier to handle analytically.

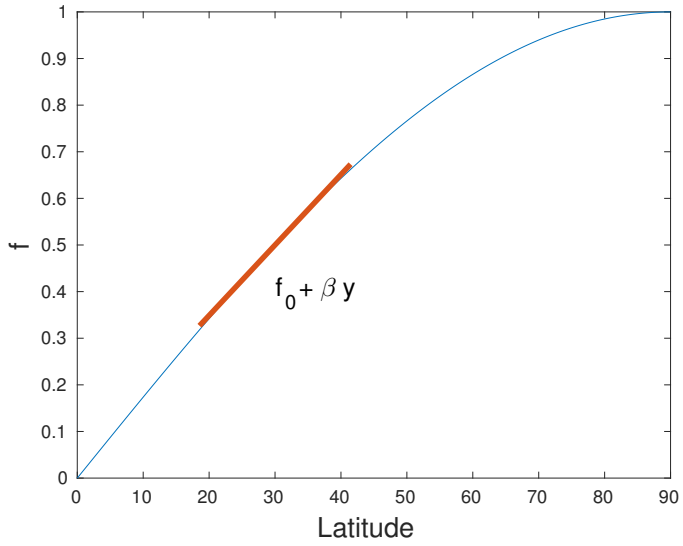

Figure 2.10: The Coriolis parameter, as a function of latitude, and the β-plane approximation with a central latitude of $\theta = 30°$.

To do this, we Taylor-expand f about the center latitude:

$$f(\theta) = f(\theta_0) + \frac{df}{d\theta}(\theta_0)\ (\theta - \theta_0) + \frac{1}{2}\frac{d^2 f}{d\theta^2}(\theta_0)\ (\theta - \theta_0)^2 + ... \qquad (2.23)$$

The subsequent terms are small if the range of latitudes is limited. Retaining the first two terms, we can write:

$$f = f_0 + \beta y$$

where:

$$f_0 = 2\Omega sin(\theta_0), \quad \beta = \frac{1}{R_e}\frac{df}{d\theta}(\theta_0) = \frac{2\Omega}{R_e}cos(\theta_0)$$

and

$$y = R_e(\theta - \theta_0)$$

The expansion is valid when the second term is much smaller than the first. This requires:

$$\frac{\beta L}{f_0} \ll 1$$

where L is the north-south extent of the domain (in distance, not degrees). So:

$$L \ll \frac{f_0}{\beta} = \frac{2\Omega sin(\theta)}{2\Omega cos(\theta)/R_e} = R_e\, tan(\theta_0) \approx R_e \tag{2.24}$$

So L must be much smaller than the earth's radius, which is roughly 6600 km.

However, you can see from Fig. (2.10) that the range of validity for the linear approximation varies with latitude; it's better nearer the equator, where $sin(\theta)$ is more linear, but more restricted at higher latitudes where the curvature is greater. Nevertheless, the great simplification with this makes it worthwhile.

Two cases are considered hereafter. Retaining only the first term, f_0, is called the *f-plane approximation*. This is appropriate for a small domain, e.g. with L on the order of a hundred kilometers or less. For larger domains, we retain the first two terms, the *β-plane approximation*. This assumes a domains of up to a couple of thousand kilometers in N-S extent.

2.4 Incompressibility

The continuity equation (1.9) can also be simplified. This is a nonlinear equation, involving products of the density, ρ, and the velocities. However, we can obtain a simpler, *linear* relation in both the atmosphere and ocean. This involves two approximations, one for each system.

2.4.1 The Boussinesq approximation

In the ocean, the density changes are very small. In particular, the terms involving the temperature and salinity in the equation of state (1.36) are typically much less than one. So if we write:

$$\rho = \rho_c + \rho'(x, y, z, t)$$

the perturbation, ρ', is much less than ρ_c. As such, the continuity equation (1.9) is:

$$\frac{d\rho'}{dt} + \rho_c(\nabla \cdot \vec{u}) \approx \rho_c(\nabla \cdot \vec{u}) = 0 \tag{2.25}$$

This implies that:

$$\nabla \cdot \vec{u} \approx 0 \tag{2.26}$$

Thus the velocities are approximately *incompressible*, meaning the *volume* is conserved. If one has a box full of water with a movable lid, it is almost impossible to press down the lid. Water does compress at great depths in the ocean, but there the pressure is enormous.

The Boussinesq approximation (named after the French physicist Joseph Boussinesq) essentially neglects density variations except where gravity is

involved. So we replace the full density with the constant reference density in the horizontal momentum equations. Thus the geostrophic relations are changed:

$$v_g = \frac{1}{\rho_c f}\frac{\partial}{\partial x}p \tag{2.27}$$

$$u_g = -\frac{1}{\rho_c f}\frac{\partial}{\partial y}p \tag{2.28}$$

As such, the geostrophic relations are now *linear*. Furthermore, under the f or β-plane approximations, the f in the denominator would be replaced by f_0, meaning that the velocities can be written thus:

$$v_g = \frac{\partial}{\partial x}\psi, \quad u_g = -\frac{\partial}{\partial y}\psi$$

where:

$$\psi \equiv \frac{p}{\rho_c f_0}$$

This is the *geostrophic streamfunction*. The velocities are exactly parallel to the ψ contours.

In addition, the geostrophic velocities, defined this way, are now horizontally non-divergent:

$$\frac{\partial}{\partial x}u_g + \frac{\partial}{\partial y}v_g = \frac{\partial}{\partial x}(-\frac{1}{\rho_c f_0}\frac{\partial}{\partial y}p) + \frac{\partial}{\partial y}(\frac{1}{\rho_c f}\frac{\partial}{\partial x}p) = 0 \tag{2.29}$$

We'll exploit this later on.

2.4.2 Pressure coordinates

We cannot responsibly use the Boussinesq approximation with the atmosphere, except possibly in the planetary boundary layer (this is often done,

for example, when considering the surface boundary layers, as in sec. 4.5). But it is possible to achieve the same simplifications if we change the vertical coordinate to *pressure* instead of height.

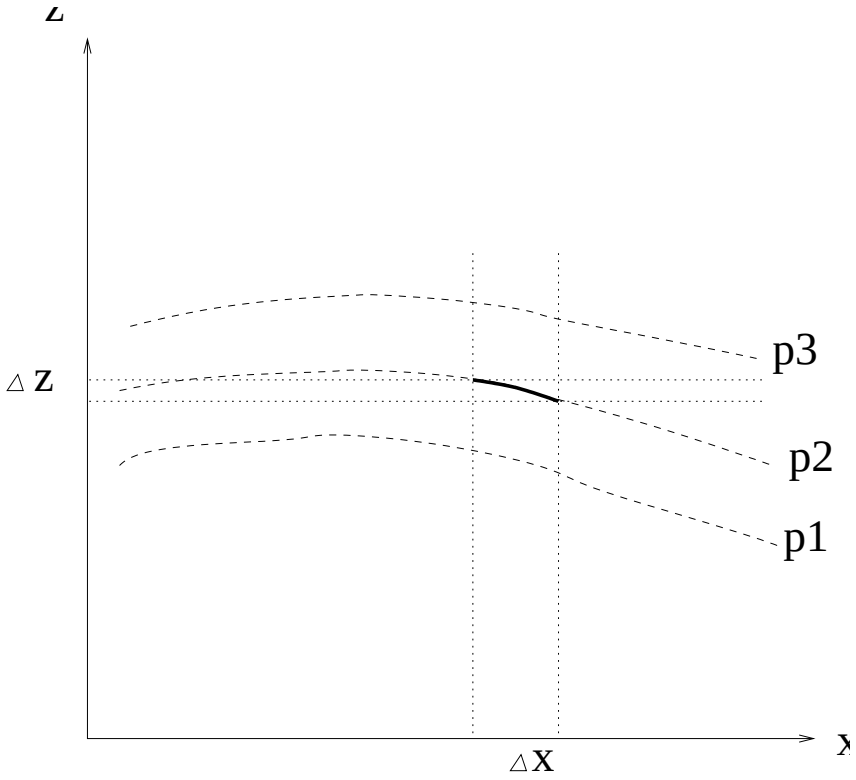

Figure 2.11: Pressure surfaces in (x, z).

We do this by exploiting the hydrostatic balance. Consider a pressure surface in two dimensions, like $p_2(x, z)$ in Fig. (2.11). As one moves along the surface, its height may change but the pressure remains the same. We can express this using the chain rule:

$$\triangle p(x, z) = \frac{\partial p}{\partial x} \triangle x + \frac{\partial p}{\partial z} \triangle z = 0 \tag{2.30}$$

Substituting the hydrostatic relation, we get:

$$\frac{\partial p}{\partial x} \triangle x - \rho g \triangle z = 0 \tag{2.31}$$

so that:

$$\frac{\partial p}{\partial x}|_z = \rho g \, \frac{\triangle z}{\triangle x}|_p \tag{2.32}$$

The left-hand side is the pressure gradient in x along a surface of constant height (hence the z subscript). The right-hand side is proportional to the *height gradient* along a surface of constant pressure—i.e. how much the pressure surface tilts in x. The gradient on the RHS thus has a p subscript, indicating pressure coordinates.

If we define the *geopotential*:

$$\Phi = gz \tag{2.33}$$

then we have:

$$\frac{\partial p}{\partial x}|_z = \rho \frac{\partial \Phi}{\partial x}|_p \tag{2.34}$$

This alteration removes the density from momentum equation, because:

$$-\frac{1}{\rho}\nabla p|_z \quad \rightarrow \quad -\nabla \Phi|_p$$

So the geostrophic balance in pressure coordinates is simply:

$$v_g = \frac{1}{f_0}\frac{\partial}{\partial x}\Phi \tag{2.35}$$

$$u_g = -\frac{1}{f_0}\frac{\partial}{\partial y}\Phi \tag{2.36}$$

(again using the β-plane approximation). As with the Boussinesq approximation, the terms on the RHS are linear. So in pressure coordinates too, the geostrophic velocities can be expressed in terms of a streamfunction:

$$\psi = \frac{\Phi}{f_0}$$

The continuity equation also simplifies with pressure coordinates. Consider our Lagrangian box, filled with a fixed number of molecules. The box has a volume:

$$\delta V = \delta x\, \delta y\, \delta z = -\delta x\, \delta y\, \frac{\delta p}{\rho g} \tag{2.37}$$

after substituting from the hydrostatic balance. Note that the volume is positive because δp is negative, with increasing height. The mass of the box is:

$$\delta M = \rho\, \delta V = -\frac{1}{g}\delta x\, \delta y\, \delta p$$

Conservation of mass implies:

$$\frac{1}{\delta M}\, \frac{d}{dt}\, \delta M = \frac{-g}{\delta x \delta y \delta p}\, \frac{d}{dt}\, (-\frac{\delta x \delta y \delta p}{g}) = 0 \tag{2.38}$$

Rearranging:

$$\frac{1}{\delta x}\, \delta(\frac{dx}{dt}) + \frac{1}{\delta y}\, \delta(\frac{dy}{dt}) + \frac{1}{\delta p}\, \delta(\frac{dp}{dt}) = 0 \tag{2.39}$$

If we let $\delta \to 0$, we get:

$$\frac{\partial u}{\partial x} + \frac{\partial v}{\partial y} + \frac{\partial \omega}{\partial p} = 0 \tag{2.40}$$

where ω (called "omega" in the literature) is the velocity perpendicular to the pressure surface. This is just as w is perpendicular to a z-surface. Hence, as with the Boussinesq approximation, the flow is *incompressible in pressure coordinates*.

The hydrostatic equation also takes a different form under pressure coordinates. It can be written:

$$\frac{d\Phi}{dp} = -\frac{RT}{p} \tag{2.41}$$

after invoking the Ideal Gas Law.

Pressure coordinates simplifies the equations considerably. But they are nonetheless awkward to work with in theoretical models. The lower boundary in the atmosphere (the earth's surface) is most naturally represented in z-coordinates, e.g. as $z = 0$. As the pressure varies at the earth's surface, it is less obvious what boundary value to use for p. So we will use z-coodinates primarily hereafter. But the solutions in p-coordinates are often very similar.[2]

2.5 Thermal wind

Often large scale flows in the atmosphere and ocean occur where there are strong temperature contrasts. The Gulf Stream, for example, lies on the boundary between the warmer waters of the Sargasso Sea (familiar to anyone who's been swimming in the Carribbean) and the cold waters off New England and Atlantic Canada (familiar to anyone who's been swimming there). This boundary is rather sharp and dynamic, meandering and pinching off eddies. The Jet Stream in the atmosphere is similar. It lies between the warm air of the tropics and the colder air at the mid-latitudes. It too is highly dynamic and generating eddies (storms).

In fact, strong temperature gradients are associated with strong *vertical*

[2] An alternative is to use *log-pressure coordinates*. These involve a coordinate change from pressure to a z-like coordinate, called z^*. However, z^* generally differs only slightly from z, so we will focus on the latter.

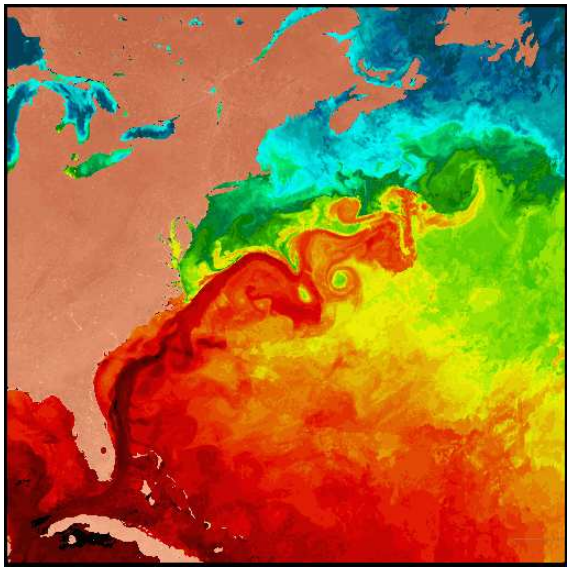

Figure 2.12: The sea surface temperature in the North Atlantic. The Gulf Stream lies between the warm Sargasso Sea and the cold waters to the north.

shear in the velocity. Shown in Fig. (2.13) is a cross section of temperature in the core of the Gulf Stream. At any given depth, the temperature increases going left to right. The current (illustrated by the dark contours) is strongest where the temperature gradients are most pronounced. In particular, the current varies greatly in the vertical, increasing towards the surface. The currents at the surface 1 m/sec, a large value in the ocean.

The relation between lateral temperature contrast and vertical shear is a consequence of the combined geostrophic and hydrostatic balances. Take, for instance, the z-derivative of the geostrophic balance for v:

$$\frac{\partial v_g}{\partial z} = \frac{1}{f_0 \rho_c} \frac{\partial}{\partial x} \frac{\partial p}{\partial z} = -\frac{g}{f_0 \rho_c} \frac{\partial \rho}{\partial x} \tag{2.42}$$

after using (2.3). Likewise:

$$\frac{\partial u_g}{\partial z} = \frac{g}{f_0 \rho_c} \frac{\partial \rho}{\partial y} \tag{2.43}$$

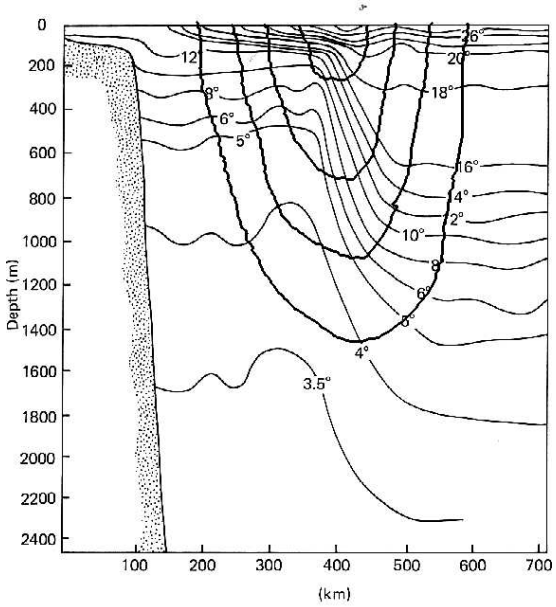

Figure 2.13: A cross section of the ocean temperature in the core of the Gulf Stream.

These are the *thermal wind relations* in z-coordinates. They state that the vertical velocity shear is proportional to the lateral gradients in the density.

The corresponding relations in pressure coordinates can be obtained by taking the p-derivative of the geostrophic relations, for example in the x-direction:

$$\frac{\partial v_g}{\partial p} = \frac{1}{f_0}\frac{\partial}{\partial x}\frac{\partial \Phi}{\partial p} = -\frac{R}{p f_0}\frac{\partial T}{\partial x} \tag{2.44}$$

after using (2.41). The p passes through the x-derivative because it is constant on an isobaric (p) surface, i.e. they are independent variables. Likewise:

$$\frac{\partial u_g}{\partial p} = \frac{R}{p f_0}\frac{\partial T}{\partial y} \tag{2.45}$$

after using the hydrostatic relation (2.41). Thus the vertical shear is proportional to the lateral gradients in the temperature.

Consider Fig. (2.14). This is reminiscent of the situation in the north-

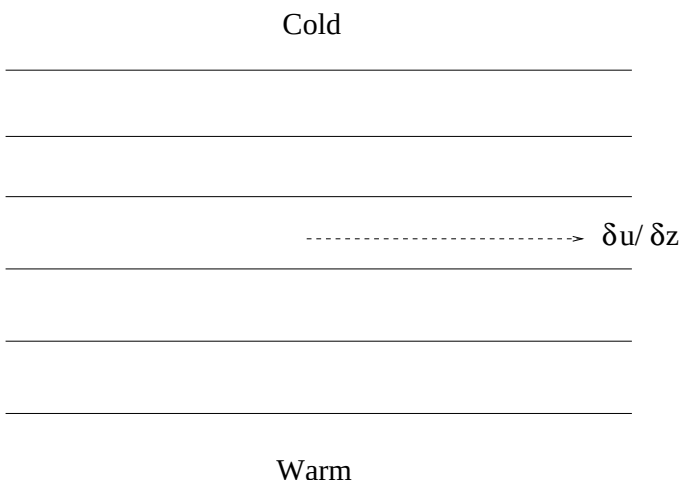

Figure 2.14: The thermal wind shear associated with a temperature gradient in the y-direction.

ern hemisphere, with cold air at the pole and warm air near the equator. The temperature gradient in y, so the thermal wind is oriented in the x-direction. As the temperature decreases to the north, $\partial T/\partial y$ is negative. From (2.45) we have that $\partial u_g/\partial p$ is also negative. This implies that $\partial u_g/\partial z$ is *positive*, because the pressure decreases going up. So the zonal velocity is increasing going up, i.e. with the cold air to the left. Notice the similarity to the geostrophic flow, which is parallel to the pressure contours with the low pressure on the left.

In the ocean, the thermal wind is parallel to the density contours, with the heavy fluid on the left. Consider the Gulf Stream case, shown in Fig. (2.13). The temperature increases moving offshore. That implies that the heavy water (cold) is to the left, so that the shear is increasing towards the surface. Assuming no flow at depth, we have a strong northward flow (into the picture).

Using thermal wind, we can derive the geostrophic velocities on a nearby pressure surface if we know the velocities on another pressure surface and

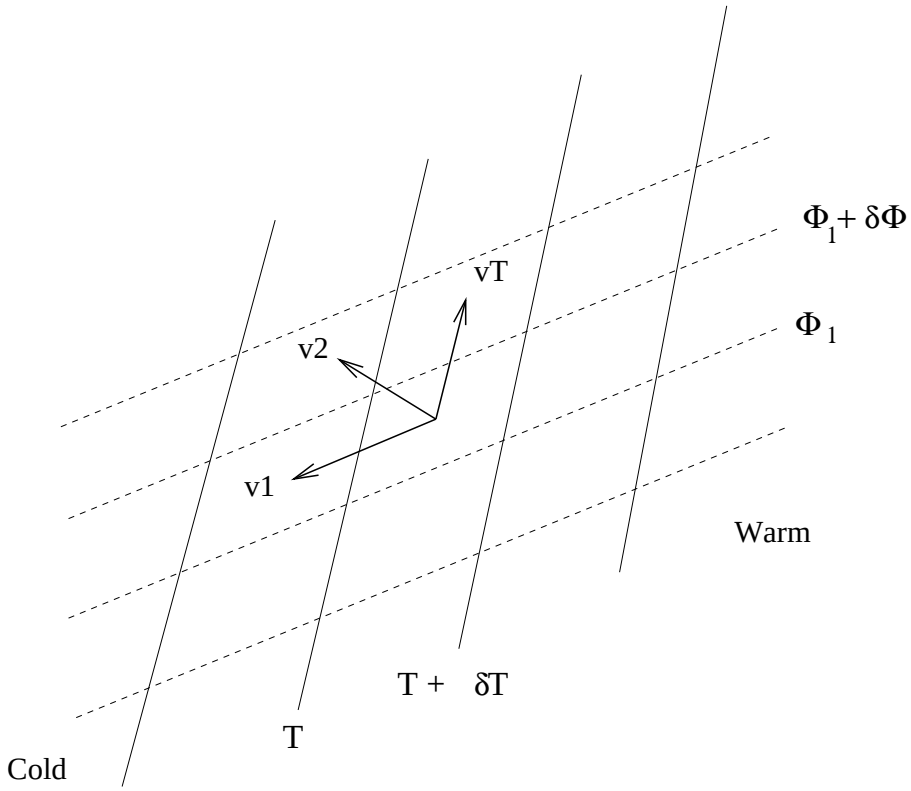

Figure 2.15: Thermal wind between two layers (1 and 2). The geopotential height contours for the lower layer, Φ_1, are the dashed lines and the temperature contours are the solid lines.

the temperature in the layer between the two. Consider Fig. (2.15). The geopotential lines for the lower surface of the layer are indicated by dashed lines. The wind at this level is parallel to these lines, with the larger values of Φ_1 to the right. The temperature contours are the solid lines, with the temperature increasing to the right. The thermal wind vector is parallel to these contours, with the larger temperatures on the right. We add the vectors v_1 and v_T to obtain the vector v_2, which is the wind at the upper surface. This is to the northwest, advecting the warm air towards the cold.

Notice that the wind vector turns clockwise with height. This is called *veering* and is typical of warm advection. Cold advection produces counter-clockwise turning, called *backing*.

Thus the geostrophic wind is parallel to the geopotential contours with larger values to the right of the wind (in the Northern Hemisphere). The thermal wind on the other hand is parallel to the mean temperature contours, with larger values to the right. Recall though that the thermal wind is not an actual wind, but the *difference* between the lower and upper level winds.

The thermal wind relations are routinely used to estimate ocean currents from density measurement made from ships. Ships collect *hydrographic* measurements of temperature and salinity, and these are used to determine $\rho(x, y, z, t)$, from the equation of state (1.36). Then the thermal wind relations are integrated upward from chosen level to determine (u, v) above the level, for example:

$$u_g(x, y, z) - u_g(x, y, z_0) = \int_{z0}^{z} \frac{1}{\rho_c f_0} \frac{\partial \rho(x, y, z)}{\partial y} \, dz \tag{2.46}$$

If (u, v, z_0) is set to zero at the lower level, it is known as a "level of no motion".

2.6 Summary of synoptic scale balances

We have a set of simplified equations, one for the ocean and one for the atmosphere, which are applicable at synoptic scales.

Equation	Boussinesq	p-coordinates	
Geostrophic u	$f_0 u = -\frac{1}{\rho_c}\frac{\partial p}{\partial y}$	$f_0 u = -\frac{\partial \Phi}{\partial y}$	(2.48)
Geostrophic v	$f_0 v = \frac{1}{\rho_c}\frac{\partial p}{\partial x}$	$f_0 v = \frac{\partial \Phi}{\partial x}$	(2.49)
Hydrostatic	$\frac{\partial p}{\partial z} = -\rho g$	$\frac{\partial \Phi}{\partial p} = -\frac{RT}{p}$	(2.50)
Thermal u	$f_0\frac{\partial u}{\partial z} = \frac{g}{\rho_c}\frac{\partial \rho}{\partial y}$	$f_0\frac{\partial u}{\partial p} = \frac{R}{p}\frac{\partial T}{\partial y}$	(2.51)
Thermal v	$f_0\frac{\partial v}{\partial z} = -\frac{g}{\rho_c}\frac{\partial \rho}{\partial x}$	$f_0\frac{\partial v}{\partial p} = -\frac{R}{p}\frac{\partial T}{\partial x}$	(2.52)
Continuity	$\frac{\partial u}{\partial x} + \frac{\partial v}{\partial y} + \frac{\partial w}{\partial z} = 0$	$\frac{\partial u}{\partial x} + \frac{\partial v}{\partial y} + \frac{\partial \omega}{\partial p} = 0$	(2.53)

For the *ocean*, we make the Boussinesq approximation and neglect density variations, except in the hydrostatic relation. For the *atmosphere*, we use pressure coordinates. The similarity between the resulting equations is striking. These equations are all linear, so they are much easier to work with than the full equations of motion.

Lastly we have the frictional boundary layers. We have Ekman layers at the base of the atmosphere and ocean, and these produce a vertical velocity proportional to the relative vorticity in the interior of the respective fluid. At the surface of the ocean we have an additional frictional layer, in which the vertical velocity is proportional to the curl of the wind stress. We'll see later how these layers interact with the interior flow.

2.7 *Exercises*

2.1. Scale the full x-momentum equation (eq. 1.32), using parameters typical of the ocean. Assume:

- $U = 10$ cm/sec
- $W = 1$ m/day
- $L = 100$ km
- $D = 5$ km

Assume an *advective time scale*, such that $T \propto L/U$ and that $sin(\theta) \approx 1$. Show that the geostrophic balance applies with these scales. Can you estimate what the scale is for $\triangle p/\rho$?

2.2. Consider a low pressure system centered at 45°S, with a sea level pressure given by:

$$p = 1000hPa - \triangle p \; e^{-r^2/R^2}$$

where r is the radial distance from the center. Determine the geostrophic wind around this storm. Find the maximum wind, and the radius where the wind is maximum, if $\triangle p = 20$ hPa, $R = 500$ km and the density at sea level is 1.3 kg/m^3. Assume $f = f_0$, with the value at 45°S.

2.3. The Gulf Stream flows north along the coast of the United States with a surface current of roughly 2 m/sec. If the flow is in geostrophic balance, what is the change of sea surface height over 100 km separation at 45°N?

2.4. Assuming $\theta = 45N$, so that $f = 10^{-4}$ sec^{-1}, and that $g \approx 10m/sec^2$:

a) Assume the pressure decreases by 0.5 Pa over 1 km to the east but does not change to the north. Which way is the geostrophic wind blowing? If the density of air is 1 kg/m^3, what is the wind speed? Note 1 Pa=1 kg/(m sec^2).

b) If the temperature of air was 10 C throughout the atmosphere and the surface pressure was 1000 hPa, what would the pressure at a height of 1 km be? Note 1 hPa=100 Pa.

c) The temperature decreases by 1/5 deg C over 1 km to the north but doesn't change to the east. What is the wind shear (in magnitude and direction)? Is this veering or backing?

Hint: Use the pressure coordinate version of thermal wind and then convert the pressure derivative to a z-derivative.

2.5. The talk show host David Letterman once called a man in South America to ask whether the water swirled clockwise when flowing out the drain in his bathtub. Is there a preferred tendency in a bathtub, due to rotation?

Assume the bathtub is 1.5 m long and that typical velocities in the water are about 1 cm/sec. The bathtub is at 45 N. Explain whether or not there is a preferred sense of rotation, and if yes, what sign?

2.6. Derive (2.41), using the Ideal Gas Law.

2.7. Say the temperature at the South Pole is -20C and it's 40C at the Equator. Assuming the average wind speed is zero at the Earth's surface (1000 hPa), what is the mean zonal speed at 250 hPa at 45S?

Assume the temperature gradient is constant with latitude and pressure. Use the thermal wind relations in pressure coordinates and integrate them with respect to pressure to find the velocity difference between the surface and 250 hPa.

2.8. Thermal wind on Venus

We know (from various space missions) that the surface density on Venus is 67 kg/m^3 and the height of the troposphere is 65 km. Also, the Venetian day is 116.5 times longer than our day(!) We want to estimate the wind velocity at the top of the tropopause.

a) Write down the thermal wind equation for the zonal wind, u, in pressure coordinates.

b) Convert the pressure derivative to a z-derivative by assuming the density decays exponentially with height, with an e-folding scale (the scale height) equal to half the height of the tropopause.

c) If the temperature gradient in the northern hemisphere is -1.087 x 10^{-4} degrees/km, what is the zonal velocity at the tropopause? Assume the temperature gradient doesn't change with height and that the velocity at the surface is zero. Note $R = 287$ J/(kg K).

Chapter 3

Shallow water flows

Now we'll begin looking at actual phenomena in the atmosphere/ocean systems. We'll start with a simpler system: a thin layer of fluid with a constant density. What we'll see is that the flow doesn't vary in the vertical, which makes it effectively two dimensional. However, the phenomena present here are also found in fully 3D flows. The system is actually quite realistic for oceanic flows, particularly at higher latitudes, but there are examples relevant to the atmosphere as well.

3.1 Fundamentals

3.1.1 Assumptions

The system is based on the *shallow water equations*. These involve two assumptions:

- The density is constant
- The *aspect ratio* is small

Having a constant density is not realistic for the atmosphere, but is for the ocean, whose density is dominated by the constant term, ρ_c.

The aspect ratio is the ratio of the depth of the fluid to its width. For an ocean basin, this might be 5 km divided by $10,000$ km, so:

$$\delta \equiv \frac{D}{L} = \frac{5}{5000} = 0.0005 \ .$$

The aspect ratio is also this small for weather systems in the troposphere.

As noted in section (2.4), the flow in the ocean and atmosphere is approximately incompressible (if the coordinates are changed, in the latter case). However, with a constant density the flow is *exactly* incompressible, following from the continuity equation (1.9):

$$\nabla \cdot \vec{u} = \frac{\partial}{\partial x} u + \frac{\partial}{\partial y} v + \frac{\partial}{\partial z} w = 0 \tag{3.1}$$

Scaling this, and assuming all three terms are equal in size, we infer:

$$W = \delta U$$

Thus the vertical velocity is much smaller than the horizontal.

The fluid is sketched in Figure (3.1). It has a free surface, given by $\eta(x, y, t)$. The lower boundary, at $z = -H(x, y)$, can be rough, with mountains and valleys. The fluid has a mean depth (with an undisturbed surface) denoted D_0 (roughly 5 km for the ocean).

The small aspect ratio guarantees that the vertical momentum equation reduces to the hydrostatic relation (sec. 2.1). This, with a constant density, yields another important simplification: that the pressure gradients driving the horizontal flow *don't vary with depth*. To see this, integrate the hydrostatic balance to the surface from a depth, z:

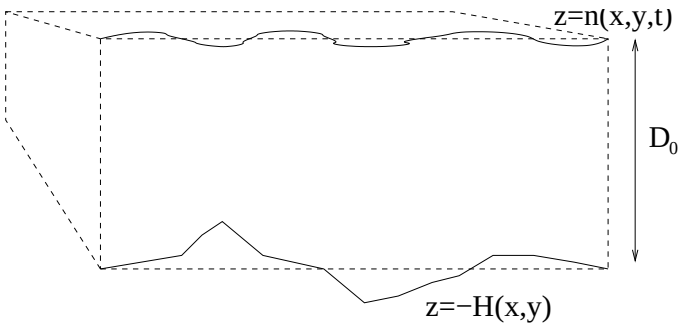

Figure 3.1: The layer of homogeneous fluid in the region shown in figure (1.4). The layer has a mean depth, D_0, and a surface elevation, $\eta(x, y, t)$. The bottom is variable and lies at $z = -H(x, y)$.

$$p(\eta) - p(z) = -\int_z^\eta \rho_c g \; dz = -\rho_c g(\eta - z) \tag{3.2}$$

Rearranging, and taking the horizontal gradient:

$$\nabla p(z) = \nabla p(\eta) + \rho_c g \nabla \eta \tag{3.3}$$

The first term on the right hand side is the gradient of the the pressure at the surface, while the second is related to gradients in the surface height. Both can vary in (x, y, t) but not in z—thus the pressure gradient terms in the x and y momentum equations likewise do not vary in the vertical. That implies that if the horizontal flow has no vertical shear initially, it cannot develop shear (in the absence of other forcing, like friction).[1]

As such, we can assume the horizontal velocities do not vary with depth. Such velocities are called *barotropic*. This is a tremendous simplification, because the formerly 3-D motion is now 2-D. Physically, the fluid moves in *columns*, because vertically-aligned fluid parcels remain aligned.

In practice, the surface height contribution in (3.3) is much greater than the surface pressure term, because the former varies on much smaller

[1]This is similar to, but not exactly equivalent to, the *Taylor-Proudman theorem*.

scales. So we will assume hereafter that the flow is driven solely by surface height variations.

3.1.2 Shallow water equations

Under these assumptions, the horizontal momentum equations (1.32) and (1.33) become:

$$\begin{aligned} \frac{d_H}{dt}u - fv &= -g\frac{\partial}{\partial x}\eta \\ \frac{d_H}{dt}v + fu &= -g\frac{\partial}{\partial y}\eta \end{aligned} \tag{3.4}$$

where:

$$\frac{d_H}{dt} \equiv \frac{\partial}{\partial t} + u\frac{\partial}{\partial x} + v\frac{\partial}{\partial y}$$

is the Eulerian derivative in the horizontal. The vertical advection terms vanish because the velocities don't vary in z. We have also neglected any forcing (e.g. from friction, or surface winds). We'll include that later on.

These are the *shallow water momentum equations*. These have three unknowns, u, v and η, meaning we require an additional equation. The incompressibility condition (3.1) provides a third equation, but this is in terms of u, v and w. However we can eliminate w in favor of η by integrating over the depth of the fluid:

$$\int_{-H}^{\eta} (\frac{\partial}{\partial x}u + \frac{\partial}{\partial y}v)\, dz + w(\eta) - w(-H) = 0 \tag{3.5}$$

Because the horizontal velocities are barotropic, they move through the integral:

$$(\eta + H)(\frac{\partial}{\partial x}u + \frac{\partial}{\partial y}v) + w(\eta) - w(-H) = 0 \tag{3.6}$$

We require the vertical velocities at the upper and lower boundaries. We get these by noting that a fluid parcel on the boundary stays on the boundary. For a parcel on the upper surface:

$$z = \eta \tag{3.7}$$

If we take the derivative of this, we get:

$$\frac{dz}{dt} = (\frac{\partial}{\partial t} + \vec{u} \cdot \nabla)z = w(\eta) = \frac{d\eta}{dt} = \frac{d_H \eta}{dt} \tag{3.8}$$

The derivative on the RHS is the horizontal one because $\eta = \eta(x, y, t)$. A similar relation applies at the lower boundary, at $z = -H$:

$$w(-H) = -\frac{d_H H}{dt} \tag{3.9}$$

The horizontal derivative here occurs because $H = H(x, y)$. The lower boundary isn't actually moving, but the term is non-zero because of the advective component, i.e.:

$$\frac{d_H H}{dt} = \vec{u}_H \cdot \nabla H \tag{3.10}$$

Putting these into the continuity equation, we get:

$$\frac{d_H}{dt}(\eta + H) + (\eta + H)(\frac{\partial}{\partial x}u + \frac{\partial}{\partial y}v) = 0 \tag{3.11}$$

This is the Lagrangian form of the continuity equation. In Eulerian terms, this is:

$$\frac{\partial}{\partial t}\eta + \nabla \cdot [\vec{u}(\eta + H)] = 0 \tag{3.12}$$

This provides us with our third equation, involving u, v and η. Now we have a closed system.

To summarize, the shallow water equations are:

$$\frac{d_H}{dt}u - fv = -g\frac{\partial}{\partial x}\eta \tag{3.13}$$

$$\frac{d_H}{dt}v + fu = -g\frac{\partial}{\partial y}\eta \tag{3.14}$$

$$\frac{d_H}{dt}(\eta + H) + (\eta + H)(\frac{\partial}{\partial x}u + \frac{\partial}{\partial y}v) = 0 \tag{3.15}$$

These constitute the shallow water system. They have several *conserved quantities*, which will be important in understanding the subsequent examples. There are two types of conservation statement: one which applies to fluid parcels and another which applies when integrated over the whole fluid volume.

3.2 Material conserved quantities

3.2.1 Volume

Equation (3.15) is a statement of mass conservation. If we imagine a fixed volume of fluid, the second term on the RHS represents the flux divergence through the sides of the volume. If there is a convergence or divergence, the height of the volume must increase or decrease.

Because the depth, H, is fixed in time, we can rewrite the continuity equation thus:

$$\frac{d_H}{dt}D + D(\frac{\partial}{\partial x}u + \frac{\partial}{\partial y}v) = 0 \tag{3.16}$$

where:

$$D = H + \eta$$

is the total fluid depth. As noted before, there is no vertical shear in shallow water flows and the fluid moves in columns. So the height of the column changes in response to divergence.

Now consider an infinitesimal area of fluid with sides δx and δy. Then the time change in the area is:

$$\frac{\delta A}{\delta t} = \delta y \frac{\delta x}{\delta t} + \delta x \frac{\delta y}{\delta t} = \delta y\, \delta u + \delta x\, \delta v \tag{3.17}$$

So the relative change in area is equal to the divergence:

$$\frac{1}{\delta A}\frac{\delta A}{\delta t} = \frac{\delta u}{\delta x} + \frac{\delta v}{\delta y}\ . \tag{3.18}$$

Using this in (3.16), we obtain:

$$A\frac{d_H}{dt}D + D\frac{d_H}{dt}A = \frac{d_H}{dt}V = 0 \tag{3.19}$$

Thus the volume of the column is conserved by the motion.

3.2.2 Vorticity

The *vorticity* is the curl of the velocity, i.e $\nabla \times \vec{u}$. This plays a central role in geophysical flows in general. The vorticity is a vector, with components:

$$\begin{aligned} \zeta_x &= \frac{\partial}{\partial y}w - \frac{\partial}{\partial z}v = \frac{\partial}{\partial y}w \\ \zeta_y &= \frac{\partial}{\partial z}u - \frac{\partial}{\partial x}w = -\frac{\partial}{\partial x}w \\ \zeta_z &= \frac{\partial}{\partial x}v - \frac{\partial}{\partial y}u \end{aligned} \tag{3.20}$$

Again, there is no vertical shear, so $\frac{\partial}{\partial z}u = \frac{\partial}{\partial z}v = 0$. Then using our scalings, we have:

$$\zeta_x = O|\frac{W}{L}| = O|\frac{\delta U}{L}|, \quad \zeta_y = O|\frac{\delta U}{L}|, \quad \zeta_z = O|\frac{U}{L}|$$

So the horizontal components are much smaller than the vertical and we can ignore them. The velocities in shallow water flows are primarily horizontal, so the most important part of the curl is in the vertical. We'll drop the z subscript on ζ because we won't consider the other components further.

We obtain an equation for the vertical vorticity, ζ, by cross-differentiating the shallow water momentum equations (3.13) and (3.14); specifically, we take the x derivative of the second equation and subtract the y derivative of the first. The result is:

$$\frac{\partial}{\partial t}\zeta + u\frac{\partial}{\partial x}\zeta + v\frac{\partial}{\partial y}\zeta + (f+\zeta)(\frac{\partial}{\partial x}u + \frac{\partial}{\partial y}v) + v\frac{\partial}{\partial y}f = 0 \qquad (3.21)$$

Note that we treat f as a function of y because it varies with latitude, i.e.:

$$f = 2\Omega sin(\theta) = 2\Omega sin(\frac{y}{R_e}) \approx f_0 + \beta y$$

Furthermore, because f does not vary in time or in x, we can re-write the equation thus:

$$\frac{d_H}{dt}(\zeta + f) = -(f+\zeta)(\frac{\partial}{\partial x}u + \frac{\partial}{\partial y}v) \qquad (3.22)$$

This is the shallow water *vorticity equation* in its Lagrangian form. This states that the *absolute vorticity* (the sum of ζ and f) on a parcel can only change if there is horizontal divergence.

Notice the Coriolis parameter, f, is on equal footing with the vorticity. Thus we refer to f as the "planetary" vorticity, and ζ the "relative" vorticity. The planetary vorticity comes about because the Earth is rotating, as explored in one of the exercises.

3.2.3 Kelvin's theorem

The absolute vorticity is not conserved following fluid parcels, because it will increase or decrease in regions with convergent or divergent flow. But we can obtain a conserved quantity if we use the fact that horizontal divergence is linked to the parcel area, via eq. (3.18). Combining this with the vorticity equation (3.22), we have:

$$\frac{d_H}{dt}(\zeta + f) = -\frac{f+\zeta}{A}\frac{d_H A}{dt} \tag{3.23}$$

Re-arranging, we get:

$$\frac{d_H}{dt}[(\zeta + f)A] = 0 \tag{3.24}$$

This is *Kelvin's circulation theorem*. The product of the absolute vorticity and the parcel area is conserved following the motion, in the absence of friction. This is a powerful result, and it helps us understand how vorticity changes with latitude and with the parcel area. Specifically, if a parcel moves to a different latitude or is compressed, so that its area changes, the vorticity must adjust so that:

$$[(\zeta + f)A] = const.$$

This is a fundamental result in rotating fluid dynamics, first derived by Lord Kelvin.

3.2.4 Potential vorticity

More often though, we use a different conserved quantity. This results from combining the conservation of volume with Kelvin's theorem. Specifically, since $V = AD$ is conserved following the motion, then:

$$\frac{d_H}{dt}\left(\frac{\zeta + f}{D}\right) = 0 \tag{3.25}$$

follows immediately from Kelvin's theorem. Here again $D = H + \eta$ is the total depth of the fluid.

The ratio of the absolute vorticity and the fluid depth is called the *potential vorticity* (PV). This is of fundamental importance in geophysical fluid dynamics. It is closely related to a more general quantity derived originally by Ertel (1942) and bearing his name ("the Ertel potential vorticity"). There are numerous examples of how PV conservation affects motion in rotating fluids.

An example is shown in Fig. (3.2). A cylinder of fluid is shown at the left, with zero vorticity. It moves to the right (as a cylinder, because there is no vertical shear), up over the hill. As it gets shorter, the relative vorticity must decrease because D is decreasing. So the vortex becomes anticyclonic over the hill. This effect is seen in the atmosphere, when air moves over a mountain range (sec. 4.8)—the compression of the fluid column generates negative vorticity.

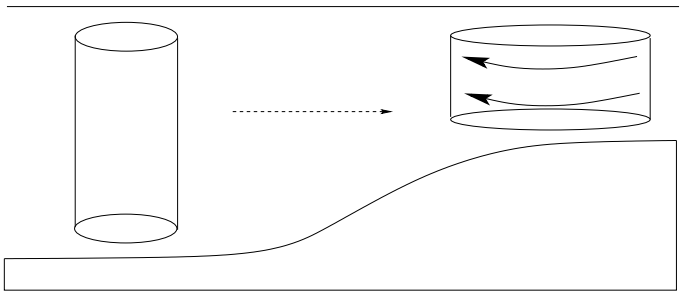

Figure 3.2: An example of the conservation of potential vorticity. The fluid column at left, with no vorticity initially, is "squashed" as it moves up over the hill, thereby acquiring negative vorticity.

3.3 Integral conserved quantities

There are additional conservation statements which apply in a volume-integrated sense. In this case, a quantity might vary locally, but when integrated over an entire region, like an enclosed basin, the quantity is conserved in the absence of forcing or dissipation.

The region can have any shape. Let's assume that it has a boundary curve which we denote Γ. The only condition we will impose is that there be no flow through this boundary, i.e.

$$\vec{u} \cdot \hat{n} = 0 \qquad on \quad \Gamma$$

This would be the case, for example, in an ocean basin or an enclosed sea. In fact, the same conservations statements will apply in *periodic* domains, i.e. domains which wrap around (like the atmosphere in the x-direction). For simplicity though, we'll focus here on the no-normal flow case.

3.3.1 Mass

The simplest example is that the total mass is conserved in the basin. Integrating the continuity equation (3.15) over the area enclosed by Γ, we

get:

$$\frac{\partial}{\partial t}\iint \eta\, dA + \iint \nabla \cdot [\vec{u}_H(\eta + H)]\, dA = 0 \tag{3.26}$$

The second term can be re-written using Gauss' theorem:

$$\iint \nabla \cdot [\vec{u}_H(\eta + H)]\, dA = \oint (\eta + H)\, \vec{u}_H \cdot \hat{n}\, dl = 0$$

This vanishes because of no-normal flow on Γ.

So the area-integrated surface height vanishes. This means positive surface deviations in one region of the basin must be offset by negative deviations in other regions.

3.3.2 Circulation

Now consider the integral of the Eulerian version of the vorticity equation (3.22):

$$\iint \frac{\partial}{\partial t}(\zeta + f)\, dA + \iint \nabla \cdot (\vec{u}_H(f + \zeta))\, dA = 0 \tag{3.27}$$

Again the second term vanishes following application of Gauss' theorem:

$$\iint \nabla \cdot (\vec{u}_H(f + \zeta))\, dA = \oint (f + \zeta)\, \vec{u} \cdot \hat{n}\, dl = 0$$

So the *absolute circulation*, the integrated absolute vorticity, is conserved in the basin:

$$\frac{\partial}{\partial t}\iint (\zeta + f)\, dA = 0 \tag{3.28}$$

This is just the basin-average version of Kelvin's circulation theorem of section (3.2.3).

Because f doesn't vary in time, this also implies:

$$\frac{\partial}{\partial t}\iint \zeta \, dA = \frac{\partial}{\partial t}\iint \nabla \times \vec{u} \, dA = 0 \tag{3.29}$$

If we now use Stokes' theorem, we can write:

$$\frac{\partial}{\partial t}\oint \vec{u} \cdot d\vec{l} = 0 \tag{3.30}$$

This is the total circulation in the basin. It is also constant in the absence of forcing.

3.3.3 Energy

In addition, the total energy is conserved. If we take the dot product of the momentum equation with $\vec{u}$, we obtain:

$$\frac{\partial}{\partial t}\frac{1}{2}|\vec{u}|^2 + \vec{u} \cdot \nabla(\frac{1}{2}|\vec{u}|^2) = -g\vec{u} \cdot \nabla\eta \tag{3.31}$$

The first term is the time change of the kinetic energy:

$$K \equiv \frac{1}{2}(u^2 + v^2) = \frac{1}{2}|\vec{u}|^2$$

So the kinetic energy changes locally due to the advection of kinetic energy and also when the pressure gradients are correlated with the velocity (the so-called pressure-work term). Note that the Coriolis force has dropped out, because it acts perpendicular to the velocity:

$$\vec{u} \cdot (f\hat{k} \times \vec{u}) = 0 \tag{3.32}$$

As such, the Coriolis force *does no work* on the flow. It just affects the direction of the flow.

Rearranging the kinetic energy equation and multiplying by the total depth, D, we get:

$$\frac{\partial}{\partial t}DK + D\vec{u} \cdot \nabla(K + g\eta) = 0 \tag{3.33}$$

Now if we multiply the shallow water continuity equation (3.15) by $(K + g\eta)$, we get:

$$(K + g\eta)\frac{\partial}{\partial t}\eta + (K + g\eta)\nabla \cdot (D\vec{u}) = 0 \tag{3.34}$$

Adding the two equations together (and noting that $\frac{\partial}{\partial t}D = \frac{\partial}{\partial t}\eta$), we have:

$$\frac{\partial}{\partial t}(DK + P) + \nabla \cdot [D\vec{u}(K + g\eta)] = 0 \tag{3.35}$$

where:

$$P = \frac{1}{2}g\eta^2$$

is the potential energy. Equation (3.35) states that the total energy changes locally by the flux divergence term. If we integrate this over the basin, the latter vanishes so that:

$$\frac{\partial}{\partial t}\iint (DK + P)\, dA = 0 \tag{3.36}$$

So the total energy is conserved (in the absence of forcing and friction).

3.4 Linear shallow water equations

The shallow water equations (3.13, 3.14, 3.15) are nonlinear—each has terms which involve products of the unknowns u, v and η—and as such, they are difficult to solve analytically. However, solutions are possible if we linearize the equations.

To do this, we make several additional assumptions. First, the height deviations are assumed to be much smaller than the stationary (non-changing) water depth, i.e.

$$|\eta| \ll H(x, y)$$

Then the nonlinear terms in the continuity equation (3.15) are removed. The assumption is reasonable e.g. in the deep ocean, where the depth is of order 5 km while the height deviations are typically less than 1 meter.

Second, we assume the temporal changes in the velocity are greater than those due to advection, or

$$\frac{U}{T} \gg \frac{U^2}{L}$$

which implies that

$$T \ll \frac{L}{U}$$

So the time scales are short compared to the *advective time scale*, L/U. Note that this can nearly always be achieved by assuming the velocities are weak enough. If the lateral scale is 100 km and the velocity scale is 10 cm/sec, the time scale must be less than 10^6 sec, or about 10 days. Longer time scales require weaker velocities and/or larger scales.

Making these approximations, the linear shallow water equations are:

$$\frac{\partial}{\partial t}u - fv = -g\frac{\partial}{\partial x}\eta \tag{3.37}$$

$$\frac{\partial}{\partial t}v + fu = -g\frac{\partial}{\partial y}\eta \tag{3.38}$$

$$\frac{\partial}{\partial t}\eta + \frac{\partial}{\partial x}(Hu) + \frac{\partial}{\partial y}(Hv) = 0 \tag{3.39}$$

Note that H remains in the parentheses in (3.39) because the bottom depth can vary in space, i.e. $H = H(x, y)$.

Linearizing is really a matter of convenience. We make the assumptions necessary to omit the nonlinear terms. Nevertheless, many observed phenomena—like gravity waves—are often nearly linear.

Because the equations are linear, we can solve them. In fact, these constitute the *Laplace Tidal Equations*, which we solve numerically when forecasting the tides. The equations can be reduced to a single equation, as shown in Appendix (6.2). But we'll focus on several special cases in the following sections.

3.5 Gravity waves

The solutions discussed hereafter are arranged in order of increasing scale of motion. At the smallest scales, for instance on scales of meters, the earth's rotation is unimportant and we can neglect the Coriolis acceleration. For simplicity, we'll also neglect topographic variations and take H to be constant. Then the equations are:

$$\frac{\partial}{\partial t}u = -g\frac{\partial}{\partial x}\eta \tag{3.40}$$

$$\frac{\partial}{\partial t}v = -g\frac{\partial}{\partial y}\eta \tag{3.41}$$

$$\frac{\partial}{\partial t}\eta + H\frac{\partial}{\partial x}u + H\frac{\partial}{\partial y}v = 0 \tag{3.42}$$

Acceleration occurs solely in response to pressure gradients, due to deviations in the surface height.

We can reduce the equations to a single one for η if we take a time derivative of the continuity equation:

$$\frac{\partial^2}{\partial t^2}\eta + H\frac{\partial}{\partial x}(\frac{\partial}{\partial t}u) + H\frac{\partial}{\partial y}(\frac{\partial}{\partial t}v) \tag{3.43}$$

$$= \frac{\partial^2}{\partial t^2}\eta - gH\frac{\partial^2}{\partial x^2}\eta - gH\frac{\partial^2}{\partial y^2}\eta \tag{3.44}$$

$$\frac{\partial^2}{\partial t^2}\eta - c_0^2\nabla^2\eta = 0 \tag{3.45}$$

after substituting in from the momentum equations. This is a second-order wave equation and straightforward to solve.

To obtain a solution, we can use a Fourier representation of the surface height:

$$\eta(x,y,t) = \iiint_{-\infty}^{\infty} \hat{\eta}(k,l,\omega)\, e^{ikx+ily-i\omega t}\, dk\, dl\, d\omega$$

(see Appendix 6.3). Here, k and l are *wavenumbers*. They are related to the wavelength, as follows. The total wavenumber is $\kappa = \sqrt{k^2+l^2}$. Then the wavelength is given by:

$$\lambda = \frac{2\pi}{\kappa} \tag{3.46}$$

The constant ω is the *frequency*. This is related to the *period* of the wave, which is like a wavelength in time:

$$T = \frac{2\pi}{\omega} \tag{3.47}$$

Since the wave equation is linear, we can study the response for a single Fourier mode. This is because linear equations allow a superposition of solutions. Thus we write:

$$\eta = Re\{\hat{\eta}(k, l, \omega)\, e^{ikx+ily-i\omega t}\}$$

The $Re\{\}$ operator implies taking the real part. Thus, for example:

$$Re\{e^{i\theta}\} = cos(\theta)$$

Substituting the wave solution into equation (3.45), we get:

$$(-\omega^2 + c_0^2\kappa^2)\, \hat{\eta} e^{ikx+ily-i\omega t} = 0 \tag{3.48}$$

where $\kappa \equiv (k^2 + l^2)^{1/2}$ is the modulus of the wavevector. So either $\hat{\eta} = 0$, in which case we have no solution at all, or:

$$\omega = \pm c_0\, \kappa \tag{3.49}$$

Thus there is a special relation between the wave's frequency and its wavenumber. Equation (3.49) is the gravity wave *dispersion relation*. It shows that short wavelength (large wavenumber) waves have higher frequencies. Short gravity waves have shorter periods than long waves.

How quickly do the waves move? Consider the wave solution in (x, t) (ignoring variations in y):

$$\eta = Re\{\hat{\eta}(k,\omega)\, e^{ikx - i\omega t}\} = Re\{\hat{\eta}(k,\omega)\, e^{i\theta}\}$$

where

$$\theta = kx - \omega t$$

is the *phase* of the wave. For simplicity, let's take $\hat{\eta}(k,\omega) = 1$. Then we have:

$$\eta = cos(\theta)$$

Consider a crest of the wave, for example at $\theta = 2\pi$. This moves, because θ is a function of time. Its position is given by:

$$\theta = 2\pi = kx - \omega t$$

Solving for the position, x, we get:

$$x = \frac{2\pi}{k} + \frac{\omega}{k}t$$

So if ω and k are both positive, the crest progresses to the right, toward larger x. The rate at which it moves is given by:

$$\frac{dx}{dt} = c = \frac{\omega}{k} \tag{3.50}$$

This is the *phase speed* of the wave.

From the dispersion relation, we see that:

$$c = \pm c_0 = \pm\sqrt{gH} \tag{3.51}$$

So the waves can propagate to the left or the right. Moreover, *all waves propagate at the same speed*, regardless of the wavelength. We say then that the waves are "non-dispersive", because an initial disturbance, which

is generally composed of different wavelengths, will not separate into long and short waves. Any initial condition will produce waves moving with speed c_0.

Consider the wave equation in one dimension:

$$\frac{\partial^2}{\partial t^2}\eta - c_0^2\frac{\partial^2}{\partial x^2}\eta = 0 \tag{3.52}$$

All solutions to this equation have the form:

$$\eta = F_l(x + c_0 t) + F_r(x - c_0 t)$$

because, substituting into (3.52) yields:

$$c_0^2(F_l'' + F_r'') - c_0^2(F_l'' + F_r'') = 0$$

where the prime indicates differentiation with respect to the argument of the function. The function F_l represents a wave which propagates to the left, towards negative x, while F_r propagates to the right. It doesn't matter what F_l and F_r look like—they can be sinusoidal or top-hat shaped. But all propagate with a phase speed c_0.

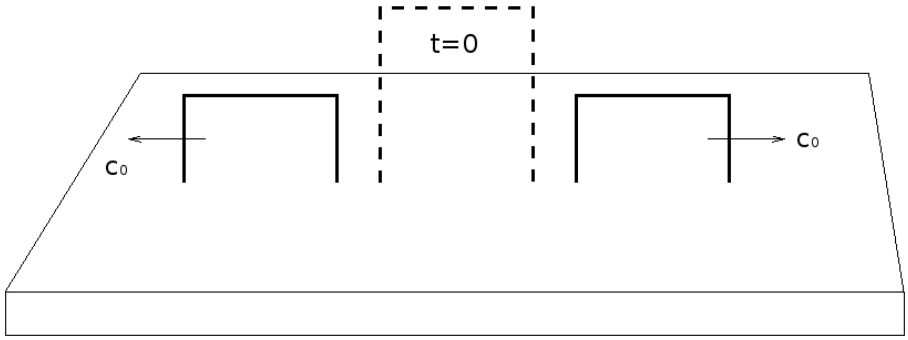

Figure 3.3: An surface height anomaly with a "top hat" distribution. The anomaly splits into two equal anomalies, one propagating left and one going right, both at the gravity wave speed, c_0.

Because there are two unknown functions, we require two sets of conditions to determine the full solution. For instance, consider the case when

$$\eta(t=0) = \mathcal{F}(x), \quad \frac{\partial}{\partial t}\eta(t=0) = 0$$

This means the height has a certain shape at $t = 0$, for example a top hat shape (Fig. 3.3), and the initial wave is not moving. Then we must have:

$$F_l = F_r = \frac{1}{2}\mathcal{F}(x)$$

So the disturbance splits in two, with half propagating to the left and half to the right, both moving with speed c_0.

3.6 Gravity waves with rotation

Now let's see what happens at larger scales, where rotation is important. We don't yet know how large the scales are for this to happen, but we'll find out along the way. The linear equations are now:

$$\frac{\partial}{\partial t}u - fv = -g\frac{\partial}{\partial x}\eta \tag{3.53}$$

$$\frac{\partial}{\partial t}v + fu = -g\frac{\partial}{\partial y}\eta \tag{3.54}$$

$$\frac{\partial}{\partial t}\eta + H\frac{\partial}{\partial x}u + H\frac{\partial}{\partial y}v = 0 \tag{3.55}$$

Notice we've left H as a constant. Again, this is only for convenience—it's much harder to solve the problem with variable topography.

The equations can again be reduced to a single one in η. This is most easily done if we ignore variations in the y direction, and consider one dimensional waves. Then the equations are:

$$\frac{\partial}{\partial t}u - fv = -g\frac{\partial}{\partial x}\eta \tag{3.56}$$

$$\frac{\partial}{\partial t}v + fu = 0 \tag{3.57}$$

$$\frac{\partial}{\partial t}\eta + H\frac{\partial}{\partial x}u = 0 \tag{3.58}$$

Notice the acceleration in v is now due solely to the Coriolis force, as in the case of inertial oscillations (sec. 2.2.3). We can eliminate v if we take a time derivative of the first equation and substitute in the second equation:

$$\frac{\partial^2}{\partial t^2}u + f^2 u = -g\frac{\partial}{\partial x}(\frac{\partial}{\partial t}\eta) \tag{3.59}$$

Taking an x derivative of this and substituting in from the continuity equation yields:

$$\frac{\partial}{\partial t}[(\frac{\partial^2}{\partial t^2} + f_0^2)\,\eta - c_0^2\,\frac{\partial^2}{\partial x^2}\eta] = 0 \tag{3.60}$$

This is the wave equation with rotation, in one dimension.

Notice the equation has three time derivatives. As such, it admits three solutions. One is a *steady* solution in which η does not vary with time; in other words, if $\eta = \eta(x, y)$, equation (3.60) is trivially satisfied. This solution is considered in section (3.7).

The portion of the equation in the brackets is similar to the gravity wave equation, except for the additional f_0^2 term. We can solve this using wave solution for η, as before. The result is:

$$\omega = \pm\sqrt{(f_0^2 + c_0^2\kappa^2)} \tag{3.61}$$

This is the dispersion relation for "Poincaré waves", which are gravity

waves with rotation. For large wavenumbers (small waves), this is approximately:

$$\omega = \pm c_0 \kappa \tag{3.62}$$

which is the same as the dispersion relation for non-rotating gravity waves. However, in the other limit, as $\kappa \to 0$, the relation is:

$$\omega = \pm f_0 \tag{3.63}$$

So the frequency asymptotes to f_0 for large waves. Thus the period is proportional to the inverse of the Coriolis parameter—it is longer at low latitudes and shorter at high.

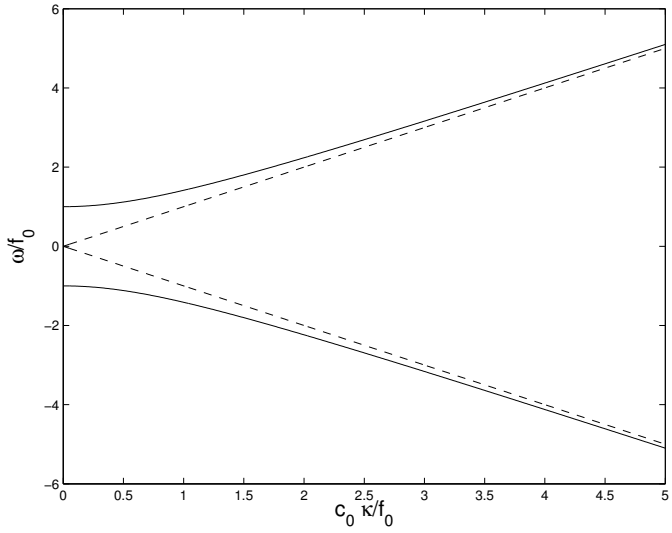

Figure 3.4: The gravity wave dispersion relations for non-rotating (dashed) and constant rotation (solid) cases. Note the frequency and wavenumber have been normalized.

We plot the non-rotating and rotating dispersion relations in Fig. (3.4). The two relations are similar when:

$$\lambda = \frac{2\pi}{\kappa} \ll \frac{\sqrt{gH}}{f_0} \equiv L_D \tag{3.64}$$

The scale, L_D, is called the Rossby *deformation radius*.[2] At wavelengths small compared to the deformation radius, the waves don't "feel" the earth's rotation.

At scales larger than the deformation radius, the frequency asymptotes to f_0. In this case, the pressure gradient terms in the momentum equations are unimportant. These are the inertial oscillations discussed in sec. (2.2.3).

We defined the phase speed as the ratio of the frequency to the wave number. As we saw, non-rotating gravity waves have the same phase speed regardless of their wavenumber and are thus non-dispersive. Rotation causes the gravity waves to disperse. The phase speed is:

$$c_x = \frac{\omega}{k} = \pm\frac{\sqrt{f_0^2 + c_0^2 k^2}}{k} = \pm c_0\sqrt{1 + (\frac{f_0}{c_0 k})^2} \tag{3.65}$$

In the short wave (large k) limit, the waves are approximately non-dispersive and traveling at speed, $\pm c_0$. But the larger waves propagate faster. So an arbitrary initial disturbance will break into sinusoidal components, with the larger wavelengths moving away fastest.

As noted, rotation becomes important at scales larger than the deformation radius. But how big is the deformation radius? Using typical values and a latitude of 45 degrees, the deformation radius is:

$$\frac{\sqrt{gH}}{f_0} \approx \frac{\sqrt{10 * 4000}}{10^{-4}} = 2000\ km$$

which is a rather large scale, corresponding to about 20 degrees of latitude. At such scales, our assumption of a constant Coriolis parameter is certainly not correct. Indeed, a more proper treatment of the large wave limit in

[2] More correctly, this is the barotropic or "external" deformation radius. Later we'll see the baroclinic deformation radius.

such deep water would have to take the variation of f into account. Of course if the depth is less, the deformation radius is smaller; this is the case for example in bays and shallow seas. We examine what happens with a variable f in Chapter (4).

3.7 Steady flow

The linear shallow water equation with rotation (eq. 3.60) admits three solutions; two are propagating waves and one is independent of time. We refer to the latter is a "steady" solution. Setting the time derivatives in the momentum equations (eqs. 3.37-3.38) to zero, we get:

$$-fv = -g\frac{\partial}{\partial x}\eta \tag{3.66}$$

$$+fu = -g\frac{\partial}{\partial y}\eta \tag{3.67}$$

Thus a steady, linear flow in shallow water is *in geostrophic balance*. We often refer to this as a "balanced state". As seen in the next section, any flow which remains, after the gravity waves have propagated away, must be a balanced one.

3.8 Geostrophic adjustment

The relaxation to a geostrophic flow is a central phenomenon in the atmosphere and ocean. An initially unbalanced flow will radiate gravity waves until it is back in balance. Interestingly, the final state can be predicted without detailed knowledge of the waves. To illustrate this, we consider an initial value problem, first without and then with rotation.

We'll stick with the one-dimensional problem, for simplicity. Assume the initial sea surface has a front (a discontinuity) at $x = 0$:

$$\eta(x, t = 0) = \eta_0 \, sgn(x)$$

where the $sgn(x)$ function is 1 if $x > 0$ and and -1 if $x < 0$ (Fig. 3.5). This could represent, for example, the initial sea surface deviation generated by an earthquake. Without rotation, the solution follows from section (3.5):

$$\eta(x, t) = \frac{\eta_0}{2} sgn(x - c_0 t) + \frac{\eta_0}{2} sgn(x + c_0 t)$$

The discontinuity splits into two fronts, one propagating to the left and one to the right (Fig.3.5). The height in the wake of the two fronts is zero (since 1 + (-1) =0). There is no motion here.

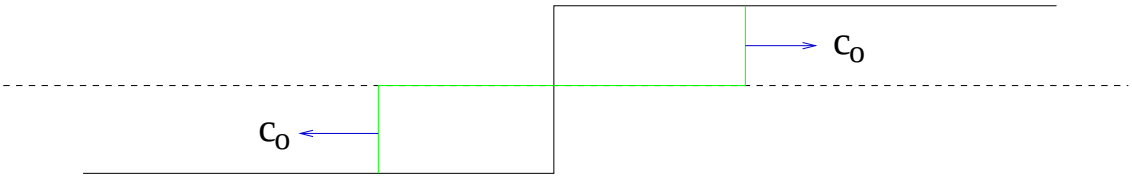

Figure 3.5: The evolution of a sea surface discontinuity in the absence of rotation.

The case with rotation is different. As noted in section (3.2.4), shallow water flows must conserve potential vorticity in the absence of forcing. This will in fact not allow a flat final state. If the PV is conserved, then from (3.25) we have:

$$\frac{\zeta + f_0}{H + \eta} = const.$$

Let's assume there is no motion in the initial state. Then we have:

$$\frac{f_0}{H + \eta_0 sgn(x)} = \frac{v_x + f_0}{H + \eta} \tag{3.68}$$

where $v_x = \frac{\partial}{\partial x} v$ (the vorticity is just v_x because the front is one-dimensional). The initial PV is on the left and final PV on the right. If the final state is flat and motionless, this would be:

$$\frac{f_0}{H + \eta_0 sgn(x)} = \frac{f_0}{H} \tag{3.69}$$

This can only work if $\eta_0 = 0$, i.e. if the initial state is also flat and motionless—not a very interesting problem!

But assume the final state isn't flat. We can use the PV to solve for η. Cross-multiplying (3.68), cancelling like terms and re-arranging, we get:

$$\left[H + \eta_0 sgn(x)\right] v_x - f_0 \eta = -f_0 \eta_0 sgn(x) \tag{3.70}$$

To be consistent with the linearization of the equations, we can assume the initial interface displacement is much smaller than the total depth, i.e. $|\eta_0| \ll H$. So we have:

$$H v_x - f_0 \eta = -f_0 \eta_0 sgn(x) \tag{3.71}$$

The final surface height will have some shape, but it does not change in time. As noted in sec. (3.7), the final state is in geostrophic balance:

$$f_0 v = g \eta_x \tag{3.72}$$

Thus the tilted surface height has an associated flow into the page (perpendicular to the initial front). Substituting into (3.71), we get:

$$\eta_{xx} - \frac{1}{L_D^2} \eta = -\frac{\eta_0}{L_D^2} sgn(x) \tag{3.73}$$

where again, $L_D = \sqrt{gH}/f_0$ is the deformation radius.

Equation (3.73) is an ordinary differential equation. We will solve it separately for $x > 0$ and $x < 0$. For $x > 0$, we have:

$$\eta_{xx} - \frac{1}{L_D^2}\eta = -\frac{\eta_0}{L_D^2} \tag{3.74}$$

The solution for this which decays as $x \to \infty$ is:

$$\eta = A\, exp(-x/L_D) + \eta_0 \tag{3.75}$$

The corresponding solution for $x < 0$ which decays as $x \to -\infty$ is:

$$\eta = B\, exp(x/L_D) - \eta_0 \tag{3.76}$$

We thus have two unknowns, A and B. We find them by matching η and η_x at $x = 0$—that way the height and the velocity, v, will be continuous at $x = 0$. The result is:

$$\begin{aligned} \eta &= \eta_0\,(1 - exp(-\frac{x}{L_D})) \quad x \geq 0 \\ &= -\eta_0\,(1 - exp(\frac{x}{L_D})) \quad x < 0 \end{aligned} \tag{3.77}$$

The final state is plotted in Fig. (3.6). Without rotation, the final state was flat, with no motion. With rotation, the initial front slumps, but does not vanish. Associated with this tilted height is a meridional jet, centered at $x = 0$:

$$v = \frac{g\eta_0}{f_0 L_D}\, exp(-\frac{|x|}{L_D}) \tag{3.78}$$

The flow is directed into the page. Thus the tilted interface is supported by the Coriolis force acting on a meridional jet.

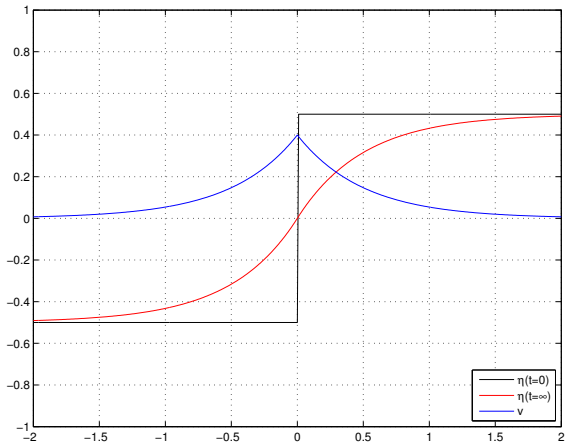

Figure 3.6: The sea surface height after geostrophic adjustment, beginning with a discontinuity, with rotation. The red curve shows the final interface shape and the blue curve the meridional velocity, v.

How does the system adjust from the initial front to the final jet? Notice that we figured out what the final interface looks like without considering gravity waves at all! We only used the conservation of PV. However, gravity waves are important. When the initial front slumps, gravity waves radiate away, to plus and minus infinity. Just enough waves are shed to adjust the interface height to its final state. So the waves *mediate* the geostrophic adjustment.

This example can be used to infer what would happen with a "top hat" distribution, discussed in sec. (3.5). This has two fronts, one on either side (Fig. 3.7). Each would relax to an exponential, with accompanying meridional flow. The result would be a structure with clockwise circulation, like a high pressure system.

3.9 Kelvin waves

So far we have examined wave properties without worrying about boundaries. Boundaries can cause waves to reflect, changing their direction of

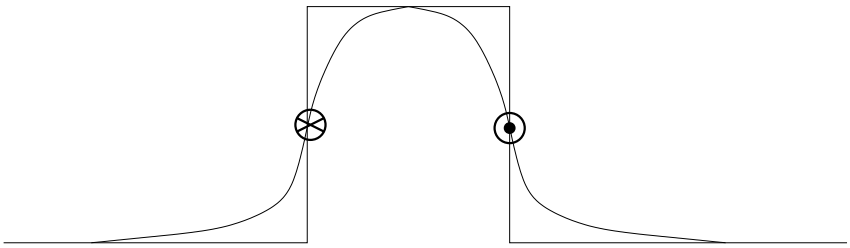

Figure 3.7: The adjustment of an initial top hat distribution. The circles indicate the meridional velocity, which has a clockwise orientation.

propagation. But in the presence of rotation, boundaries can also support gravity waves which are *trapped* there; these are called Kelvin waves.

The simplest example of a Kelvin wave occurs with an infinitely long wall. Let's assume this is parallel to the x-axis and lies at $y = 0$. The wall permits no normal flow, so we have $v = 0$ at $y = 0$. In fact, we will seek solutions which have $v = 0$ everywhere. We start with the linearized shallow water equations (3.37-3.39) and set $v = 0$:

$$\frac{\partial}{\partial t}u = -g\frac{\partial}{\partial x}\eta \tag{3.79}$$

$$f_0 u = -g\frac{\partial}{\partial y}\eta \tag{3.80}$$

$$\frac{\partial}{\partial t}\eta + \frac{\partial}{\partial x}Hu = 0 \tag{3.81}$$

An equation for η can be derived with only the x-momentum and continuity equations:

$$\frac{\partial^2}{\partial t^2}\eta - c_0^2\frac{\partial^2}{\partial x^2}\eta = 0 \tag{3.82}$$

Notice this is just the linearized shallow water equation in one dimension *without* rotation. Indeed, rotation drops out of the x-momentum equation because $v = 0$. So we expect that Kelvin waves will be non-dispersive

and propagate with a phase speed, c_0. Furthermore, from section (3.5), we know the general solution to equation (3.82) involves two waves, one propagating towards negative x and one towards positive x:

$$\eta(x, y, t) = F_l(x + c_0 t, y) + F_r(x - c_0 t, y)$$

We allow for structure in the y-direction and this remains to be determined.

This is where rotation enters. From the x-momentum equation, (3.79), we deduce that the velocity component parallel to the wall has the following form:[3]

$$u = -\frac{g}{c_0}(F_l - F_r)$$

Substituting this into the y-momentum equation, (3.80), and equating the terms involving F_l and F_r (which must be satisfied independently), we obtain:

$$\frac{\partial}{\partial y}F_l = \frac{f_0}{c_0}F_l, \quad \frac{\partial}{\partial y}F_r = -\frac{f_0}{c_0}F_r$$

The solutions are exponentials, with an e-folding scale of $\sqrt{gH}/f = L_D$, the deformation radius:

$$F_l \propto exp(y/L_D), \quad F_r \propto exp(-y/L_D)$$

We choose the solution which decays away from the wall (the one that is trapped there) rather than one which grows indefinitely. Which solution to choose depends on the where the wall is. If the ocean lies south of the wall, then the only solution decaying (in the negative y-direction) is F_l. If the ocean lies north of the wall, only F_r is decaying. Thus in both cases

[3] You can see this by assuming that $u = aF_l + bF_r$ and substituing into equation (3.79).

the Kelvin wave propagates at the gravity wave speed with the wall *to its right*.

Note that the decay is also affected by the sign of f. If we are in the southern hemisphere, where $f < 0$, the Kelvin waves necessarily propagate with the wall to their left.

3.10 Equatorial Kelvin waves

Kelvin waves also occur at the equator, where f vanishes. To consider this case, we use the β-plane approximation (2.3) centered on the equator, so that $f_0 = 0$. Thus:

$$f = \beta y \tag{3.83}$$

Assuming there is no flow perpendicular to the equator ($v = 0$), the linearized shallow water equations are:

$$\frac{\partial}{\partial t} u = -g \frac{\partial}{\partial x} \eta \tag{3.84}$$

$$\beta y u = -g \frac{\partial}{\partial y} \eta \tag{3.85}$$

$$\frac{\partial}{\partial t} \eta + \frac{\partial}{\partial x} H u = 0 \tag{3.86}$$

The first and third equations are the same as previously, and yield the non-rotating gravity wave equation:

$$\frac{\partial^2}{\partial t^2} \eta - c_0^2 \frac{\partial^2}{\partial x^2} \eta = 0 \tag{3.87}$$

So again, the surface height can be expressed in terms of left-going and right-going solutions:

$$\eta(x, y, t) = F_l(x + c_0 t, y) + F_r(x - c_0 t, y)$$

and as before, the velocity, u, can be written:

$$u = -\frac{g}{c_0}(F_l - F_r)$$

Plugging this into the second equation yields:

$$\frac{\partial}{\partial y} F_l = \frac{\beta y}{c_0} F_l, \quad \frac{\partial}{\partial y} F_r = -\frac{\beta y}{c_0} F_r$$

The solutions in this case are Gaussian functions:

$$F_l \propto exp(y^2/L_B^2), \quad F_r \propto exp(-y^2/L_B^2)$$

where:

$$L_B = (\frac{2c_0}{\beta})^{1/2}$$

Notice that we require a solution which decays *both* towards to the north and the south, moving away from the equator. The leftward solution grows away from the equator, so we reject it. The rightward solution on the other hand decays for large positive or negative y, and thus is the one we're after. The solution also implies a scale, of L_B. This is approximately:

$$L_B \approx (\frac{2(200)}{2 \times 10^{-11}})^{1/2} \approx 4500\,\text{km}$$

Equatorial Kelvin waves exist in both the atmosphere and ocean. In the ocean, the waves are an important part of the adjustment process which occurs prior to an El Nino.

3.11 *Exercises*

3.1. The surface pressure in the atmosphere is due to the weight of all the air in the atmospheric column above the surface. Use the hydrostatic relation to estimate how large the surface pressure is. Assume that the atmospheric density decays exponentially with height:

$$\rho(z) = \rho_s \, exp(-z/H)$$

where $\rho_s = 1.2\, kg/m^3$ and the scale height, $H = 8.6$ km. Assume too that the pressure at $z = \infty$ is zero.

3.2. Planetary vorticity. Imagine looking down on the North Pole. The earth spinning in *solid body rotation*, because every point is rotating with the same frequency, 2π rad/day. This implies that the azimuthal velocity at any point is just Ωr. Write the vorticity in cylindrical coordinates. For a solid body rotating at a frequency ω, $v_r = 0$ and $v_\theta = \omega r$. Use this to show that $\zeta = 2\Omega$.

The analogy carries over to a local region, centered at latitude θ, where the vertical component of the rotation is $2\Omega sin(\theta)$, the planet's vorticity at this latitude.

3.3. Let $\eta = 0$. Imagine a column of fluid at 30N, with H=200 m and with no vorticity. That column is moved north, to 60N, where the depth is 300 m. What is the final vorticity of the column?

3.4. Imagine that a fluid parcel is moving into a region where there is a constant horizontal divergence, i.e.:

$$\frac{\partial}{\partial x}u + \frac{\partial}{\partial y}v = D = \text{const.} \tag{3.88}$$

Solve the vorticity equation, assuming $D > 0$. What can you conclude about the parcel's vorticity at long times? Now consider $D < 0$ (convergent flow). What happens? Consider two cases, one where the absolute vorticity is initially positive and a second where it is negative. Note that the storm initially should have a small Rossby number.

3.5. Consider again a region where the horizontal divergence is constant and equal to - 0.5 day^{-1}. Use the vorticity equation to deduce what the vorticity on a parcel will be after 2 days if:

a) $\zeta(t = 0) = f/2$

b) $\zeta(t = 0) = -f/2$

c) $\zeta(t = 0) = -2f$

Are these reasonable values of vorticity? Explain why or why not.

3.6. Consider waves near a beach. What is a typical length scale? If the velocity associated with the waves is on the order of 10 cm/sec, how short does the wave period have to be to justify the linearity assumption? Is it reasonable to consider the waves to be linear?

3.7. A wave has the form:

$$\eta = Asin(6.28x - 3.14y - \omega t) \tag{3.89}$$

What is the wavelength in the x-direction? In the y-direction? What is the frequency is the wave is in 100 m of water? What is the phase velocity in the x-direction?

Calculate the u velocity associated with the wave. If the maximum velocity is 10 cm/sec, what is A?

3.8. A meteor strikes the surface of the ocean, causing a disturbance at the surface at $x = 0$. We'll model this as:

$$\eta(x,0) = -e^{-x^2}; \quad \frac{\partial}{\partial t}\eta(x,0) = 2c_0 x e^{-x^2} \tag{3.90}$$

Where is it safer to view the waves, at $x = L$ or $x = -L$ ($L \gg 1$)? You can neglect rotation.

3.9. Consider a wave with a wavelength of 10 km in a lake 200 m deep. How accurate would you be if you used the non-rotating phase speed, c_0, to estimate the wave's speed?

3.10. A meteor strikes the surface of the ocean again, causing a depression in the surface at $x = 0$. This time we will include rotation. The initial depression has the form:

$$\eta(x,0) = -Ae^{-c|x|} \tag{3.91}$$

What will the final, adjusted state be after the gravity waves have radiated away?

3.11. How does the radius of deformation vary with latitude? Calculate the radius of deformation using the depth of a typical bathtub. How large does the tub have to be in order for rotational effects to be important for waves on the surface?

3.12. Assume there is an initial elevation in sea surface height along a wall at $y = 0$ (the ocean lies south of the wall) with:

$$\eta(x,0) = exp(-x^2) \tag{3.92}$$

What is the solution at later times, if we are in the Southern Hemisphere? Compare to the solution in the non-rotating case.

Chapter 4

Synoptic scale barotropic flows

As noted in discussing Poincaré and Kelvin waves, the deformation radius, L_D, above which rotational effects are important in shallow water flows, is very large. So large, in fact, that we ought to take into account the variation of f as well. Doing this though introduces a number of interesting phenomena. From now on, we examine large scale flows with longer time scales. We will employ a modified set of equations, designed with these scales in mind.

4.1 The Quasi-geostrophic equations

The quasi-geostrophic system of equations was originally developed by Jules Charney, Arnt Eliassen and others for weather prediction. As suggested in the name, the equations pertain to motions which are nearly in geostrophic balance, i.e. for which the Rossby number is small. They pertain then to weather systems in the atmosphere and ocean eddies.

An advantage of the QG system is that it *filters out gravity waves*. This is similar in spirit to the geostrophic adjustment problem (sec. 3.8), where we derived the final state, in geostrophic balance, without taking account of the gravity waves which were radiated away. QG similiarly focuses

on the "slow modes" while ignoring the "fast modes". As such, the QG system can be used with a larger time step, when using numerical models.

The QG system is rigorously derived by a perturbation expansion in the Rossby number (see Pedlosky, 1987). But we will derive the main results heuristially. The primary assumptions are:

- The Rossby number, ϵ, is small
- $|\zeta|/f_0 = O|\epsilon|$
- $|\beta L|/f_0 = O|\epsilon|$
- $|h_b|/D_0 = O|\epsilon|$
- $|\eta|/D_0 = O|\epsilon|$

The expression $O|\epsilon|$ means "of the order of ϵ", i.e. roughly the same size as ϵ. Thus all the stated ratios are about as large as the Rossby number.

The second assumption follows from the first. If you note that the vorticity scales as U/L, then:

$$\frac{|\zeta|}{f_0} \propto \frac{U}{f_0 L} = \epsilon$$

Thus the relative vorticity is much smaller than f_0 if ϵ is small.

The third assumption says that the change in f over the domain is much less than f_0 itself. As noted in sec. (2.3), this implies the N-S extent of the domain is small compared to the Earth's radius (6600 km), at mid-latitudes. Also we assume we're not at the equator, where $f_0 = 0$.

The fourth and fifth assumptions imply the bottom topography and the surface elevation are both much less than the total depth. We write:

$$H = D_0 - h_b + \eta$$

where D_0 is the (constant) average depth in the fluid. Then both h_b and η are much smaller than D_0.

An important point here is that all the small terms are assumed to be roughly *the same size*. We don't take $|h_b|/D_0$ to scale like ϵ^2, for example. The reason we do this is that all these terms enter into the dynamics. If the topography were this week, it wouldn't affect the flow much.

Let's consider how these assumptions alter the shallow water vorticity equation (3.22):

$$\frac{d_H}{dt}(\zeta + f) = -(f + \zeta)(\frac{\partial}{\partial x}u + \frac{\partial}{\partial y}v) \tag{4.1}$$

With a small Rossby number, the velocities are nearly geostrophic, so we can replace the Lagrangian derivative thus:

$$\frac{d_H}{dt} \quad \rightarrow \quad \frac{\partial}{\partial t} + u_g\frac{\partial}{\partial x} + v_g\frac{\partial}{\partial y} \equiv \frac{d_g}{dt}$$

The new Lagrangian derivative then is following the geostrophic flow, rather than the total horizontal flow.

Similarly, the vorticity is replaced by its geostrophic counterpart:

$$\zeta \rightarrow \zeta_g$$

Thus the LHS of the equation becomes:

$$\frac{d_g}{dt}\zeta_g + \beta v_g$$

On the RHS, the term:

$$(f + \zeta) \rightarrow f_0$$

This is because:

$$(f + \zeta) = f_0 + \beta y + \zeta_g$$

and the two last terms are much smaller than f_0, by assumption.

Lastly, we have the horizontal divergence:

$$\frac{\partial}{\partial x}u + \frac{\partial}{\partial y}v = (\frac{\partial}{\partial x}u_g + \frac{\partial}{\partial y}v_g) + (\frac{\partial}{\partial x}u_a + \frac{\partial}{\partial y}v_a)$$

But the geostrophic velocities are non-divergent (sec. 2.4.1). So this is:

$$= \frac{\partial}{\partial x}u_a + \frac{\partial}{\partial y}v_a = -\frac{\partial}{\partial z}w$$

Collecting all the terms, we have:

$$(\frac{\partial}{\partial t} + u_g\frac{\partial}{\partial x} + v_g\frac{\partial}{\partial y})(\zeta_g + \beta y) = f_0\frac{\partial}{\partial z}w \tag{4.2}$$

This is the *quasi-geostrophic vorticity equation*. Though we used the shallow water vorticity equation to derive this, the exact same result is obtained for *baroclinic* flows, i.e. flows with vertical shear. The equation in has two unknowns. The geostrophic velocities and vorticity can be derived from the surface height, but there is also the vertical velocity. With baroclinic flows, this can be eliminated by using the QG density equation.

For shallow water flows though we can eliminate w by simply integrating (4.2) from the bottom to the surface:

$$\int_{-H}^{\eta} \frac{d_g}{dt}(\zeta_g + \beta y)\, dz = f_0(w(\eta) - w(-H)) \tag{4.3}$$

Because the horizontal velocities don't vary with height, they pass through the integral, so the LHS is simply:

$$(\eta + H)\frac{d_g}{dt}(\zeta_g + \beta y) = (\eta + D_0 - h_b)\frac{d_g}{dt}(\zeta_g + \beta y) \approx D_0 \frac{d_g}{dt}(\zeta_g + \beta y)$$

after using the last two assumptions above.

On the RHS, we have the vertical velocities at the upper and lower surface. Following the arguments in sec. (3.1.2), we can write:

$$w(\eta) = \frac{d}{dt}\eta \to \frac{d_g}{dt}\eta$$

and:

$$w(-H) = -\frac{d}{dt}H \to -\frac{d_g}{dt}(D_0 - h_b) = \frac{d_g}{dt}h_b$$

Collecting terms, the integrated vorticity equation becomes:

$$\frac{d_g}{dt}(\zeta_g + \beta y) = \frac{f_0}{D_0}[\frac{d_g}{dt}\eta - \frac{d_g}{dt}h_b]$$

or:

$$(\frac{\partial}{\partial t} + u_g\frac{\partial}{\partial x} + v_g\frac{\partial}{\partial y})(\zeta_g + \beta y - \frac{f_0}{D_0}\eta + \frac{f_0}{D_0}h_b) = 0 \tag{4.4}$$

This is the barotropic QG *potential vorticity equation*, without forcing. The great advantage of this is that it has only one unknown: the pressure. From the geostrophic relations, we have:

$$u_g = -\frac{g}{f_0}\frac{\partial}{\partial y}\eta\ , \quad v_g = \frac{g}{f_0}\frac{\partial}{\partial x}\eta \tag{4.5}$$

The relative vorticity can also be expressed solely in terms of the pressure:

$$\zeta_g = \frac{\partial}{\partial x}v - \frac{\partial}{\partial y}u = \frac{g}{f_0}\nabla^2\eta \tag{4.6}$$

We can simplify this somewhat by defining a *streamfunction*:

$$\psi = \frac{g\eta}{f_0} \tag{4.7}$$

Then we have:

$$u_g = -\frac{\partial}{\partial y}\psi, \qquad v_g = \frac{\partial}{\partial x}\psi, \qquad \zeta_g = \nabla^2\psi \tag{4.8}$$

Using these, the potential vorticity equation is:

$$(\frac{\partial}{\partial t} + u_g\frac{\partial}{\partial x} + v_g\frac{\partial}{\partial y})(\nabla^2\psi - \frac{f_0^2}{c_0^2}\psi + \beta y + \frac{f_0}{D_0}h_b) = 0 \tag{4.9}$$

with:

$$u_g = -\frac{\partial}{\partial y}\psi,\ v_g = \frac{\partial}{\partial x}\psi$$

Having a single equation with one unknown is an enormous simplification and is a major reason we use the quasi-geostrophic system for studying geophysical fluid dynamics.

Like the name suggests, the QGPV equation is closely related to the shallow water PV equation (sec. 3.2.4). In fact, we can derive the QGPV equation directly from the shallow water equation (3.25), under the assumptions given above. Replacing the velocities and vorticity with their geostrophic counterparts, the equation is:

$$\frac{d_g}{dt}\frac{\zeta_g + f_0 + \beta y}{D_0 + \eta - h_b} = 0 \tag{4.10}$$

With the assumptions above, the PV can be approximated:

$$\frac{\zeta_g + f_0 + \beta y}{D_0 + \eta - h_b} = \frac{f_0}{D_0}\left(\frac{1 + \zeta/f_0 + \beta y/f_0}{1 + \eta/D_0 - h_b/D_0}\right) \tag{4.11}$$

$$\approx \frac{f_0}{D_0}\left(1 + \frac{\zeta}{f_0} + \frac{\beta y}{f_0}\right)\left(1 - \frac{\eta}{D_0} + \frac{h_b}{D_0}\right) \tag{4.12}$$

$$\approx \frac{f_0}{D_0} + \frac{\zeta}{D_0} + \frac{\beta y}{D_0} - \frac{f_0 \eta}{D_0^2} + \frac{f_0 h_b}{D_0^2} \tag{4.13}$$

The last four terms are all order Rossby number compared to the first term. Moreover, the terms we've dropped involve the products of the small terms and are hence of order Rossby number squared. Substituting this into (4.10) yields:

$$\frac{d_g}{dt}\left(\zeta_g + \beta y - \frac{f_0}{D_0}\eta + \frac{f_0}{D_0}h_b\right) = 0 \tag{4.14}$$

after dropping the constant term, f_0/D_0, and multiplying through by the constant, D_0. This is just the QGPV equation (4.4) again.

4.1.1 The rigid lid assumption

Having a moveable free surface is obviously important for gravity waves, but it is less important for synoptic scale flows. Since we have filtered out the faster modes, by assuming the flows are geostrophically balanced, we no longer really require the moveable surface.

So replace it with a "rigid lid", a flat surface where the vertical velocity vanishes. It might seem that this would remove all flows in the barotropic system, but it doesn't—this is because the lid can support pressure differences in the fluid.

The changes with a rigid lid are relatively minor. First, we omit the second term in the potential vorticity in (4.9). So the PV is simply:

$$\zeta_g + \beta y + \frac{f_0}{D_0} h_b$$

Second, the streamfunction changes. By assuming a rigid lid, we are setting $\eta = 0$. However, the rigid lid can still support pressure anomalies. Thus $p(z = 0)$ doesn't vanish. As such it makes more sense to define the streamfunction in terms of the pressure:

$$\psi \equiv \frac{p}{\rho_c f_0} \tag{4.15}$$

4.2 Geostrophic contours

The conservation of PV following the motion is a strong constraint. The PV is comprised of a time-varying portion (the vorticity) and a time-independent part (due to β and the bottom topography). So we can rewrite equation (4.9) this way:

$$\frac{d_g}{dt} \nabla^2 \psi + \vec{u}_g \cdot \nabla q_s = 0 \tag{4.16}$$

where the function:

$$q_s \equiv \beta y + \frac{f_0}{D_0} h$$

defines the *geostrophic contours*, the stationary (unchanging) part of the potential vorticity.

If a parcel crosses the geostrophic contours, its relative vorticity must change to conserve the total PV. Consider the example in figure (4.1). Here there is no topography, so the contours are just latitude lines ($q_s = \beta y$). Northward motion is accompanied by a *decrease* in relative vorticity: as

y increases, ζ_g must decrease. If the parcel has zero vorticity initially, it acquires negative vorticity (clockwise circulation) in the northern hemisphere. Southward motion likewise generates positive vorticity. This is just Kelvin's theorem again.

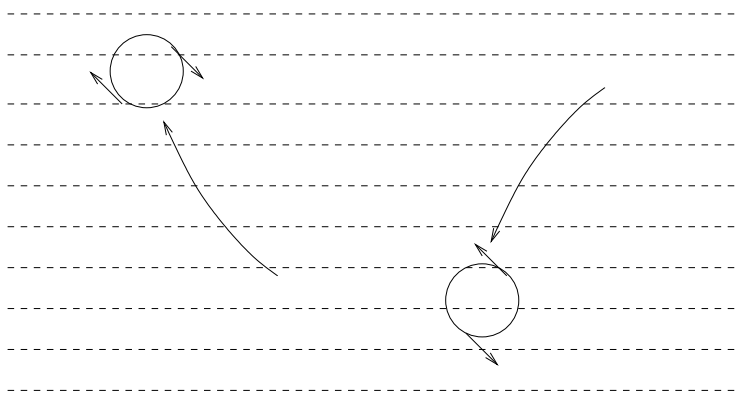

Figure 4.1: The change in relative vorticity due to northward or southward motion relative to βy.

Topography generally distorts the geostrophic contours. If large enough, it can overwhelm the βy term locally, even causing *closed* contours (near mountains or basins). But the same principle holds, as shown in Fig. (4.2). Motion towards larger values of q_s generates negative vorticity and motion to lower values of q_s generates positive vorticity.

If the flow is steady, then (4.14) is just:

$$\vec{u}_g \cdot \nabla(\zeta_g + q_s) = 0 \tag{4.17}$$

This implies a steady geostrophic flow is *parallel to the total PV contours*, $q = \zeta_g + q_s$. If the relative vorticity is weak, so that $\zeta_g \ll q_s$, then:

$$\vec{u}_g \cdot \nabla q_s = 0 \tag{4.18}$$

So the flow follows the geostrophic contours.

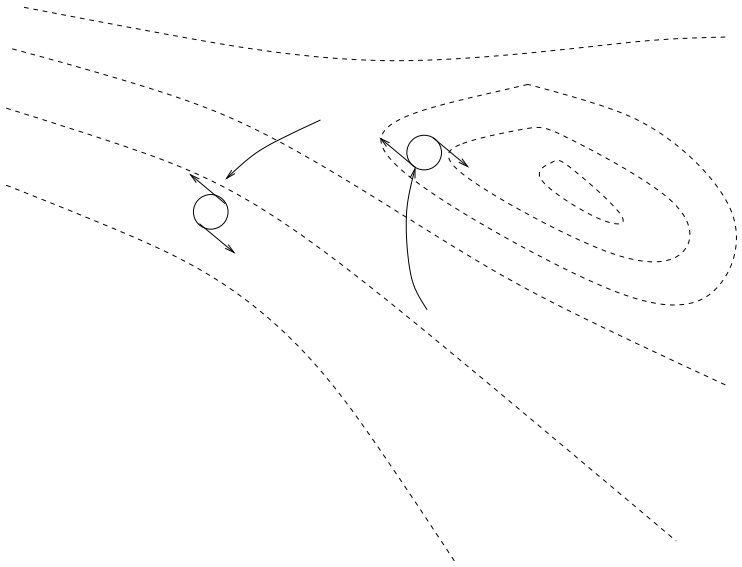

Figure 4.2: The change in relative vorticity due to motion across geostrophic contours with topography.

Take the case again of no topography. Then:

$$\vec{u}_g \cdot \nabla \beta y = \beta v_g = 0 \tag{4.19}$$

So the steady flow is purely *zonal*. This is because meridional motion necessarily implies a changing relative vorticity. An example are the Jet Streams in the atmosphere. These are approximately zonal flows.

Alternately if the region is small enough so that we can ignore changes in the Coriolis parameter, then:

$$\vec{u}_g \cdot \nabla h = 0 \tag{4.20}$$

(after dropping the constant f_0/D_0 factor). Then the flow follows the topographic contours. This is why many major currents in the ocean are parallel to the isobaths.

Whether such steady flows actually exist depends in addition on the boundary conditions. The atmosphere is a *re-entrant domain*, so a zonal

wind can simply wrap around the earth (Fig. 4.3, left). But most ocean basins have lateral boundaries (continents), and these block the flow. As such, steady, along-contour flows in a basin can occur *only where topography causes the contours to close* (Fig. 4.3, right). This can happen in basins.

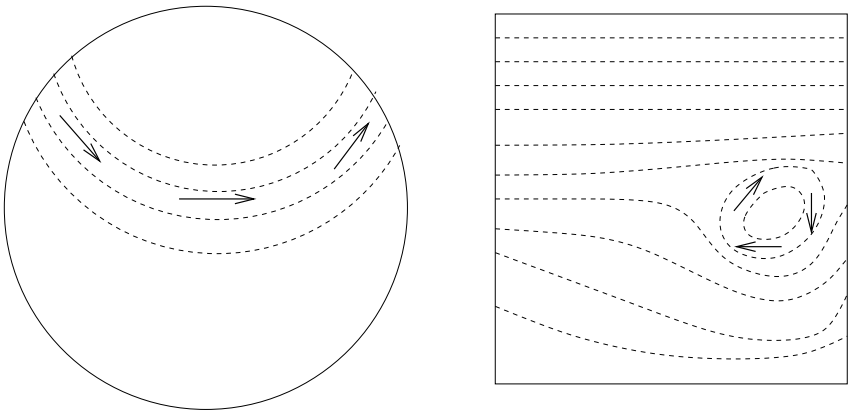

Figure 4.3: Steady, along-geostrophic contour flow in the atmosphere (left) and in the ocean (right).

Consider Fig. (4.4). This is a plot of the mean surface velocities, derived from surface drifters, in and near the Lofoten Basin off the west coast of Norway. The strong current on the right hand side is the Norwegian Atlantic Current, which flows in from the North Atlantic and proceeds toward Svalbard. Notice how this follows the continental slope (the steep topography between the continental shelf and deeper ocean). In the basin itself, the flow is more variable, but there is a strong, clockwise circulation in the deepest part of the basin, where the topographic contours are closed. Thus both closed and open geostrophic contour flows are seen here.

If the relative vorticity is not small compared to q_s, the flow will deviate from the latter contours. This can be seen for example with the Gulf Stream, which crosses topographic contours as it leaves the east coast of

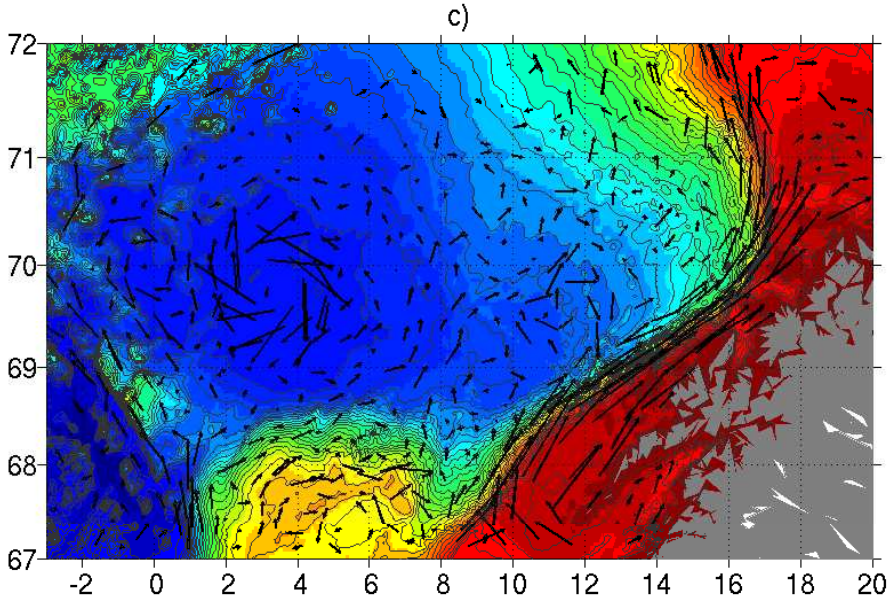

Figure 4.4: Mean velocities estimated from surface drifters in the Lofoten Basin west of Norway. The color contours indicate the water depth. Note the strong flow along the continental margin and the clockwise flow in the center of the basin, near 2° E. From Koszalka et al. (2010).

the U.S. If the relative vorticity is much stronger than q_s, then we have:

$$\vec{u}_g \cdot \nabla \zeta_g \approx 0 \tag{4.21}$$

as a condition for a steady flow. Then the flow follows contours of constant vorticity. An example is flow in a vortex. The vorticity contours are circular or ellipsoidal and the streamlines have the same shape. The vortex persists for long times precisely because it is near a steady state.

We will return to the q_s contours repeatedly hereafter. Often these are the key to understanding how a particular system evolves in time.

4.3 Linear wave equation

As in sec. (3.4), we will linearize the QGPV equation, to facilitate analytical solutions. We assume the motion is weak, as this allows us to neglect

terms which are quadratic in the streamfunction.

Suppose we have a mean flow, $\vec{U} = (U, V)$. Note that this can vary in space. So we can write:

$$u = U + u', \quad v = V + v'$$

The perturbations are weak, so that:

$$|u'| \ll |U|, \quad |v'| \ll |V|$$

Both the mean and the perturbation velocities have vorticity:

$$\mathcal{Z} \equiv \frac{\partial}{\partial x}V - \frac{\partial}{\partial y}U, \quad \zeta' = \frac{\partial}{\partial x}v' - \frac{\partial}{\partial y}u'$$

Only the latter varies in time. The mean vorticity in turn affects the geostrophic contours:

$$q_s = \mathcal{Z} + \beta y + \frac{f_0}{D_0}h$$

This will become important with regards to the stability of the mean flow.

Substituting these into the PV equation (4.14), we get:

$$\frac{\partial}{\partial t}\zeta' + (U+u')\frac{\partial}{\partial x}\zeta' + (V+v')\frac{\partial}{\partial y}\zeta' + \vec{U}\cdot\nabla q_s + u'\frac{\partial}{\partial x}q_s + v'\frac{\partial}{\partial y}q_s = 0 \quad (4.22)$$

We can separate out the terms in (4.22) with respective to perturbation velocities. The only term with no primed terms is:

$$\vec{U} \cdot \nabla q_s = 0 \quad (4.23)$$

Thus the mean flow must be parallel to the mean PV contours, as inferred in sec. (4.2). If this were not the case, the mean flow would have to evolve in time.

Collecting terms with one perturbation quantity yields:

$$\frac{\partial}{\partial t}\zeta' + U\frac{\partial}{\partial x}\zeta' + V\frac{\partial}{\partial y}\zeta' + u'\frac{\partial}{\partial x}q_s + v'\frac{\partial}{\partial y}q_s = 0 \tag{4.24}$$

This is the linearized QGPV equation for barotropic flows. We'll use this in the next few examples. For simplicity, we'll drop the primes hereafter, but keep in mind that it is the perturbation fields which we're interested in.

4.4 Barotropic Rossby waves

Consider a constant mean flow, $\vec{U} = U\hat{i}$, without bottom topography. Then:

$$q_s = \beta y$$

The mean flow doesn't contribute to q_s because it has no shear and hence no vorticity. Moreover, the mean flow, which is purely zonal, is parallel to q_s, which is only a function of y. So the linear PV equation is simply:

$$\frac{\partial}{\partial t}\zeta' + U\frac{\partial}{\partial x}\zeta' + \beta v' = 0 \tag{4.25}$$

Or, written in terms of the geostrophic streamfunction:

$$(\frac{\partial}{\partial t} + U\frac{\partial}{\partial x})\nabla^2\psi + \beta\frac{\partial}{\partial x}\psi = 0 \tag{4.26}$$

This is the *barotropic Rossby wave equation*.

4.4.1 Wave solution

To solve this, we use a wave solution. Because the coefficients in the wave equation are constants, we can use a general plane wave solution (Appendix 6.3):

$$\psi = Re\{\hat{\psi} e^{ikx+ily-i\omega t}\} \tag{4.27}$$

where $Re\{\}$ signifies the real part (we will drop this hereafter, but remember it in the end). Substituting this in yields:

$$(-i\omega + ikU)(-k^2 - l^2)\,\hat{\psi} e^{ikx+ily-i\omega t} + i\beta k\,\hat{\psi} e^{ikx+ily-i\omega t} = 0 \tag{4.28}$$

Notice that both the wave amplitude and the exponential term drop out. This is typical of linear wave problems: we get no information about the amplitude from the equation itself (that requires specifying initial conditions). Solving for ω, we get:

$$\omega = kU - \frac{\beta k}{k^2 + l^2} \tag{4.29}$$

This is the *Rossby wave dispersion relation*. It relates the frequency of the wave to its wavenumbers. The corresponding phase speed (in the x-direction) is:

$$c_x = \frac{\omega}{k} = U - \frac{\beta}{k^2 + l^2} \equiv U - \frac{\beta}{\kappa^2} \tag{4.30}$$

where $\kappa = (k^2 + l^2)^{1/2}$ is the total wavenumber.

There are a number of interesting features about this. First, the phase speed depends on the wavenumbers, so the waves are dispersive. The

largest speeds occur when k and l are small, corresponding to long wavelengths. Thus large waves move faster than small waves.

Second, all waves propagate *westward* relative to the mean velocity, U. If $U = 0$, $c < 0$ for *all* (k, l). This is a distinctive feature of Rossby waves. Satellite observations of Rossby waves in the Pacific Ocean show that the waves, originating off of California and Mexico, sweep westward toward Asia (as seen hereafter).

The phase speed also has a meridional component, and this can be either towards the north or south:

$$c_y = \frac{\omega}{l} = \frac{Uk}{l} - \frac{\beta k}{l(k^2 + l^2)} \tag{4.31}$$

The sign of c_y thus depends on the signs of k and l. So Rossby waves can propagate northwest, southwest or west—but not east.

With a mean flow, the waves can be swept eastward, producing the appearance of eastward propagation. This happens frequently in the atmosphere, where the mean westerlies advect Rossby waves (pressure systems) eastward. If

$$\kappa > \kappa_s \equiv (\frac{\beta}{U})^{1/2}$$

the wave moves eastward. Longer waves move westward, opposite to the mean flow, and short waves are advected eastward. If $\kappa = \kappa_s$, the wave is *stationary* and the crests don't move at all—the wave is propagating west at exactly the same speed that the background flow is going east. Stationary waves can only occur if the mean flow is eastward, because the waves propagate westward.

Example: How big is the stationary wave if the mean flow is 20 m/sec to the east? Assume we are at 45 degrees N and that $k = l$.

At 45N:

$$\beta = \frac{1}{6.3 \times 10^6} \frac{4\pi}{86400} cos(45) = 1.63 \times 10^{-11}\, m^{-1} sec^{-1}$$

so:

$$\kappa_s = \frac{\beta}{U} = (\frac{1.63 \times 10^{-11}\, m^{-1} sec^{-1}}{20\, m/sec})^{1/2} = 9.03 \times 10^{-7}\, m^{-1}$$

Assuming $\lambda_x = \lambda_y$, we have that:

$$\kappa_s = \frac{2\sqrt{2}\pi}{\lambda_s}$$

so:

$$\lambda_s = 9.84 \times 10^6\, m \approx 9000\, km$$

Remember that this is a wavelength, so it includes positive and negative pressure anomalies. But it still is larger than our typical storm scale of 1000 km, implying the storms are in the eastward-propagating regime.

4.4.2 Westward propagation: mechanism

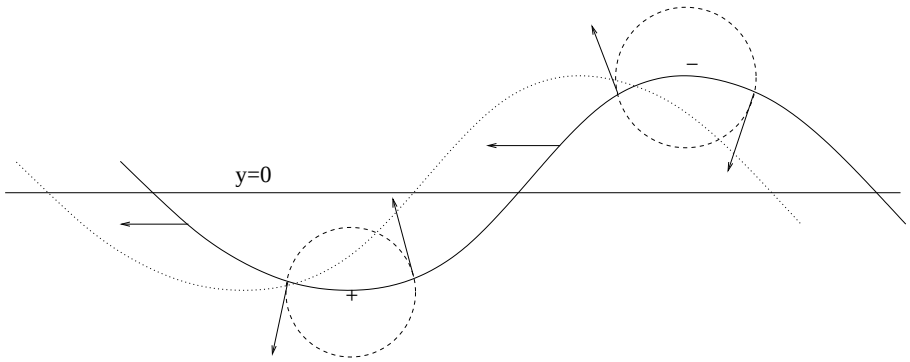

Figure 4.5: Relative vorticity induced in a Rossby wave. Fluid advected northwards acquires negative vorticity and fluid advected southwards positive vorticity.

We have discussed how motion across the mean PV contours, q_s, induces relative vorticity. The same is true with a Rossby wave. Fluid

parcels which are advected north in the wave acquire negative vorticity, while those advected south acquire positive vorticity (Fig. 4.5). Thus one can think of a Rossby wave as a string of negative and positive vorticity anomalies (Fig. 4.6).

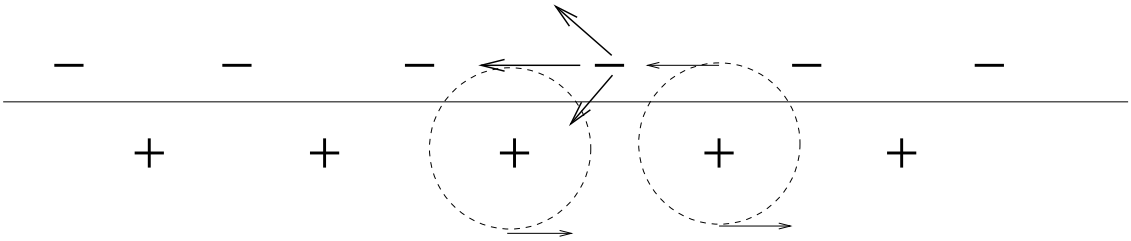

Figure 4.6: The Rossby wave as a string of vorticity anomalies. The cyclone in the right hand circle advects the negative anomaly to the southwest, while the left cyclone advects it toward the northwest. The net effect is westward motion.

Now the negative anomalies to the north will act on the positive anomalies to the south, and vice versa. Consider the two positive anomalies shown in Fig. (4.6). The right one advects the negative anomaly between them southwest, while the left one advects it northwest. Adding the two velocities together, the net effect is a westward drift for the anomaly. Similar reasoning suggests the positive anomalies are advected westward by the negative anomalies.

4.4.3 Observations of Rossby waves

What does a Rossby wave look like? In the atmosphere, Rossby waves are superimposed on the Jet Stream, giving the latter a meandering aspect (Fig. 4.7). The meanders tend to propagate downstream. They also have meaning for the weather. Since the temperatures to the north are colder, the temperature in a trough is colder than in a crest.

In addition, the meanders often grow in amplitude and break. This leads

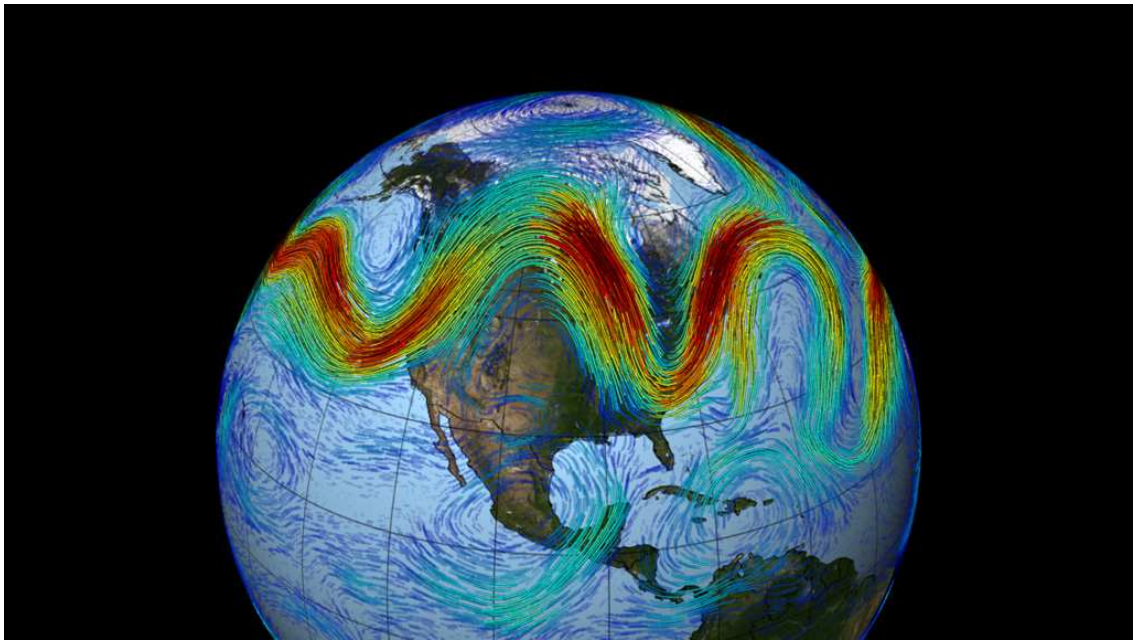

Figure 4.7: An example of Rossby waves in the atmosphere. The Jet Stream, flowing eastward, is superimposed over westward-propagating Rossby waves. Courtesy of NASA.

to regions of anomalous temperature and vorticity, as for example in a so-called "cut-off" or "blocking" high pressure. Such instability is considered later on.

In the ocean, the mean zonal flow in regions is near zero ($U = 0$), so the observed phase propagation is generally westward. Westward phase propgation is clearly visible in satellite measurements of sea surface height. An example is shown in Fig. (4.8), from the Pacific. In the upper panel is the sea surface height anomaly[1] from April, 1993. The corresponding field from July is shown in the lower panel. There is a large positive anomaly (red) off the Americas in April, surrounded by a (blue) negative anomaly. The latter is indicated by the white curve. In July the anomalies have all shifted westward. The waves are basin scale, covering 1000s of kilometers.

[1]The stationary part of the surface height, due to mean flows and also irregularities in the graviational field, have been removed.

From the figure, you can see that the phase speed varies with latitude, being largest at the equator and decreasing away from that. In fact this is a *baroclinic* effect. Baroclinic Rossby waves are discussed in sec. (5.5).

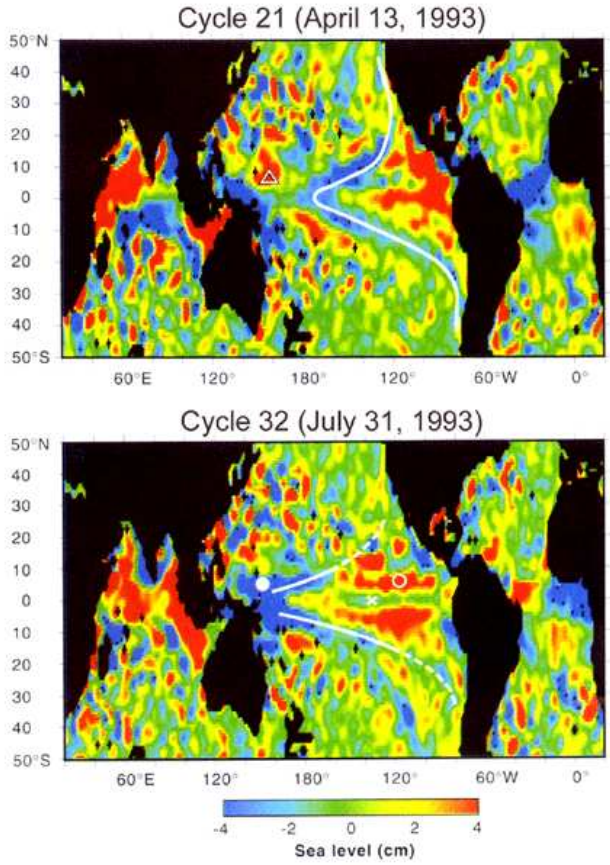

Figure 4.8: Sea surface height anomalies at two successive times. Westward phase propagation is clear at low latitudes, with the largest speeds occurring near the equator. From Chelton and Schlax (1996).

4.4.4 Group Velocity

Rossby waves propagate westward. But this actually poses a problem. Say we are in an ocean basin, with no mean flow ($U = 0$). If there is a disturbance on the eastern wall, Rossby waves will propagate westward into the interior. Thus changes on the eastern wall are *communicated* to the

rest of the basin by Rossby waves. Because they propagate westward, the whole basin will soon know about these changes. But say the disturbance is on the *west wall*. If the waves can go only toward the wall, the energy would necessarily be trapped there. How do we reconcile this?

The answer is that the phase velocity tells us only about the motion of the crests and troughs—it does not tell us how the energy is moving. To see how energy moves, it helps to consider a *packet* of waves with different wavelengths. If the Rossby waves were initiated by a localized source, say a meteor crashing into the ocean, they would start out as a wave packet. Wave packets have both a phase velocity and a "group velocity". The latter tells us about the movement of packet itself, and this reflects how the energy is moving. It is possible to have a packet of Rossby waves which are moving eastwards, while the crests of the waves in the packet move westward.

Consider the simplest example, of two waves with different wavelengths and frequencies, but the same (unit) amplitude:

$$\psi = cos(k_1 x + l_1 y - \omega_1 t) + cos(k_2 x + l_2 y - \omega_2 t) \tag{4.32}$$

Imagine that k_1 and k_2 are almost equal to k, one slightly larger and the other slightly smaller. We'll suppose the same for l_1 and l_2 and ω_1 and ω_2. Then we can write:

$$\begin{aligned} \psi = cos[(k + \delta k)x + (l + \delta l)y - (\omega + \delta\omega)t] \\ + cos[(k - \delta k)x + (l - \delta l)y - (\omega - \delta\omega)t] \end{aligned} \tag{4.33}$$

From the cosine identity:

$$cos(a \pm b) = cos(a)cos(b) \mp sin(a)sin(b) \tag{4.34}$$

So we can rewrite the streamfunction as:

$$\psi = 2\, cos(\delta kx + \delta ly - \delta\omega t)\, cos(kx + ly - \omega t) \tag{4.35}$$

The combination of waves has two components: a plane wave (like we considered before) multiplied by a *carrier wave*, which has a longer wavelength and lower frequency. The carrier wave has a phase speed of:

$$c_x = \frac{\delta\omega}{\delta k} \approx \frac{\partial\omega}{\partial k} \equiv c_{gx} \tag{4.36}$$

and

$$c_y = \frac{\delta\omega}{\delta l} \approx \frac{\partial\omega}{\partial l} \equiv c_{gy} \tag{4.37}$$

The phase speed of the carrier wave is the *group velocity*, because this is the speed at which the group (in this case two waves) moves. While the phase velocity of a wave is the ratio of the frequency and the wavenumber, the group velocity is the *derivative* of the frequency by the wavenumber.

This is illustrated in Fig. (4.9). This shows two waves, $cos(1.05x)$ and $cos(0.095x)$. Their sum yields the wave packet in the lower panel. The smaller ripples propagate with the phase speed, $c = \omega/k = \omega/1$, westward. But the larger scale undulations move with the group velocity, and this can be either west *or* east.

The group velocity concept applies to any type of wave. For Rossby waves, we take derivatives of the Rossby wave dispersion relation for ω. This yields:

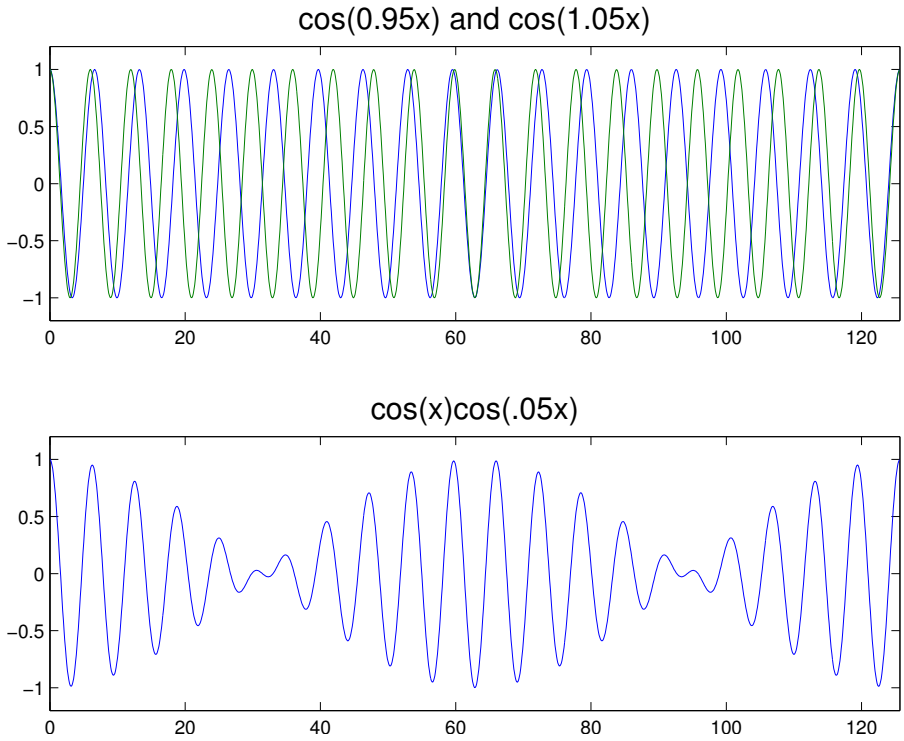

Figure 4.9: Two waves with nearly the same wavelength (upper panel) and their sum (lower panel).

$$c_{gx} = \frac{\partial \omega}{\partial k} = \beta \frac{k^2 - l^2}{(k^2 + l^2)^2}\,, \quad c_{gy} = \frac{\partial \omega}{\partial l} = \frac{2\beta k l}{(k^2 + l^2)^2} \tag{4.38}$$

Consider for example the group velocity in the zonal direction, c_{gx}. The sign of this depends on the relative sizes of the zonal and meridional wavenumbers. If

$$k > l$$

the wave packet has a positive (eastward) zonal velocity. Then the energy is moving in the *opposite* direction to the phase speed. This answers the question about the disturbance on the west wall. Energy can indeed spread eastward into the interior, if the zonal wavelength is shorter than the merid-

ional one. Note that for such waves, the phase speed is still westward. So the crests will move toward the west wall while energy is carried eastward!

Another interesting aspect is that the group velocity in the y-direction is *always* in the opposite direction to the phase speed in y, because:

$$\frac{c_{gy}}{c_y} = -\frac{2l^2}{k^2 + l^2} < 0\,. \tag{4.39}$$

So northward propagating waves have southward energy flux!

The group velocity can also be derived by considering the energy equation for the wave. This is shown in Appendix (6.4).

4.4.5 Rossby wave reflection

A good illustration of Rossby wave properties is the case of a wave reflecting off a solid boundary. Consider what happens to a westward propagating plane Rossby wave which encounters a straight wall, oriented along $x = 0$. The incident wave can be written:

$$\psi_i = A_i\, e^{ik_i x + il_i y - i\omega_i t}$$

where:

$$\omega_i = \frac{-\beta k_i}{k_i^2 + l_i^2}$$

The incident wave has a westward group velocity, so that

$$k_i < l_i$$

Let's assume too that the group velocity has a northward component (so that the wave is generated somewhere to the south). As such, the phase velocity is oriented toward the *southwest*.

The wall will produce a reflected wave. If this weren't the case, all the energy would have to be absorbed by the wall. We assume instead that all the energy is reflected. The reflected wave is:

$$\psi_r = A_r\, e^{ik_r x + il_r y - i\omega_r t}$$

The total streamfunction is the sum of the incident and reflected waves:

$$\psi = \psi_i + \psi_r \tag{4.40}$$

In order for there to be no flow into the wall, we require that the zonal velocity vanish at $x = 0$, or:

$$u = -\frac{\partial}{\partial y}\psi = 0 \quad at \;\; x = 0 \tag{4.41}$$

This implies:

$$-il_i\, A_i\, e^{il_i y - i\omega_i t} - il_r\, A_r\, e^{il_r y - i\omega_r t} = 0 \tag{4.42}$$

In order for this condition to hold at all times, the frequencies must be equal:

$$\omega_i = \omega_r = \omega \tag{4.43}$$

Likewise, if it holds for all values of y along the wall, the meridional wavenumbers must also be equal:

$$l_i = l_r = l \tag{4.44}$$

Note that because the frequency and meridional wavenumbers are preserved on reflection, the meridional phase velocity, $c_y = \omega/l$, remains unchanged. Thus (4.42) becomes:

$$il\,A_i\,e^{ily-i\omega t} + il\,A_r\,e^{ily-i\omega t} = 0 \tag{4.45}$$

which implies:

$$A_i = -A_r \equiv A \tag{4.46}$$

So the amplitude of the wave is preserved, but the phase is changed by 180°.

Now let's go back to the dispersion relations. Because the frequencies are equal, we have:

$$\omega = \frac{-\beta k_i}{k_i^2 + l^2} = \frac{-\beta k_r}{k_r^2 + l^2}\ . \tag{4.47}$$

This is possible because the dispersion relation is quadratic in k and thus admits two different values of k. Solving the Rossby dispersion relation for k, we get:

$$k = -\frac{\beta}{2\omega} \pm \frac{\sqrt{\beta^2 - 4\omega^2 l^2}}{2\omega} \tag{4.48}$$

The incident wave has a smaller value of k because it has a westward group velocity; so it is the additive root. The reflected wave thus comes from the difference of the two terms.

This implies the zonal wavenumber *increases* on reflection, by an amount:

$$|k_r - k_i| = 2\sqrt{\frac{\beta^2}{4\omega^2} - l^2} \tag{4.49}$$

So if the incident waves are long, the reflected waves are *short*.

We can also show that the meridional velocity, v, *increases* upon reflection and also that the mean energy (Appendix 6.4) increases on reflection. The reflected wave is more energetic because the energy is squeezed into

a shorter wave. However, the *flux* of energy is conserved; the amount of energy going in equals that going out. So energy does not accumulate at the wall.

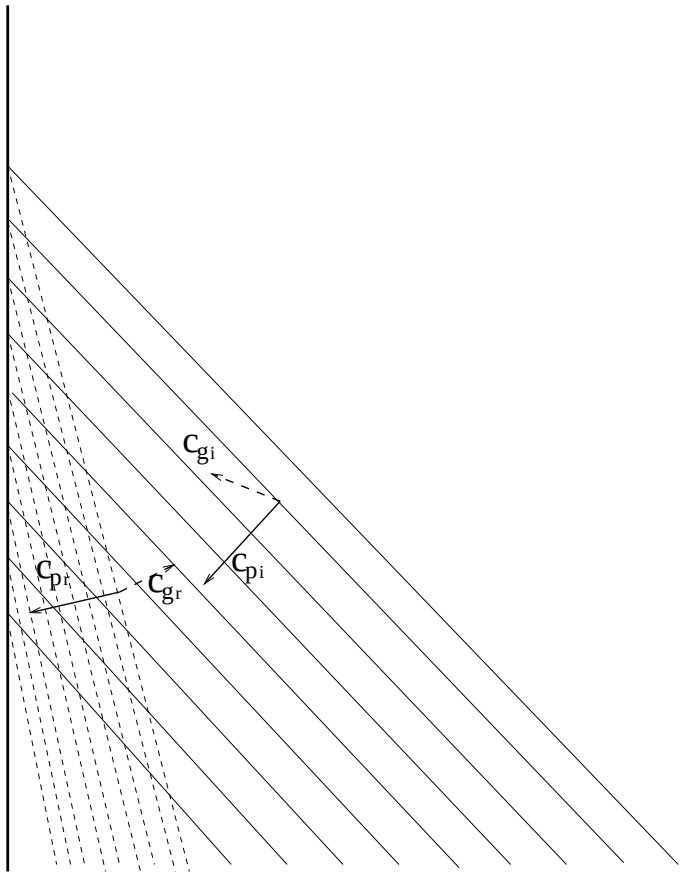

Figure 4.10: A plane Rossby wave reflecting at a western wall. The incident wave is shown by the solid lines and the reflected wave by the dashed lines. The phase velocities are indicated by the solid arrows and the group velocities by the dashed arrows. Note the wavelength in y doesn't change, but the reflected wavelength in x is much shorter. Note too the reflected wave has a phase speed directed toward the wall, but a group velocity away from the wall.

Thus Rossby waves change their character on reflection. Interestingly, the change depends on the *orientation* of the boundary. A tilted boundary (e.g. northwest) will produce different results. In fact, the case with a zonally-oriented boundary (lying, say, along $y = 0$) is *singular*; you must

introduce other dynamics, like friction, to solve the problem.

4.5 Boundary layers

So far we have ignored forcing and friction. Without wind forcing, we would not have many of the major ocean currents, like the Gulf Stream. And without friction, there would be nothing to remove energy supplied by the sun (to the atmosphere) or the winds (to the ocean) and the velocities would accelerate to infinity. Stresses, by which forcing and friction act, are important in the boundary layers at the earth's surface in the atmosphere, and at the surface and bottom of the ocean. How do these layers affect the interior motion?

The important feature of the boundary layers is that the velocities are *sheared*. So we can distinguish the interior of the fluid, where there is no shear, and the boundary layers. In the bottom boundary layers, the velocity goes to zero at the ground, to satisfy the "no-slip condition". At the ocean surface on the other hand, the stress exerted by the wind will drive flow. In both surface and bottom layers, friction permits the smooth variation of the velocities to the interior values.

We represent friction as the gradient of a stress. Think of the surface layer as a series of thin layers. The stress at the surface acts on the upper-most layer. That layer in turn exerts a stress on the layer below it. But that layer exerts an equal and opposite force on the upper-most layer. So the acceleration of the layer is the difference between these two stresses. If we think of a series of thin layers, it is then the vertical derivative of the stress which accelerates the fluid. Because the aspect ratio is small, we can focus solely on the vertical derivative, and ignore the horizontal stress

derivatives.

Perhaps the simplest boundary layer model possible includes the geostrophic relations (2.27) and (2.28) with the vertical stress terms:

$$-f_0 v = -\frac{1}{\rho_c}\frac{\partial}{\partial x}p \; + \; \frac{\partial}{\partial z}\frac{\tau_x}{\rho_c} \tag{4.50}$$

$$f_0 u = -\frac{1}{\rho_c}\frac{\partial}{\partial y}p \; + \; \frac{\partial}{\partial z}\frac{\tau_y}{\rho_c} \tag{4.51}$$

where τ_x and τ_y are stresses acting in the x and y directions. Thus friction *breaks the geostrophic balance* in the boundary layers.

We can rewrite these relations thus:

$$-f_0(v - v_g) \equiv -f_0 v_a = \frac{\partial}{\partial z}\frac{\tau_x}{\rho_c} \tag{4.52}$$

$$f_0(u - u_g) \equiv f_0 u_a = \frac{\partial}{\partial z}\frac{\tau_y}{\rho_c} \tag{4.53}$$

where (u_a, v_a) are the *ageostrophic velocities* (the departures from purely geostrophic flow). The ageostrophic velocities in the boundary layer are proportional to the stresses and these are the components which are sheared.

We are mainly concerned with how the boundary layer affects the motion in the interior. As seen below, it is the *vertical velocity* from the boundary layers which forces the flow in the interior.

4.5.1 Surface Ekman layer

Consider the boundary layer at the ocean surface. This was first considered in a paper by Ekman (1905), which in turn was motivated by observations by Fridtjof Nansen. Nansen noticed that icebergs in the Arctic drift to the right of the wind. Ekman's model explains why. Hereafter, we refer to the boundary layers as "Ekman layers", following his derivation.

Let's say the surface is at $z = 0$ and that the Ekman layer extends down to $z = -\delta_e$ (which we take to be constant). The lower depth is defined as the location where the stress vanishes; below that, in the ocean interior, the flow is in geostrophic balance. We are interested in $w(\delta_e)$, as this will effect the interior flow. To obtain this, we use the continuity equation (2.26):

$$\frac{\partial}{\partial z}w = -\frac{\partial}{\partial x}u - \frac{\partial}{\partial y}v = -\frac{\partial}{\partial x}u_a - \frac{\partial}{\partial y}v_a \tag{4.54}$$

The horizontal divergence involves only the ageostrophic velocities because the geostrophic velocities are horizontally non-divergent (sec. 2.4.1). Integrating this over the layer yields:

$$w(0) - w(-\delta_e) = -\int_{-\delta_e}^{0} (\frac{\partial}{\partial x}u_a + \frac{\partial}{\partial y}v_a)\, dz \tag{4.55}$$

Since there is no flow out of the ocean surface, we can write $w(0) = 0$. Then we have:

$$w(-\delta_e) = \frac{\partial}{\partial x}U_s + \frac{\partial}{\partial y}V_s \tag{4.56}$$

where (U_s, V_s) are the horizontal ageostrophic *transports* in the surface layer:

$$U_s \equiv \int_{-\delta_e}^{0} u_a\, dz, \qquad V_s \equiv \int_{-\delta_e}^{0} v_a\, dz \tag{4.57}$$

We obtain these by integrating (4.52) and (4.53) vertically.

The stress at the surface ($z = 0$) is due to the wind:

$$\vec{\tau}^w = (\tau_x^w, \tau_y^w)$$

The stress at the base of the Ekman layer is zero, by definition. So we obtain:

$$U_s = \frac{\tau_y^w}{\rho_c f_0}, \qquad V_s = -\frac{\tau_x^w}{\rho_c f_0}$$

Notice the transport in the layer is *90 degrees to the right of the wind stress*. If the wind is blowing to the north, the transport is to the east. This is consistent with Nansen's observations.

To get the vertical velocity, we take the divergence of these transports:

$$w(\delta_e) = \frac{\partial}{\partial x}\frac{\tau_y^w}{\rho_c f_0} + \frac{\partial}{\partial y}(-\frac{\tau_x^w}{\rho_c f_0}) = \frac{1}{\rho_c f_0}\hat{k} \cdot \nabla \times \vec{\tau}^w \tag{4.58}$$

So the vertical velocity is *proportional to the curl of the wind stress*. It is the curl, not the stress itself, which is most important for the interior flow in the ocean at synoptic scales.

Interestingly, we haven't made any assumptions about the stress in the surface layer itself. By integrating over the layer, we only need to know the stress at the surface. So the result (4.58) is *independent* of the stress distribution, $\tau(z)/\rho_c$, in the layer.

4.5.2 Bottom Ekman layer

Then there is the bottom boundary layer, which exists in both the ocean and atmosphere. Let's assume the bottom is flat and that the Ekman layer goes from $z = 0$ to $z = \delta_e$. The integral of the continuity equation is:

$$w(\delta_e) - w(0) = w(\delta_e) = -(\frac{\partial}{\partial x}U_B + \frac{\partial}{\partial y}V_B) \tag{4.59}$$

where now U_B, V_B are the integrated (ageostrophic) transports in the bottom layer. Note the vertical velocity vanishes at the *bottom* of the layer—there is no flow into the bottom surface.

Again we integrate (4.52) and (4.53) to find the transports. However, *we don't know the stress at the bottom*. All we know is that the bottom boundary isn't moving.

This problem was solved by Ekman (1905). Ekman's solution requires that we *parametrize* the stress in the boundary layer. To do this, we make a typical assumption, that the stress is proportional to the velocity shear:

$$\frac{\vec{\tau}}{\rho_c} = A_z \frac{\partial}{\partial z}\vec{u} \tag{4.60}$$

Here A_z, is a *mixing coefficient*. Thus the stress acts down the gradient of the velocity. If the vertical shear is large, the stress is large and vice versa. Generally, A_z varies with height, and often in a non-trivial way, but in such cases it is difficult to find analytical solutions. So we'll assume A_z is constant.

Again, we assume the interior flow is in geostrophic balance, with velocities (u_g, v_g). The boundary layer's role is to bring the velocities to rest at the lower boundary. Substituting the parametrized stresses (4.60) into the boundary layer equations (4.52-4.53) yields:

$$-f_0 v_a = A_z \frac{\partial^2}{\partial z^2} u_a \tag{4.61}$$

$$f_0 u_a = A_z \frac{\partial^2}{\partial z^2} v_a \tag{4.62}$$

Because the geostrophic velocity is independent of height, it doesn't contribute to the RHS. If we define a variable χ thus:

$$\chi \equiv u_a + i v_a \tag{4.63}$$

we can combine the two equations into one:

$$\frac{\partial^2}{\partial z^2}\chi = i\frac{f_0}{A_z}\chi \tag{4.64}$$

The general solution to this is:

$$\chi = A\, exp(\frac{z}{\delta_e})\, exp(i\frac{z}{\delta_e}) + B\, exp(-\frac{z}{\delta_e})\, exp(-i\frac{z}{\delta_e}) \tag{4.65}$$

The scale, δ_e, is the layer depth that we assumed before. Now we see that this is related to the mixing coefficient, A_z:

$$\delta_e = (\frac{2A_z}{f_0})^{1/2} \tag{4.66}$$

Thus the *Ekman depth* is determined by the mixing coefficient and by the Coriolis parameter.

To proceed, we need boundary conditions. The solutions should decay moving upward, into the interior of the fluid, as the boundary layer solutions should be confined to the boundary layer. Thus we can set:

$$A = 0$$

From the definition of χ, we have:

$$\begin{aligned} u_a = Re\{\chi\} = Re\{B\}\, exp(-\frac{z}{\delta_e})\, cos(\frac{z}{\delta_e}) \\ +Im\{B\}\, exp(-\frac{z}{\delta_e})\, sin(\frac{z}{\delta_e}) \end{aligned} \tag{4.67}$$

and:

$$\begin{aligned} v_a = Im\{\chi\} = -Re\{B\}\, exp(-\frac{z}{\delta_e})\, sin(\frac{z}{\delta_e}) \\ +Im\{B\}\, exp(-\frac{z}{\delta_e})\, cos(\frac{z}{\delta_e}) \end{aligned} \tag{4.68}$$

Thus there are two unknowns. To determine these, we evaluate the velocities at $z = 0$. To satisfy the no-slip condition, we require:

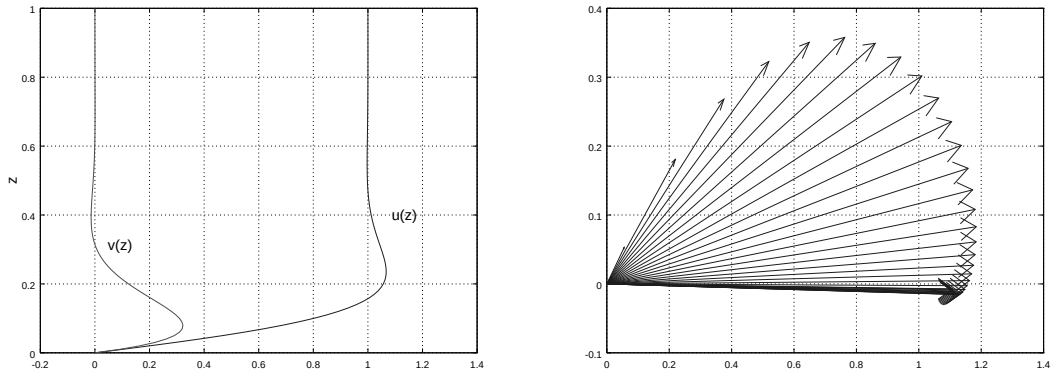

Figure 4.11: The Ekman velocities for a case with $v_g = 0$. In the left panel are the velocities as a function of height. In the right panel are the velocity vectors, looking down from above.

$$u_a = -u_g, \quad v_a = -v_g \quad at \;\; z = 0$$

Then the total velocity will vanish. So we must have:

$$Re\{B\} = -u_g$$

and:

$$Im\{B\} = -v_g$$

The resulting total velocities, the sum of geostrophic and ageostrophic parts, are shown in the left panel of Fig. (4.11) for a case with $v_g = 0$. Outside the boundary layer, the velocity reverts to $(u_g, 0)$. Both velocities go to zero at the bottom, to satisfy the no-slip condition. But above that, both increase somewhat as well. This reflects the decaying/sinusoidal nature of the solutions.

The figure masks the actual behavior of the velocities, which is seen more clearly in the right panel. This shows the velocity vectors when

viewed from above. Outside the layer, the vector is parallel with the x-axis. As one descends into the layer, the vectors veer *to the left*. They first increase slightly in magnitude and then decrease smoothly to zero. The result is a curving *Ekman spiral*.

If one solves the same problem in the surface layer, one also finds a solution which spirals with depth. But since it is the stress which is matched at the surface, the vectors spiral to the right. That's why the depth-averaged velocity is to the right in the surface layer. In the bottom layer, the transport is to the left.

Strictly speaking, the integrals are over the depth of the layer. But as the ageostrophic velocities decay with height, we can just as well integrate them to infinity. So, we have:

$$\begin{aligned} U_a = -u_g \int_0^\infty exp(-\frac{z}{\delta_e})\, cos(\frac{z}{\delta_e})\, dz - v_g \int_0^\infty exp(-\frac{z}{\delta_e})\, sin(\frac{z}{\delta_e})\, dz \\ = -\frac{\delta_e}{2}(u_g + v_g) \end{aligned} \tag{4.69}$$

(using a standard table of integrals). Likewise:

$$\begin{aligned} V_a = u_g \int_0^\infty exp(-\frac{z}{\delta_e})\, sin(\frac{z}{\delta_e})\, dz - v_g \int_0^\infty exp(-\frac{z}{\delta_e})\, cos(\frac{z}{\delta_e})\, dz \\ = \frac{\delta_e}{2}(u_g - v_g) \end{aligned} \tag{4.70}$$

where (u_g, v_g) are the velocities in the interior. Thus for the case shown in Fig. (4.11), the transport is:

$$(U_a, V_a) = \frac{\delta_e}{2}(-u_g, u_g)$$

This is 135° to the left of the geostrophic velocity.

What about the stress at the bottom? From the definition above, we have $\tau/\rho_c = Au_z$. Only the ageostrophic velocity varies with height, by assumption. It can be shown (see exercises) that the transport is 90 degrees to the left of the bottom stress.

But the primary factor of interest for the interior flow is the vertical velocity at the top of the Ekman layer, as this will be seen to force the interior flow. This is:

$$
\begin{aligned}
w(\delta_e) &= -\frac{\partial}{\partial x}U_a - \frac{\partial}{\partial y}V_a && (4.71)\\
&= \frac{\delta_e}{2}(\frac{\partial u_g}{\partial x} + \frac{\partial v_g}{\partial x}) + \frac{\delta_e}{2}(-\frac{\partial u_g}{\partial y} + \frac{\partial v_g}{\partial y}) && (4.72)\\
&= \frac{\delta_e}{2}(\frac{\partial v_g}{\partial x} - \frac{\partial u_g}{\partial y}) && (4.73)\\
&= \frac{\delta_e}{2}\nabla \times \vec{u}_g && (4.74)\\
&= \frac{\delta_e}{2}\zeta_g && (4.75)
\end{aligned}
$$

Recall that the horizontal divergence of the geostrophic velocities is zero. Thus the vertical velocity at the top of a bottom Ekman layer is *proportional to the relative vorticity in the interior*. So there is updrafting beneath a cyclonic vortex.

These two results represent a tremendous simplification. We can include the boundary layers without actually worrying about what is happening in the layers themselves. The bottom layer causes relative vorticity to decay in time (sec. 4.7) and the stress at the ocean surface forces the ocean.

4.6 The QGPV equation with forcing

We include the Ekman layers to the interior dynamics by adding two additional terms on the RHS of the vertically-integrated vorticity equation (4.4), thus:

$$\frac{d_g}{dt}\left(\zeta + \beta y - \frac{f_0}{D_0}\eta + \frac{f_0}{D_0}h\right) = \frac{f_0}{D_0}[w_e(z_1) - w_e(z_0)] \tag{4.76}$$

The first term on the RHS is the vertical velocity associated with the boundary layer on the upper surface and the second term is that with the layer on the lower surface.

In the atmosphere, we set the vertical velocity at the top boundary to zero (there is no Ekman layer on the tropopause). For the ocean, we include the wind stress term from (4.58):

$$w_e(z_1) = \frac{1}{\rho_c f_0}\hat{k}\cdot\nabla\times\tau^w \tag{4.77}$$

The bottom Ekman layer exists in both the atmosphere and ocean. From (4.75), we have:

$$w_e(z_0) = \frac{\delta}{2}\zeta_g \tag{4.78}$$

The Ekman layers thus affect the motion in the interior when there is vorticity.

Combining the terms, we arrive at the full QG barotropic PV equation:

$$\frac{d_g}{dt}\left(\nabla^2\psi + \beta y + \frac{f_0}{D_0}h\right) = \frac{1}{\rho_c D_0}\hat{k}\cdot\nabla\times\vec{\tau}_w - r\nabla^2\psi \tag{4.79}$$

The constant, r, is called the "Ekman drag coefficient" and is defined:

$$r = \frac{f_0 \delta}{2D_0}$$

An important point is that the forcing terms exert themselves over the entire depth of the fluid, because there is no vertical shear in the barotropic system.

4.7 Spin down

Bottom friction damps the velocities, causing the winds to slow. The simplest example of this is with no bottom topography and a constant f. Then the barotropic vorticity equation is:

$$\frac{d_g}{dt}\zeta = -r\zeta \tag{4.80}$$

This is a nonlinear equation. However it is easily solved in the Lagrangian frame. Following a parcel, we have that:

$$\zeta(t) = \zeta(0)e^{-rt} \tag{4.81}$$

implying the vorticity decreases exponentially. The e-folding time scale is known as the Ekman *spin-down time*:

$$T_e = r^{-1} = \frac{2D_0}{f_0 \delta} \tag{4.82}$$

Typical atmospheric values are:

$$D_0 = 10km, \quad f_0 = 10^{-4} sec^{-1}, \quad \delta = 1km$$

So:

$$T_e \approx \ 2.3 \ days$$

If all the forcing (including the sun) were suddenly switched off, the winds would slow down, over this time scale. After about a week or so, the winds would be weak.

If we assume the atmospheric barotropic layer does not extend all the way to the tropopause but lies nearer the ground, the spin-down time will be even shorter. This is actually what happens in the stratified atmosphere, with the winds near the ground spinning down but the winds aloft being less affected. So bottom friction favors flows intensified further up. The same is true in the ocean.

4.8 Mountain waves

Barotropic Rossby waves have been used to study the mean surface pressure distribution in the atmosphere. This is the pressure field you get when averaging over long periods of time (e.g. years). The central idea is that the mean wind, U, blowing over topography can excite stationary waves ($c_x = 0$). As demonstrated by Charney and Eliassen (1949), one can find a reasonable first estimate of the observed distribution using the linear, barotropic vorticity equation.

We begin with the vorticity equation without forcing:

$$\frac{d_g}{dt}\left(\zeta + \beta y + \frac{f_0}{D_0}h\right) = 0 \tag{4.83}$$

(we'll add friction later on). We linearize about a mean zonal flow:

$$u = U + u', \quad v = v', \quad \zeta = \zeta'$$

We will also assume the topography is weak:

$$h = h'$$

Then the Rossby wave equation has one additional term:

$$(\frac{\partial}{\partial t} + U\frac{\partial}{\partial x})\zeta' + \beta v' + U\frac{\partial}{\partial x}\frac{f_0}{D_0}h' = 0 \tag{4.84}$$

Substituting in the streamfunction, we have:

$$(\frac{\partial}{\partial t} + U\frac{\partial}{\partial x})\nabla^2\psi + \beta\frac{\partial}{\partial x}\psi = -\frac{f_0}{D_0}U\frac{\partial}{\partial x}h' \tag{4.85}$$

We put the topographic term on the RHS because it does not involve the streamfunction, and so acts instead like a forcing term. The winds blowing over the mountains generate the response.

The homogeneous solution to this equation are the Rossby waves discussed earlier. These are called "free Rossby waves". If we were to suddenly "turn on" the wind, we would excite free waves. The particular solution, or the "forced wave", is the part generated by the topographic term on the RHS. This is the portion of the flow that remains after the free waves have propagated away.

Thus the forced wave is what determines the time mean flow. To find it, we ignore the time derivative:

$$U\frac{\partial}{\partial x}\nabla^2\psi + \beta\frac{\partial}{\partial x}\psi = -\frac{f_0}{D_0}U\frac{\partial}{\partial x}h' \tag{4.86}$$

All the terms involve a derivative in x, so we can simply integrate the equation once in x to get rid of that. We will also ignore the constant of integration.[2]

[2]This would add a constant to the streamfunction. The latter would have no effect on the velocity field (why?).

In line with our previous derivations, we write the topography as a sum of Fourier modes:

$$h'(x,y) = Re\{\sum_k \sum_l h_0(k,l)\, e^{ikx+ily}\} \tag{4.87}$$

and for simplicity, we focus on the response to a single wave mode:

$$h' = h_0 e^{ikx+ily} \tag{4.88}$$

We can always construct the response to more complicated topography by adding the solutions for different (k,l), because the Rossby wave equation is linear (see exercise 2.7). We'll also use a single wave expression for ψ:

$$\psi = Ae^{ikx+ily} \tag{4.89}$$

Substituting these into the wave yields:

$$(U(-k^2-l^2)+\beta)\, A = -\frac{f_0 h_0}{D_0} U \tag{4.90}$$

or:

$$A = \frac{f_0 h_0}{D_0(\kappa^2 - \beta/U)} = \frac{f_0 h_0}{D_0(\kappa^2 - \kappa_s^2)} \tag{4.91}$$

where:

$$\kappa_s \equiv (\frac{\beta}{U})^{1/2}$$

is the wavenumber of the stationary Rossby wave with a background velocity, U (sec. 4.4.1). So the forced solution is:

$$\psi = \frac{f_0 h_0}{D_0(\kappa^2 - \kappa_s^2)} e^{ikx+ily} \tag{4.92}$$

The pressure field thus *resembles the topography*. If the wavenumber of the topography, κ, is greater than the stationary wavenumber, the amplitude is positive. Then the forced wave is *in phase* with the topography. If the topographic wavenumber is smaller, the atmospheric wave is 180° out of phase with the topography. The latter case applies to large scale topography, for which the wavenumber is small. So there are negative pressures over mountains and positive pressures over valleys. With small scale topography, the pressure over the mountains will instead be positive.

What happens though when $\kappa = \kappa_S$? Then the streamfunction is infinite! This is typical with forced oscillations. If the forcing is at the natural frequency of the system, the response is infinite (we say the response is *resonant*). Having infinite winds is not realistic, so we must add additional dynamics to correct for this. In particular, we can add friction.

So we return to the barotropic vorticity equation, but with a bottom Ekman layer:

$$\frac{d_g}{dt}\left(\zeta + \beta y + \frac{f_0}{D_0}h\right) = -r\zeta \tag{4.93}$$

Linearizing as before, we obtain:

$$U\frac{\partial}{\partial x}\nabla^2\psi + \beta\frac{\partial}{\partial x}\psi = -\frac{f_0}{D_0}U\frac{\partial}{\partial x}h' - r\nabla^2\psi \tag{4.94}$$

or:

$$(U\frac{\partial}{\partial x} + r)\nabla^2\psi + \beta\frac{\partial}{\partial x}\psi = \frac{f_0}{D_0}\frac{\partial}{\partial x}h' \tag{4.95}$$

Using the wave expressions for the topography and streamfunction, we get:

$$[(ikU + r)(-k^2 - l^2) + ik\beta]\, A = -\frac{ikf_0 U}{D_0} h_0 \tag{4.96}$$

after cancelling the exponential terms. Solving for A, we get:

$$A = \frac{f_0 h_0}{D_0(\kappa^2 - \kappa_s^2 - iR)} \tag{4.97}$$

where:

$$R \equiv \frac{r\kappa^2}{kU} \tag{4.98}$$

The difference from before is that now the wave amplitude is *complex*.

The result is similar to that without friction, except for the additional term in the denominator. This term does two things. First, it removes the singularity. At $\kappa = \kappa_s$, we have:

$$A = i\frac{f_0 h_0}{D_0 R} \tag{4.99}$$

So the response is no longer infinite. It is however still greatest at this wavenumber; having $\kappa \neq \kappa_s$ produces a weaker amplitude.

Second, friction causes a *phase shift* in the pressure field relative to the topography. Consider the response at $\kappa = \kappa_S$. Then the amplitude is purely imaginary, as seen above. Using the relation:

$$i = e^{i\pi/2}$$

we can write:

$$\psi = Ae^{ikx+ily} = \frac{f_0 h_0}{D_0 R} e^{ikx+i\pi/2+ily} \tag{4.100}$$

So the streamfunction is 90° out of phase with the mountains. Plotting the streamfunction, we find that the low pressure is downstream of the mountain and the high pressure is upstream.

For non-resonant waves, the phase shift depends on the difference between κ and κ_s. The larger the difference, the more aligned the pressure field is with the topography (either in phase, or 180° out of phase).

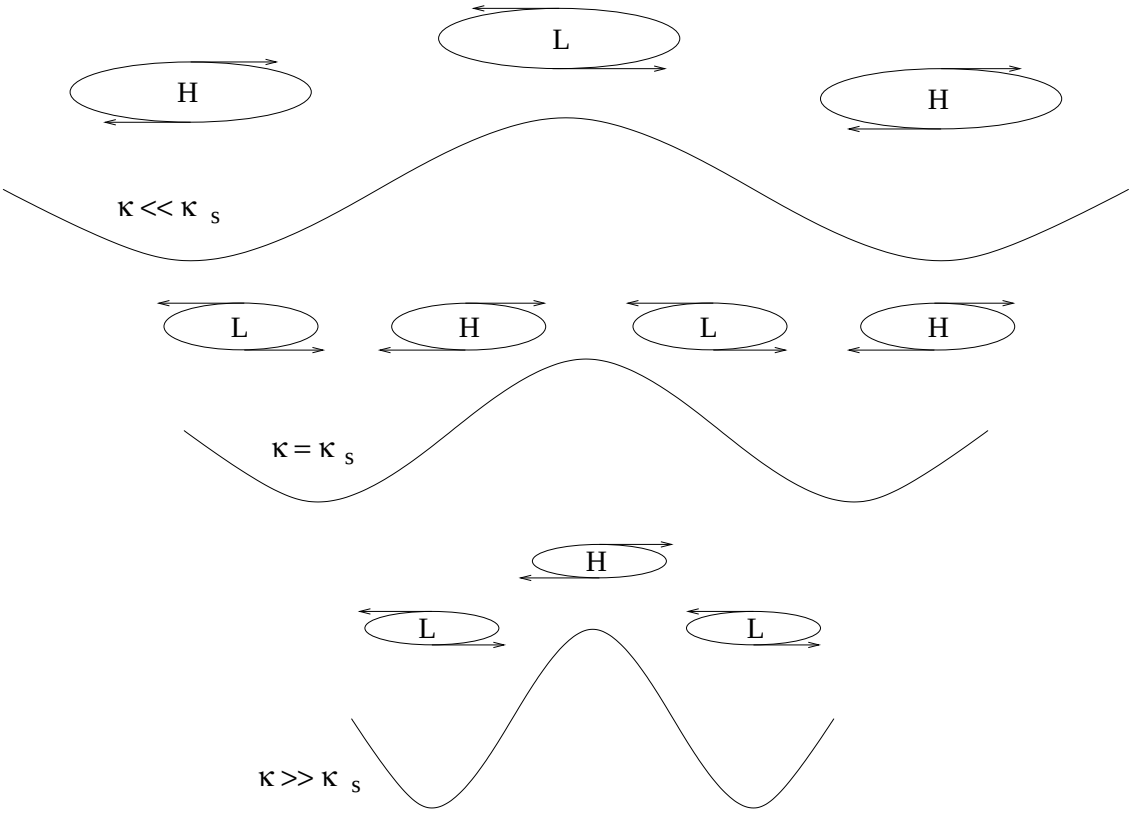

Figure 4.12: The mean pressure distribution over a sinusoidal mountain range. The topographic wavenumber is less than (upper), greater than (bottom) and equal to (middle) the stationary wavenumber.

We summarize the results with sinusoidal topography and Ekman friction graphically in Fig. (4.12). When the topographic wavenumber is much less than κ_s, the pressure field is aligned but anti-correlated with the topography. When the wavenumber is much greater than κ_s, the pressure is aligned and correlated. When $\kappa = \kappa_s$, the pressure is 90 ° out of phase with the mountains.

Charney and Eliassen (1949) applied this approach using actual atmo-

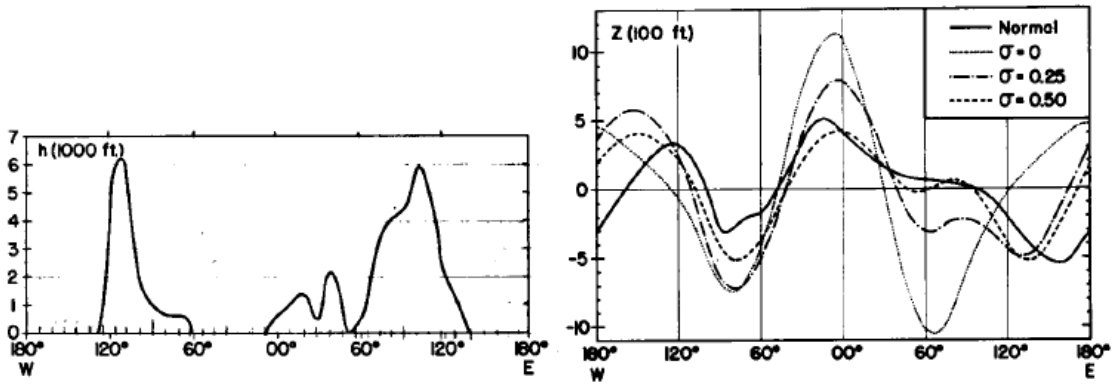

Figure 4.13: Charney and Eliassen's (1949) solution of the barotropic mountain wave problem at 45N. The topographic profile is shown in the left panel (their Fig. 3). The mean pressure at 500 mb is shown in the right panel (their Fig. 4) as the solid line. The dashed lines indicate the theoretical solutions, using three different values of friction.

spheric fields. But instead of using sinusoidal topography, they took the observed topographic profile at 45 N. The result of their calculation is shown in Fig. (4.13). The topography (left panel) has two large maxima, from the Himalayas and the Rocky Mountains. Their solutions, using three different friction parameters, is compared with the observed mean pressure at 500 mb in the right panel. The model pressure exhibits much of the same structure as the observed. Both have low pressure regions downwind of the mountains.

The agreement between the model and observations is surprisingly good, given the simplicity of the model. In fact, it is probably too good. Charney and Eliassen used a zonally-reentrant channel for their calculation (as one would do with a QG β-plane), but if one does the calculation on a sphere, the Rossby waves can disperse meridionally and the amplitude is decreased (Held, 1983). Nevertheless, the relative success of the model demonstrates the utility of Rossby wave dynamics in understanding the low frequency atmospheric response.

4.9 The Gulf Stream

Figure 4.14: Benjamin Franklin's map of the Gulf Stream. From Wikipedia.

The next example is one of the most famous in dynamical oceanography. It was known at least since the mid 1700's, when Benjamin Franklin mapped the principal currents of the North Atlantic (Fig. 4.14), that the Gulf Stream is an intense current which lies on the *western* side of the basin, near North America. The same is true of the Kuroshio Current, on the western side of the North Pacific, the Agulhas Current on the western side of the Indian Ocean, and numerous other examples. Why do these currents lie in the west? A plausible answer came from a work by Stommel (1948), based on the barotropic vorticity equation. We will consider this problem, which also illustrates the technique of *boundary layer analysis*.

We retain the β-effect and bottom Ekman drag, but neglect topography (the bottom is flat). We also include the surface Ekman layer, to allow for

wind forcing. The result is:

$$\frac{d_g}{dt}(\zeta + \beta y) = \frac{d_g}{dt}\zeta + \beta v = \frac{1}{\rho_c D_0}\nabla \times \vec{\tau}_w - r\zeta \tag{4.101}$$

We will search for steady solutions, as with the mountain waves. Moreover, we will not linearize about a mean flow—it is the mean flow itself we're after. So we neglect the first term in the equation entirely. Using the streamfunction, we get:

$$\beta \frac{\partial}{\partial x}\psi = \frac{1}{\rho_c D_0}\nabla \times \vec{\tau}_w - r\nabla^2\psi \tag{4.102}$$

For our "ocean", we will assume a square basin. The dimensions of the basin aren't important, so we will just use the region $x = [0, L]$ and $y = [0, L]$ (L might be 5000 km).

It is important to consider the geostrophic contours in this case:

$$q_s = \beta y \tag{4.103}$$

which are just latitude lines. In this case, all the geostrophic contours intersect the basin walls. From the discussion in sec. (4.2), we know that there can be no steady flows without forcing, because such a flow would be purely zonal and would have to continue through the walls. However, with forcing there can be steady flow; we will see that this flow *crosses* the geostrophic contours.

Solutions to (4.102) can be obtained in a general form, once the wind stress is specified. But Stommel used a more elegant method. The main idea is as follows. Since the vorticity equation is linear, we can express the solution as the sum of two components:

$$\psi = \psi_I + \psi_B \tag{4.104}$$

The first part, ψ_I, is that driven by the wind forcing. We assume that this part is present in the whole domain. We assume moreover that the friction is weak, and does not affect this interior component. Then the interior component is governed by:

$$\beta \frac{\partial}{\partial x} \psi_I = \frac{1}{\rho_c D_0} \nabla \times \vec{\tau} \tag{4.105}$$

This is the *Sverdrup relation*, after H. U. Sverdrup. It is perhaps the most important dynamical balance in oceanography. It states that vertical flow from the base of the surface Ekman layer, due to the wind stress curl, drives meridional motion. This is the motion across the geostrophic contours, mentioned above.

We can solve (4.105) if we know the wind stress and the boundary conditions. For the wind stress, Stommel assumed:

$$\vec{\tau} = -\frac{L}{\pi} cos(\frac{\pi y}{L}) \hat{i}$$

The wind is purely zonal, with a cosine dependence. The winds in the northern half of the domain are eastward, and they are westward in the southern half. This roughly resembles the situation over the subtropical North Atlantic. Thus the wind stress curl is:

$$\nabla \times \vec{\tau} = -\frac{\partial}{\partial y} \tau^x = -sin(\frac{\pi y}{L})$$

Again, this is the vertical component of the curl. From the Sverdrup relation (4.105), this corresponds to southward flow over the whole basin, with

the largest velocities occurring at the mid-basin ($y = L/2$). We can then integrate equation (4.105) to obtain the streamfunction in the interior.

However, one can do this in two ways: either by integrating from the western wall or *to* the eastern wall (the reason why these produce different results will become clear). Let's do the latter case first. Then:

$$\int_x^L \frac{\partial}{\partial x}\psi_I \, dx = \psi_I(L,y) - \psi_I(x,y) = -\frac{1}{\beta\rho_c D_0} \, sin(\frac{\pi y}{L})(L-x) \quad (4.106)$$

To evaluate this, we need to know the value of the streamfunction on the eastern wall, $\psi_I(L,y)$.

The boundary condition here is that there is no normal flow, i.e. $u(L,y) = 0$. From the definition of u:

$$u(L,y) = -\frac{\partial}{\partial y}\psi_I(L,y) \quad (4.107)$$

this implies that $\psi(L,y)$ must be a constant. But what is the constant? In fact, we can take this to be zero, because using any other constant would not change the velocity field. So we have:

$$\psi_I(x,y) = \frac{1}{\beta\rho_c D_0} \, sin(\frac{\pi y}{L})(L-x) \quad (4.108)$$

However, this solution has flow into the *western* wall, because:

$$u_I(0,y) = -\frac{\partial}{\partial y}\psi_I(0,y) = -\frac{\pi}{\beta\rho_c D_0} cos(\frac{\pi y}{L}) \neq 0 \quad (4.109)$$

This can't occur.

To fix the flow at the western wall, we use the second component of the flow, ψ_B. Let's go back to the vorticity equation, with the interior and boundary streamfunctions substituted in:

$$\beta\frac{\partial}{\partial x}\psi_I + \beta\frac{\partial}{\partial x}\psi_B = \frac{1}{\rho_c D_0}\nabla\times\vec{\tau}_w - r\nabla^2\psi_B \tag{4.110}$$

We have ignored the term $r\nabla^2\psi_I$. We assume this is much smaller than $r\nabla^2\psi_B$, because ψ_B has rapid variations near the wall, so the second derivative will be much larger than that of ψ_I (which has a large scale structure). Using (4.105), the vorticity equation reduces to:

$$\beta\frac{\partial}{\partial x}\psi_B = -r\nabla^2\psi_B \tag{4.111}$$

ψ_B is assumed to be vanishingly small in the interior. But it will not be small in a boundary layer, which occupies a narrow region near the western wall. Rather ψ_B will be large enough to cancel the zonal interior flow at the wall.

Thus the boundary layer will be narrow in the x-direction, but the changes in y should be more gradual (as the boundary layer will cover the entire west wall). Thus the derivatives in x will be much greater than in y. So we have:

$$\beta\frac{\partial}{\partial x}\psi_B = -r\nabla^2\psi_B \approx -r\frac{\partial^2}{\partial x^2}\psi_B \tag{4.112}$$

This has a general solution:

$$\psi_B = A\,exp(-\frac{\beta x}{r}) + B$$

In order for the boundary correction to vanish in the interior, the constant B must be zero. We then determine A by making the zonal flow vanish at the west wall (at $x = 0$). This again implies that the streamfunction is constant. That constant must be zero, because we took it to be zero on the east wall. If it were a different constant, then ψ would have to

change along the northern and southern walls, meaning $v = \frac{\partial}{\partial x}\psi$ would be non-zero. Thus we demand:

$$\psi_I(0, y) + \psi_B(0, y) = 0 \tag{4.113}$$

Thus:

$$A = -\frac{L}{\beta \rho_c D_0} \, sin(\frac{\pi y}{L}) \tag{4.114}$$

So the total solution is:

$$\psi = \frac{1}{\beta \rho_c D_0} \, sin(\frac{\pi y}{L}) \, [L - x - Lexp(-\frac{\beta x}{r})] \tag{4.115}$$

We examine the character of this solution below. But first let's see what would have happened if we integrated the Sverdrup relation (4.105) from the *western* wall instead of to the eastern. Then we would get:

$$\beta \int_0^x \frac{\partial}{\partial x}\psi \, dx = \beta\psi(x, y) - \beta\psi(0, y) = -x \, sin(\frac{\pi y}{L}) \tag{4.116}$$

Setting $\psi(0, y) = 0$, we get:

$$\psi(x, y) = -\frac{x}{\beta \rho_c D_0} \, sin(\frac{\pi y}{L}) \tag{4.117}$$

This solution has flow into the eastern wall, implying we must have a boundary layer there. Again the boundary layer should have more rapid variation in x than in y, so the appropriate boundary layer equation is (4.112), with a solution:

$$\psi_B = Aexp(-\frac{\beta x}{r}) + B$$

We take B to be zero again, so the solution vanishes in the interior.

But does it? To satisfy the zero flow condition at $x = L$, we have:

$$\psi_I(L, y) + \psi_B(L, y) = 0 \tag{4.118}$$

or:

$$-\frac{L}{\beta\rho_c D_0}\, sin(\frac{\pi y}{L}) + Aexp(-\frac{\beta L}{r}) = 0 \tag{4.119}$$

Solving for A, we get:

$$A = \frac{L}{\beta\rho_c D_0}\, exp(\frac{\beta L}{r})\ sin(\frac{\pi y}{L}) \tag{4.120}$$

So the total solution in this case is:

$$\psi = \frac{1}{\beta\rho_c D_0}\, sin(\frac{\pi y}{L})\ [-x + Lexp(\frac{\beta(L-x)}{r})] \tag{4.121}$$

Now there is a problem. The exponential term in this case does not decrease moving away from the eastern wall. Rather, it grows exponentially. So the boundary layer solution *isn't confined* to the eastern wall! Thus we reject the possibility of an eastern boundary layer. The boundary layer must lie on the western wall. This is why, Stommel concluded, the Gulf Stream lies on the western boundary of the North Atlantic.

Another explanation for the western intensification was proposed by Pedlosky (1965). Recall that Rossby waves propagate to the west as long waves, and reflect off the western wall as short waves. The short waves move more slowly, with the result that the energy is intensified in the region near the west wall (sec. 4.4.5). Pedlosky showed that in the limit of low frequencies (long period waves), the Rossby wave solution converges to the Stommel solution. So western intensification occurs because Rossby waves propagate to the west.

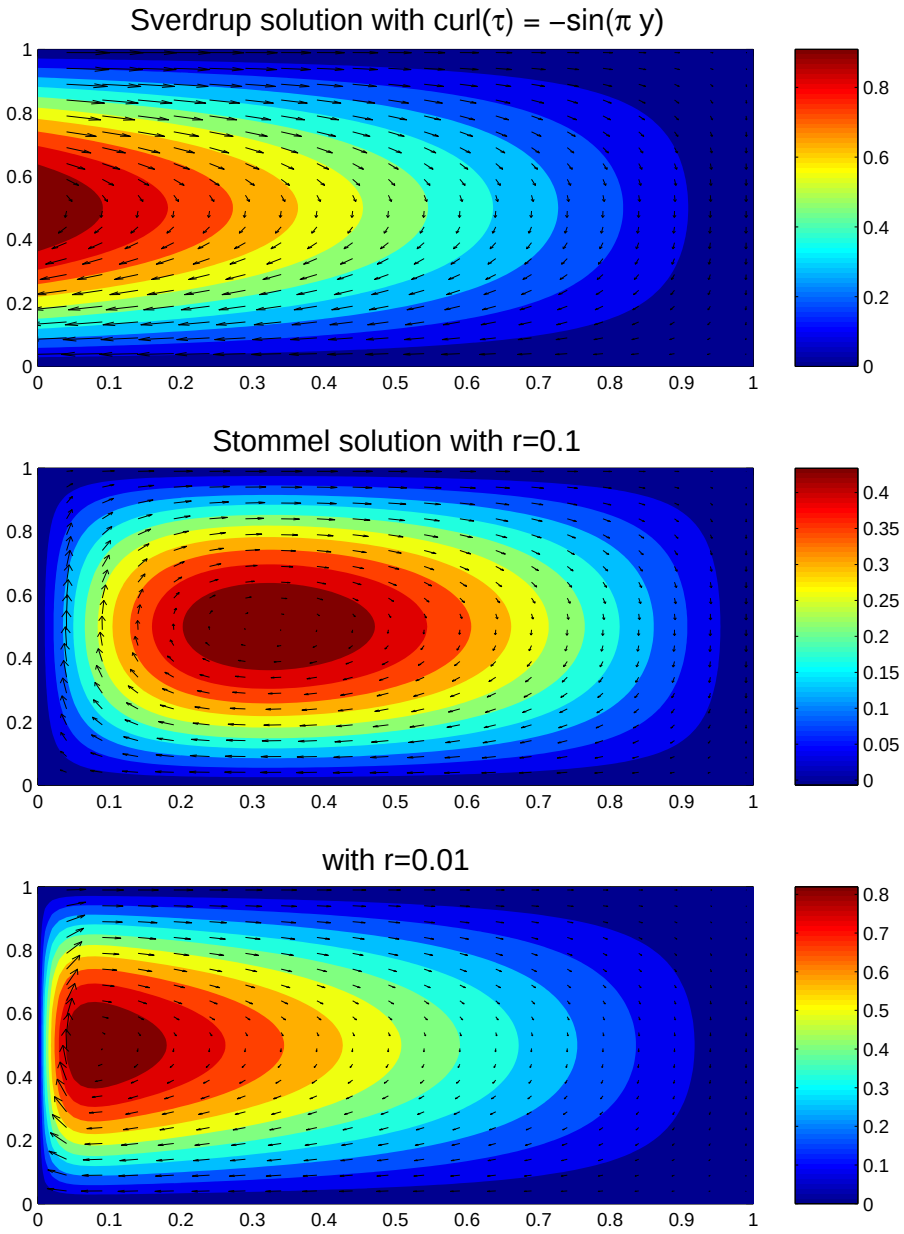

Figure 4.15: Solutions of Stommel's model for two different values of the friction coefficient, r.

Let's look at the (correct) Stommel solution. Shown in figure (4.15) is the Sverdrup solution (upper panel) and two full solutions with different r (lower panels). The Sverdrup solution has southward flow over the whole basin. So the mean flow crosses the geostrophic contours, as suggested earlier. There is, in addition, an eastward drift in the north and a westward drift in the south.

With the larger friction coefficient, the Stommel solution has a broad, northward-flowing western boundary current. With the friction coefficient 10 times smaller, the boundary current is ten times narrower and the northward flow is roughly ten times stronger. This is the Stommel analogue of the Gulf Stream.

Consider what is happening to a fluid parcel in this solution. The parcel's potential vorticity decreases in the interior, due to the negative wind stress curl, which causes the parcel to drift southward. We know the parcel needs to return to the north to complete its circuit, but to do that it must somehow acquire vorticity. Bottom friction permits the parcel to acquire vorticity in the western layer. You can show that if the parcel were in an eastern boundary layer, it's vorticity would *decrease* going northward. So the parcel would not be able to re-enter the northern interior.

The Stommel boundary layer is like the bottom Ekman layer (sec. 4.5), in several ways. In the Ekman layer, friction, which acts only in a boundary layer, brings the velocity to zero to satisfy the no-slip condition. This yields a strong vertical shear in the velocities. In the Stommel layer, friction acts to satisfy the no-normal flow condition and causes strong *lateral* shear. Both types of boundary layer also are passive, in that they do not force the interior motion; they simply modify the behavior near the boundaries.

Shortly after Stommel's (1948) paper came another (Munk, 1950) appeared which also modelled the barotropic North Atlantic. The model is similar, except that Munk used lateral friction rather than bottom friction. The lateral friction was meant to represent horizontal stirring by oceanic eddies. Munk's model is considered in one of the exercises.

4.10 Closed ocean basins

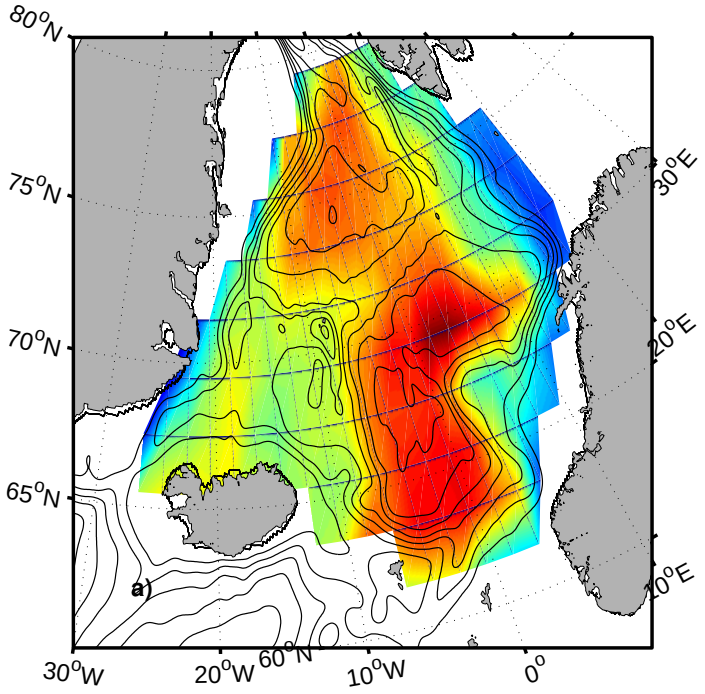

Figure 4.16: Geostrophic contours (solid lines) in the Nordic seas. Superimposed are contours showing the first EOF of sea surface height derived from satellite measurements. The latter shows strong variability localized in regions of closed q_s contours. From Isachsen et al. (2003).

Next we consider an example with bottom topography. As discussed in sec. (4.2), topography can cause the geostrophic contours to close on themselves. This is an entirely different situation because mean flows can

exist on the closed contours (they do not encounter boundaries; Fig. 4.3). Such mean flows can be excited by wind-forcing and can be very strong.

There are several regions with closed geostrophic contours in the Nordic Seas (Fig. 4.16), specifically in three basins: the Norwegian, Lofoten and Greenland gyres. The topography is thus steep enough here as to overwhelm the β-effect. Isachsen et al. (2003) examined how wind-forcing could excite flow in these gyres.

This time we take equation (4.79) with wind forcing and bottom topography:

$$\frac{d_g}{dt}(\zeta + \beta y + \frac{f_0}{D_0}h) = \frac{1}{\rho_c D_0}\nabla \times \vec{\tau} - r\zeta \tag{4.122}$$

We will linearize the equation, without a mean flow. We can write the result this way:

$$\frac{\partial}{\partial t}\zeta + \vec{u} \cdot \nabla q_s = \frac{1}{\rho_c D_0}\nabla \times \vec{\tau} - r\zeta \tag{4.123}$$

where:

$$q_s \equiv \beta y + \frac{f_0}{D_0}h$$

defines the geostrophic contours (sec.4.2). Recall that these are the so-called "f/H" contours in the shallow water system. As noted, the q_s contours can close on themselves if the topography is strong enough to overwhelm the βy contribution to q_s (Fig. 4.3). This is the case in the Nordic Seas (Fig. 4.16).

As in the Gulf Stream model, we will assume the bottom friction coefficient, r, is small. In addition, we will assume that the wind forcing and the time derivative terms are as small as the bottom friction term (of order r).

Thus the first, third and fourth terms in equation (4.123) are of comparable size. We can indicate this by writing the equation this way:

$$r\frac{\partial}{\partial t'}\zeta + \vec{u}\cdot\nabla q_s = r\frac{1}{\rho_c D_0}\nabla\times\vec{\tau}' - r\zeta \tag{4.124}$$

where $t' = rt$ and $\tau' = \tau/r$ are the small variables normalized by r, so that they are order one.

Now we use a *perturbation expansion* and expand the variables in r. For example, the vorticity is:

$$\zeta = \zeta_0 + r\zeta_1 + r^2\zeta_2 + ...$$

Likewise, the velocity is:

$$\vec{u} = \vec{u}_0 + r\vec{u}_1 + r^2\vec{u}_2 + ...$$

We plug this into the vorticity equation and then collect terms which are multiplied by the same factor of r. The largest terms are those multiplied by one. These are just:

$$\vec{u}_0\cdot\nabla q_s = 0 \tag{4.125}$$

So the first order component *follows the q_s contours*. In other words, the first order streamfunction is everywhere parallel to the q_s contours. Once we plot the q_s contours, we know what the flow looks like.

But this only tells us the *direction* of $\vec{u}_o$, not its strength or structure (how it varies from contour to contour). To find that out, we go to the next order in r:

$$\frac{\partial}{\partial t'}\zeta_0 + \vec{u}_1\cdot\nabla q_s = \frac{1}{\rho_c D_0}\nabla\times\vec{\tau}' - \zeta_0 \tag{4.126}$$

This equation tells us how the zeroth order field changes in time. However, there is a problem. In order to solve for the zeroth order field, we need to know the first order field because of the term with u_1. But it is possible to eliminate this, as follows. First, we can rewrite the advective term thus:

$$\vec{u}_1 \cdot \nabla q_s = \nabla \cdot (\vec{u}_1 q_s) - q_s(\nabla \cdot \vec{u}_1) \tag{4.127}$$

The second term on the RHS vanishes by incompressibility. In particular:

$$\nabla \cdot \vec{u} = 0 \tag{4.128}$$

This implies that the velocity is incompressible at each order. So the vorticity equation becomes:

$$\frac{\partial}{\partial t'}\zeta_0 + \nabla \cdot (\vec{u}_1 q_s) = \frac{1}{\rho_c D_0}\nabla \times \vec{\tau}' - r\zeta_0 \tag{4.129}$$

Now, we can eliminate the second term if we integrate the equation over an area bounded by a closed q_s contour. This follows from Gauss's Law, which states:

$$\iint \nabla \cdot \vec{A}\, dx\, dy = \oint \vec{A} \cdot \hat{n}\, dl \tag{4.130}$$

Thus:

$$\iint \nabla \cdot (\vec{u} q_s)\, dA = \oint q_s \vec{u} \cdot \hat{n}\, dl = q_s \oint \vec{u} \cdot \hat{n}\, dl = 0 \tag{4.131}$$

We can take the q_s outside the line integral because q_s is constant on the bounding contour. The closed integral of $\vec{u} \cdot \hat{n}$ vanishes because of incompressibility:

$$\oint \vec{u} \cdot \hat{n}\, dl = \iint \nabla \cdot \vec{u}\, dA = 0$$

Thus the integral of (4.132) in a region bounded by a q_s contour is:

$$\frac{\partial}{\partial t'} \iint \zeta_0\, dxdy = \frac{1}{\rho_c D_0} \iint \nabla \times \vec{\tau}'\, dxdy - \iint \zeta_0\, dxdy \qquad (4.132)$$

Notice this contains only zeroth order terms. We can rewrite (4.132) by exploiting Stoke's Law, which states:

$$\iint \nabla \times \vec{A}\, dx\, dy = \oint \vec{A} \cdot\, \vec{dl} \qquad (4.133)$$

So (4.132) can be rewritten:

$$\frac{\partial}{\partial t'} \oint \vec{u} \cdot \vec{dl} = \frac{1}{\rho_c D_0} \oint \vec{\tau}' \cdot \vec{dl} - \oint \vec{u} \cdot \vec{dl} \qquad (4.134)$$

We have dropped the zero subscripts, since this is the only component we will consider. In terms of the real time and wind stress, this is:

$$\frac{\partial}{\partial t} \oint \vec{u} \cdot \vec{dl} = \frac{1}{\rho_c D_0} \oint \vec{\tau} \cdot \vec{dl} - r \oint \vec{u} \cdot \vec{dl} \qquad (4.135)$$

Isachsen et al. (2003) solved (4.135) by decomposing the velocity into Fourier components in time:

$$\vec{u}(x, y, t) = \sum \tilde{u}(x, y, \omega)\, e^{i\omega t}$$

Then it is easy to solve (4.135) for the velocity integrated around the contour:

$$\oint \vec{u} \cdot \vec{dl} = \frac{1}{r + i\omega} \frac{1}{\rho_c D_0} \oint \vec{\tau} \cdot \vec{dl} \qquad (4.136)$$

Note the solution is actually for the integral of the velocity around the contour (rather than the velocity at every point). We can divide by the length of the contour to get the average velocity on the contour:

$$< u > \equiv \frac{\oint \vec{u} \cdot \vec{dl}}{\oint dl} = \frac{1}{r + i\omega} \frac{1}{\rho_c D_0} \frac{\oint \vec{\tau} \cdot \vec{dl}}{\oint dl} \tag{4.137}$$

Isachsen et al. (2003) derived a similar relation using the shallow water equations. Their expression is somewhat more complicated but has the same meaning. They tested this prediction using various types of data from the Nordic Seas. One example is shown in figure (4.16). This shows the principal Empirical Orthogonal Function (EOF) of the sea surface height variability measured from satellite. The EOF shows that there are regions with spatially coherent upward and downward sea surface motion. These regions are exactly where the q_s contours are closed. This height variability reflects strong gyres which are aligned with the q_s contours.

Isachsen et al. took wind data, the actual bottom topography and an approximate value of the bottom drag to predict the transport in the three gyres (corresponding to the Norwegian, Lofoten and Greenland basins). The results are shown in figure (4.17). The simple model does astonishingly well, predicting the intensification and weakening of the gyres in all three basins.

4.11 Barotropic instability

Many of the "mean" flows in the atmosphere and ocean, like the Jet and Gulf Streams, are not steady at all. They meander and generate eddies (storms). The reason is that these flows are *unstable*. If the flow is perturbed slightly, for instance by a slight change in heating or wind forcing,

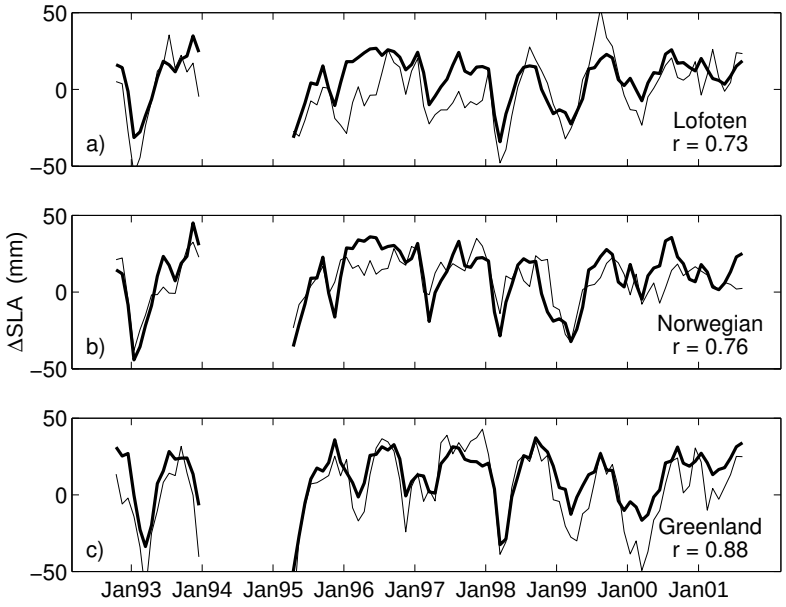

Figure 4.17: Time series of observed (thin line) and predicted (thick line) sea surface height displacements between the outer rim and the center of each of the principal gyres in the Nordic seas. The linear bottom drag coefficient was $R = 5 \times 10^{-4}$ m/sec. From Isachsen et al. (2003).

the perturbation will grow, extracting energy from the mean flow. These perturbations then develop into mature storms, both in the atmosphere and ocean.

We'll first study instability in the barotropic context. In this we ignore forcing and dissipation, and focus exclusively on the interaction between the mean flow and the perturbations. A constant mean flow, like we used when deriving the dispersion relation for free Rossby waves, is stable. But a mean flow which is *sheared* can be unstable. To illustrate this, we examine a mean flow which varies in y. We will see that wave solutions exist in this case too, but that they can grow in time.

The barotropic vorticity equation with a flat bottom and no forcing or bottom drag is:

$$\frac{d_g}{dt}(\zeta + \beta y) = 0 \tag{4.138}$$

We again linearize the equation assuming a zonal flow, but we now allow this to vary in y, i.e. $U = U(y)$. As a result, the mean flow now has *vorticity*:

$$\overline{\zeta} = -\frac{\partial}{\partial y}U \tag{4.139}$$

So the PV equation is now:

$$\frac{d_g}{dt}(\zeta' - \frac{\partial}{\partial y}U + \beta y) = 0 \tag{4.140}$$

Because the mean flow is time independent, its vorticity doesn't change in time and as such, the mean vorticity *alters the geostrophic contours*:

$$q_s = \beta y - \frac{\partial}{\partial y}U \tag{4.141}$$

This implies the mean flow will affect the way Rossby waves propagate in the system.

The linearized version of the vorticity equation is:

$$(\frac{\partial}{\partial t} + U\frac{\partial}{\partial x})\zeta' + v'\frac{\partial}{\partial y}q_s = 0 \tag{4.142}$$

Written in terms of the streamfunction, this is:

$$(\frac{\partial}{\partial t} + U\frac{\partial}{\partial x})\nabla^2\psi + (\frac{\partial}{\partial y}q_s)\frac{\partial\psi}{\partial x} = 0 \tag{4.143}$$

Now because the mean flow varies in y, we have to be careful about our choice of wave solutions. We can in any case assume a sinusoidal dependence in x and t. The form we will use is:

$$\psi = Re\{\hat{\psi}(y)\, e^{ik(x-ct)}\} \tag{4.144}$$

Recall that the amplitude can be complex, i.e.:

$$\hat{\psi} = \hat{\psi}_r + i\hat{\psi}_i$$

However, now the phase speed, c, *also* can be complex:

$$c = c_r + ic_i \tag{4.145}$$

This is an important point. With a complex c, we have:

$$e^{ik(x-ct)} = e^{ik(x-(c_r+ic_i)\,t)} = e^{ik(x-c_rt)+kc_it} \tag{4.146}$$

Thus the argument of the exponential has both real and imaginary parts. The real part determines how the phases change, as with the mountain waves. But the imaginary part affects the wave amplitude. In particular, if $c_i > 0$, the amplitude will *grow exponentially in time*. If this happens, we say the flow is *barotropically unstable*. This growth will continue such that the wave eventually becomes as strong as the background flow itself.

If we substitute the wave solution into (4.143), we get:

$$(-ikc + ikU)(-k^2\hat{\psi} + \frac{\partial^2}{\partial y^2}\hat{\psi}) + ik\hat{\psi}\frac{\partial}{\partial y}q_s = 0 \tag{4.147}$$

Cancelling the ik yields:

$$(U-c)\,(\frac{\partial^2}{\partial y^2}\hat{\psi} - k^2\hat{\psi}) + \hat{\psi}\frac{\partial}{\partial y}q_s = 0 \tag{4.148}$$

This is known as the "Rayleigh equation". The solution of this determines which waves are unstable. However, because U and q_s are functions of y, the equation is not trivial to solve.

One alternative is to solve it numerically. If you know $U(y)$, you can put that into the equation and crank out a solution (see sec. 4.11.2). But imagine you then want to examine a slightly different flow; you would have to solve the equation all over again. It would be nice if we could figure out a way to determine if the flow is unstable without actually solving (4.148). It turns out this is possible.

4.11.1 Rayleigh-Kuo criterion

We do this as follows. First we divide (4.148) by $U - c$:

$$(\frac{\partial^2}{\partial y^2}\hat{\psi} - k^2\hat{\psi}) + \frac{\hat{\psi}}{U-c}\frac{\partial}{\partial y}q_s = 0 \tag{4.149}$$

This assumes that $U \neq c$ anywhere in the flow.[3] Then we multiply by the complex conjugate of the streamfunction:

$$\hat{\psi}^* = \hat{\psi}_r - i\hat{\psi}_i$$

This yields:

$$(\hat{\psi}_r\frac{\partial^2}{\partial y^2}\hat{\psi}_r + \hat{\psi}_i\frac{\partial^2}{\partial y^2}\hat{\psi}_i) + i(\hat{\psi}_r\frac{\partial^2}{\partial y^2}\hat{\psi}_i - \hat{\psi}_i\frac{\partial^2}{\partial y^2}\hat{\psi}_r) - k^2|\hat{\psi}|^2 + \frac{|\hat{\psi}|^2}{U-c}\frac{\partial}{\partial y}q_s = 0 \tag{4.150}$$

The denominator in the last term is complex, but we can write it in a more convenient form this way:

$$\frac{1}{U-c} = \frac{1}{U-c_r-ic_i} = \frac{U-c_r+ic_i}{|U-c|^2}$$

Now the denominator is purely real. So we have:

[3] When $U = c$ at some point, the flow is said to have a *critical layer*. Then the analysis is more involved than that here.

$$(\hat{\psi}_r \frac{\partial^2}{\partial y^2}\hat{\psi}_r + \hat{\psi}_i \frac{\partial^2}{\partial y^2}\hat{\psi}_i) + i(\hat{\psi}_r \frac{\partial^2}{\partial y^2}\hat{\psi}_i - \hat{\psi}_i \frac{\partial^2}{\partial y^2}\hat{\psi}_r) - k^2|\hat{\psi}|^2$$
$$+(U - c_r + ic_i)\frac{|\hat{\psi}|^2}{|U-c|^2}\frac{\partial}{\partial y}q_s = 0 \tag{4.151}$$

This equation has both real and imaginary parts, and each must separately equal zero.

Consider the imaginary part of (4.151):

$$(\hat{\psi}_r \frac{\partial^2}{\partial y^2}\hat{\psi}_i - \hat{\psi}_i \frac{\partial^2}{\partial y^2}\hat{\psi}_r) + c_i \frac{|\hat{\psi}|^2}{|U-c|^2}\frac{\partial}{\partial y}q_s = 0 \tag{4.152}$$

Let's integrate this in y, over a region from $y = [0, L]$:

$$\int_0^L (\hat{\psi}_i \frac{\partial^2}{\partial y^2}\hat{\psi}_r - \hat{\psi}_r \frac{\partial^2}{\partial y^2}\hat{\psi}_i)\, dy = c_i \int_0^L \frac{|\hat{\psi}|^2}{|U-c|^2}\frac{\partial}{\partial y}q_s\, dy \tag{4.153}$$

We can rewrite the first terms by noting:

$$\hat{\psi}_i \frac{\partial^2}{\partial y^2}\hat{\psi}_r - \hat{\psi}_r \frac{\partial^2}{\partial y^2}\hat{\psi}_i = \frac{\partial}{\partial y}(\hat{\psi}_i \frac{\partial}{\partial y}\hat{\psi}_r - \hat{\psi}_r \frac{\partial}{\partial y}\hat{\psi}_i) - \frac{\partial}{\partial y}\hat{\psi}_i \frac{\partial}{\partial y}\hat{\psi}_r + \frac{\partial}{\partial y}\hat{\psi}_r \frac{\partial}{\partial y}\hat{\psi}_i$$
$$= \frac{\partial}{\partial y}(\hat{\psi}_i \frac{\partial}{\partial y}\hat{\psi}_r - \hat{\psi}_r \frac{\partial}{\partial y}\hat{\psi}_i) \tag{4.154}$$

Substituting this into the LHS of (4.153), we get:

$$\int_0^L \frac{\partial}{\partial y}(\hat{\psi}_i \frac{\partial}{\partial y}\hat{\psi}_r - \hat{\psi}_r \frac{\partial}{\partial y}\hat{\psi}_i)\, dy = (\hat{\psi}_i \frac{\partial}{\partial y}\hat{\psi}_r - \hat{\psi}_r \frac{\partial}{\partial y}\hat{\psi}_i)\,|_0^L \tag{4.155}$$

To evaluate this, we need the boundary conditions on ψ at $y = 0$ and $y = L$. If the flow is confined to a channel, then the normal flow vanishes at the northern and southern walls. This implies that the streamfunction is constant on those walls, and we can take the constant to be zero:

$$\hat{\psi}(0) = \hat{\psi}(L) = 0$$

Then (4.155) vanishes. Alternately we could simply choose $y = 0$ and $y = L$ to be latitudes where the perturbation vanishes (i.e. far away from the mean flow), and then (4.155) would also vanish. If the flow was periodic in y, it would also vanish because the streamfunction and its y-derivative would be the same at $y = 0$ and L.

Either way, the equation for the imaginary part reduces to:

$$c_i \int_0^L \frac{|\hat{\psi}|^2}{|U-c|^2} \frac{\partial}{\partial y} q_s \, dy = 0 \tag{4.156}$$

In order for this to be true, either c_i or the integral must be zero. If $c_i = 0$, the wave amplitude is not growing and the wave is stable. For unstable waves, $c_i > 0$. Then the integral must vanish to satisfy the equation. The squared terms in the integrand are always greater than zero, so a necessary condition for instability is that:

$$\frac{\partial}{\partial y} q_s = \beta - \frac{\partial^2}{\partial y^2} U = 0 \tag{4.157}$$

somewhere in the domain. If this is true, then the integrand is positive in part of the domain and negative in another part, and the integral is thus possibly zero. This is the *Rayleigh-Kuo criterion*. It states that *the meridional gradient of the background PV must change sign somewhere in the domain*, and that:

The PV gradient can only change sign if there is a mean flow. If $U = 0$, then $q_s = \beta y$ and we have Rossby waves, all of which propagate westward. But with $U_{yy} \neq 0$, the wave propagation changes with latitude, and instability is possible.

However, we can only state that the flow *may* be unstable (because the integral in 4.156 may still not be zero). As such, the Rayleigh-Kuo criterion is a *necessary condition* for instability, but it is not a *sufficient condition*. Having $\frac{\partial}{\partial y}q_s$ vanish doesn't guarantee that a jet will be unstable. On the other hand, the opposite case is a sufficient condition; if the gradient does *not* change sign, the jet must be stable.

As noted, the Rayleigh-Kuo condition is useful because we don't actually need to solve for the unstable waves to see if the jet is unstable. We can evaluate the potential for instability by making a simply calculation involving the jet profile.

One can derive another stability criterion, following Fjørtoft (1950), by taking the real part of (4.151). The result is similar to the Rayleigh-Kuo criterion, but a little more specific. Some flows which are unstable by the Rayleigh criterion may be stable by Fjørtoft's. However this is fairly rare. Details are given in Appendix (6.5).

4.11.2 Stability of a barotropic jet

Now we examine a specific example of a barotropically unstable jet. This has the following profile:

$$U(y) = U_0\, sech^2(by) \tag{4.158}$$

This is called a "Bickley jet", a well-known profile in fluid dynamics. It is similar to a Gaussian, and is frequently used in the literature. The jet profile, with $b = 5$, is plotted in the left panel of Fig. (4.18). Note the parameters have been set so that that $\beta = L = 1$, to simplify things.

Shown in the middle and right panels is $\beta - \frac{\partial^2}{\partial y^2}U$. Taking derivatives, this is:

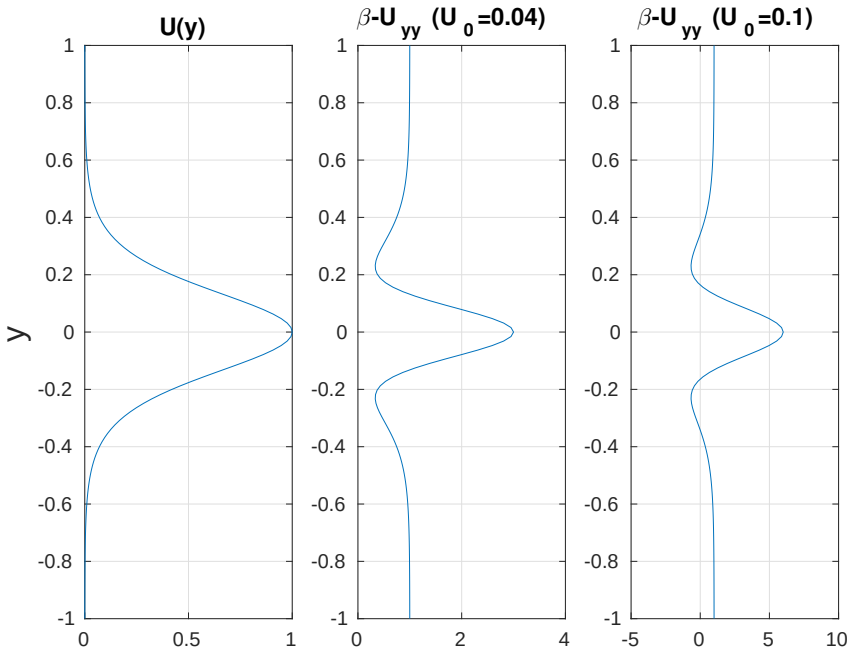

Figure 4.18: An eastward jet (left panel). The middle and right panels show $\beta - \frac{\partial^2}{\partial y^2} u$ for the jet with amplitudes of 0.04 and 0.1, respectively. Only the latter satisfies Rayleigh's criterion for instability.

$$\beta - Uyy = \beta - 2b^2\, U_0\, sech^2(by)[3\, tanh^2(by) - 1] \tag{4.159}$$

This is plotted for two jet amplitudes, U_0. With $U_0 = 0.04$ (middle panel), the PV gradient is positive everywhere, so the jet is stable. With $U_0 = 0.1$ (right panel), the PV gradient changes sign both to the north and south of the jet maximum. So the latter jet *may* be unstable.

What happens if the jet is westward? This is shown in Fig. (4.19). Now with both amplitudes, $\beta - \frac{\partial^2}{\partial y^2} U$ is negative at the centers of the jets, meaning the jet may be unstable in both cases. Generally westward jets tend to be more unstable than eastward ones.

To know what type of eddies result from the instability requires solving the instability equation (4.148), with this profile. This is very difficult to

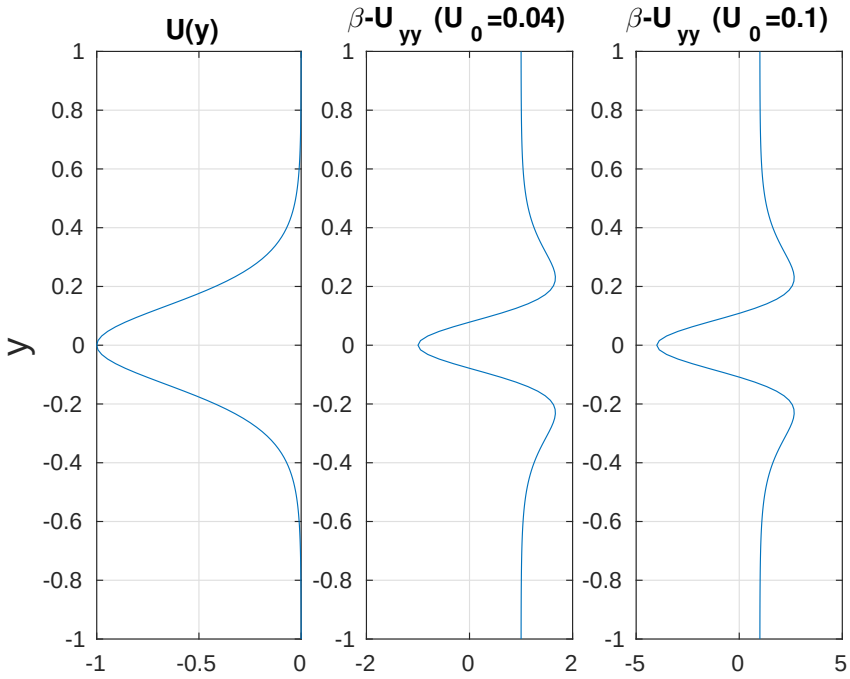

Figure 4.19: A westward jet (left panel). The middle and right panels again show $\beta - \frac{\partial^2}{\partial y^2} u$ for the jet, with amplitudes of 0.04 and 0.1. Note that both satisfy Rayleigh's criterion for instability.

do analytically (as with most mean velocity profiles). But it is relatively straightforward to do this numerically.

To solve the problem, we re-write equation (4.148) this way:

$$U\,(\frac{\partial^2}{\partial y^2}\hat{\psi} - k^2\hat{\psi}) + \hat{\psi}\frac{\partial}{\partial y}q_s = c(\frac{\partial^2}{\partial y^2}\hat{\psi} - k^2\hat{\psi}) \tag{4.160}$$

We can write this as a matrix equation:

$$A\psi = cB\psi \tag{4.161}$$

where:

$$A = U(y)(D^2 - k^2) + \frac{\partial}{\partial y}q_s, \quad B = (D^2 - k^2)$$

if D is a differentiation matrix. This is known as a *generalized eigenvalue*

problem. The eigenvalues are the phase speeds, c, and each c has a corresponding eigenvector. The Matlab routine "eig" can be used to solve this, given appropriate boundary conditions.

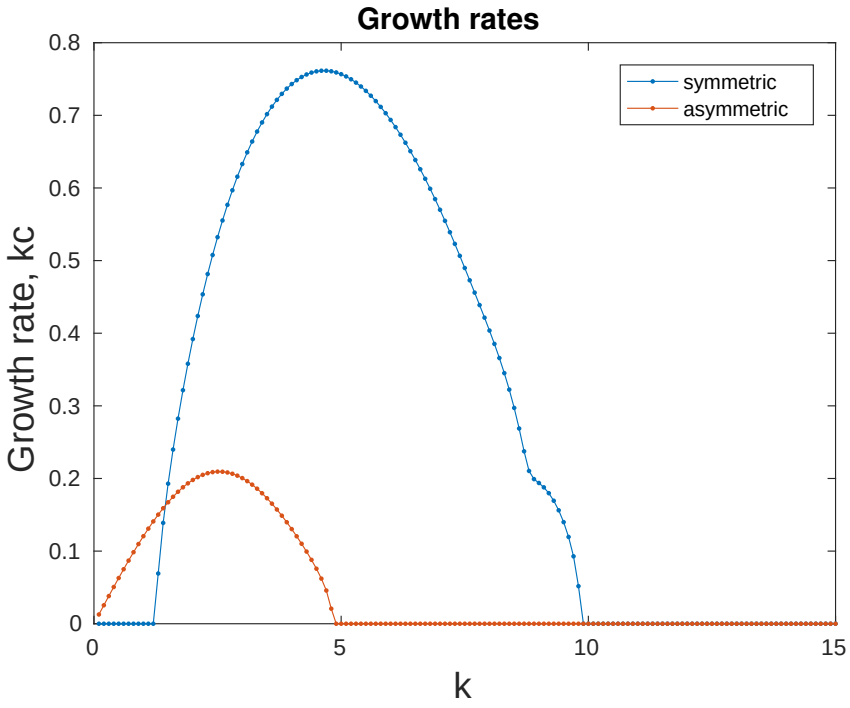

Figure 4.20: The growth rates, kc_i, for symmetric and asymmetric modes, for an eastward $sech^2$ jet with amplitude $U_0 = 1$ and a width $L = 0.2$.

We'll assume the flow is confined to an east-west channel, from $x = [0, 2\pi]$ and $y = [-1, 1]$, with a $sech^2$ jet centered on $y = 0$ (as in Fig. 4.18). We set $\beta = U_0 = 1$ (this can be done by "non-dimensionalizing" the governing equation). The jet width, which is given by $1/b$, is 0.2 here.

As discussed above, this profile should be unstable from the Rayleigh-Kuo criterion. We solve the problem in Matlab, using 200 grid points in the cross-channel direction. We do this for a range of values of the zonal wavenumber, k, and obtain the phase speed for each value.

Since the jet is symmetric around $y = 0$, it's possible to show the solutions are either symmetric or asymmetic about $y = 0$. Shown in Fig.

(4.20) are the growth rates, kc_i, for both types of mode. The rates are plotted against the wavenumber, k.

The curves show that there are a range of wavenumbers which produce unstable solutions. Also, there are *no* unstable solutions if the wavenumber is greater than roughly $k = 10$. This means that small scale disturbances will not grow, they will simply be advected by the jet. Thus the instability has a "short wave cut-off", because short waves are stable.

Larger waves on the other hand will grow in time. The fastest growing are the symmetric waves (blue curve). These are unstable over a range of wavenumbers, from roughly $k = 1.5 - 10$. Thus the largest symmetric waves are also stable (this is due to the β-effect). The maximum occurs at $k = 4.8$, with a maximum growth rate of 0.9. We refer to this as the "most unstable wave". If there was a range of disturbances initially, we'd expect to see this wave emerge first, with a wavelength of $2\pi/(4.8)$.

The asymmetric modes (red curve) have smaller growth rates. However, for wavenumbers less than $k = 1.5$, only the asymmetric modes are unstable. Thus if the initial disturbance is large enough, it will yield an asymmetric unstable mode (growing more slowly than the smaller symmetric modes). The maximum growth for the asymmetric modes occurs at $k = 2.9$.

The most unstable modes are plotted in Fig. (4.21). The symmetric mode (upper panel) has maxima centered on the jet axis and resembles a train of high and low pressures. The maxima have a meridional extent which mirrors that of the jet, i.e. twice $0.2 = 0.4$. The asymmetric mode (lower panel), has a longer wavelength than the symmetric mode, and has maxima on the flanks of the jet axis.

What happens in such cases is that as the unstable waves grow in time,

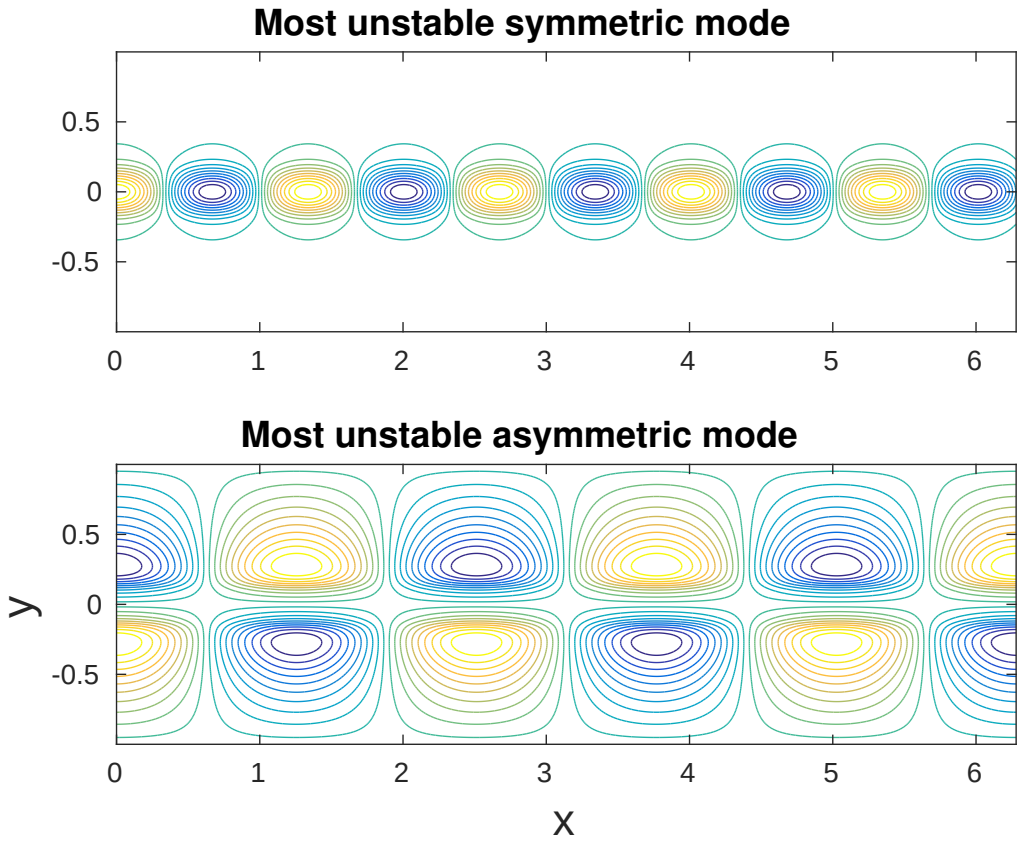

Figure 4.21: The most unstable symmetric and asymmetric waves for the eastward $sech^2$ jet.

they extracts energy from the jet. At some point, the waves become as strong as the jet itself, and then the jet is obscured by the waves. An asymmetric mode, like that in Fig. (4.21b), causes the jet to bulge and narrow and as such is often referred to as a "varicose mode". A symmetric mode on the other hand causes the jet to *meander*, i.e. to shift north and south. Given that the symmetric mode grows faster here, we expect that meandering would be favored with this profile. Meandering is common in the atmosphere and ocean, occurring both in the atmospheric Jet Streams and in the major oceanic jets, like the Gulf Stream.

4.11.3 Simulations and observations

To capture the eddies depleting energy from a jet requires a fully nonlinear numerical simulation. In the linear instability calculation, the jet profile is fixed, and thus it cannot weaken. An example of a nonlinear simulation is shown in Fig. (4.22). This involves a jet with a Gaussian profile of relative vorticity:

$$\zeta = -\frac{\partial}{\partial y}U = Ae^{-y^2/L^2} \tag{4.162}$$

The author chose moreover to set $\beta = 0$, so the PV gradient is:

$$\frac{\partial}{\partial y}q_s = -\frac{\partial^2}{\partial y^2}U = -\frac{2y}{L^2}Ae^{-y^2/L^2} \tag{4.163}$$

This is zero at $y = 0$, and thus satisfies Rayleigh's criterion. In the simulation (Fig. 4.22), the jet begins to meander and then wraps up, into a "street" of vortices. These have positive vorticity, like the jet itself.

An actual example of barotropic instability, in the atmosphere, is seen in Fig. (4.23). This shows three infrared satellite images of water vapor above the US. Note the dark band which stretches over the western US in into Canada. This is a dark filament of air, near the tropopause. This is dry air, probably from the stratosphere. We see the filament is rolling up into vortices, much like in the numerical simulation in (4.22).

An example of barotropic instability in the ocean, from the southern Indian and Atlantic Oceans, is shown in Figs. (4.24-4.26). Shown in (4.24) is a Stommel-like solution for the region. Africa is represented by a barrier attached to the northern wall, and the island to its east represents Madagascar. The wind stress curl is indicated in the right panel; this is negative in the north, positive in the middle and negative in the south.

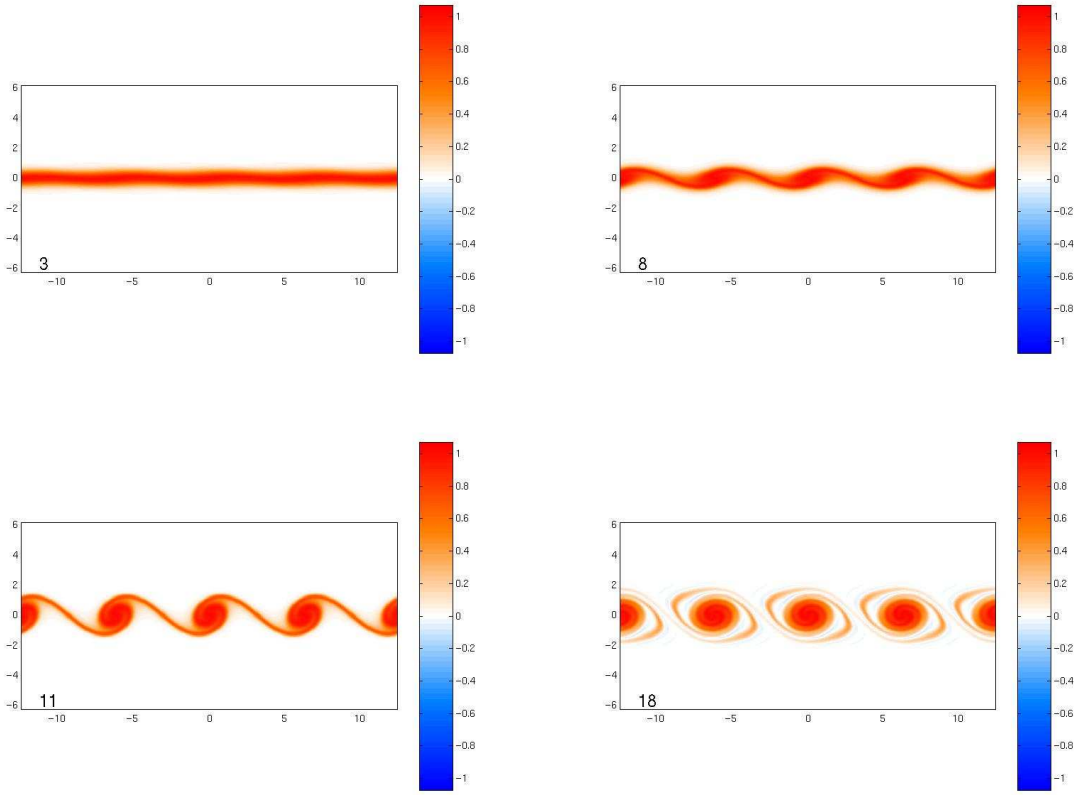

Figure 4.22: Barotropic instability of a jet with a Gaussian profile in relative vorticity. Courtesy of G. Hakim, Univ. of Washington.

In the southern part of the domain, the flow is eastward. This represents the Antarctic Circumpolar Current (the largest ocean current in the world). In the "Indian Ocean", the flow is to the west, towards Madagascar. This corresponds to the South Equatorial Current, which impinges on Madagascar. There are western boundary currents to the east of Africa and Madagascar. The boundary currents east of Madagascar flow westward toward Africa in two jets, to the north and south of the Island. Similarly, the western boundary current leaves South Africa to flow west and join the flow in the South Atlantic.

Shown in Fig. (4.25) is the PV gradient for this solution, in the region near South Africa and Madagascar. Clearly the gradient is dominated by

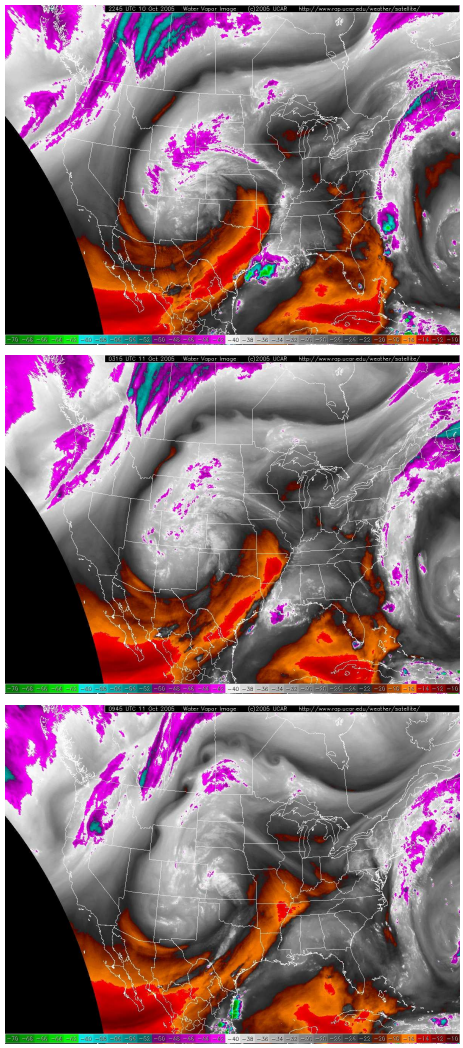

Figure 4.23: Barotropic instability of a filament of dry air, observed from water vapor infrared satellite imagery. The images were taken on the 11th of October, 2005, at 22:45 pm, 3:15 am and 9:45 am, respectively. Courtesy of G. Hakim, Univ. of Washington.

the separated jets. Moreover, the gradient changes sign several times in each of the jets. So we would expect the jets might be unstable, by the Rayleigh-Kuo criterion.

A snapshot from a numerical solution of the barotropic flow is shown in Fig. (4.26). In this simulation, the mean observed winds were used to drive the ocean, which was allowed to spin-up to a statistically steady state. The figure shows a snapshot of the sea surface height, after the model has spun

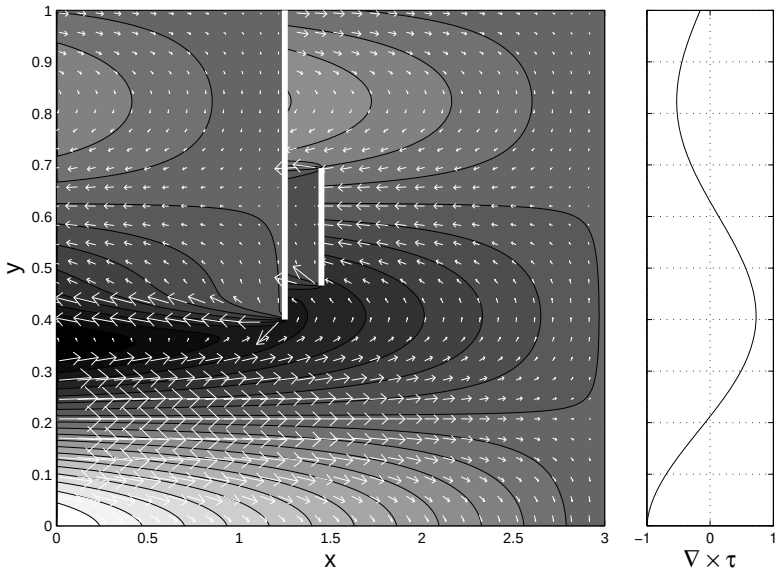

Figure 4.24: A Stommel-like solution for the Indian Ocean. The curl of the wind stress is indicated in the right panel. From LaCasce and Isachsen (2007).

up. We see that all three of the eastward jets have become unstable and are generating eddies (of both signs). The eddies drift westward, linking up with the boundary currents to their west.

Barotropic instability occurs when the lateral shear in a current is too large. The unstable waves extract energy from the mean flow, reducing the shear by mixing momentum laterally. However, in the atmosphere *baroclinic instability* is more important, and this results in storm formation. Under baroclinic instability, unstable waves act to reduce the *vertical shear* of the mean flow. In order to study that, we have to take account of density changes.

4.12 *Exercises*

4.1. Barotropic Rossby waves

a) Write down the expression for the Rossby wave phase speed, given

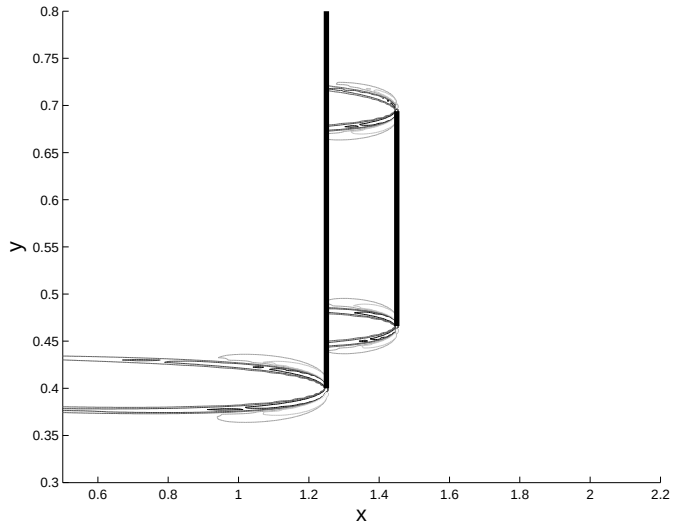

Figure 4.25: The PV gradient for the solution in Fig. (4.24). The gradient changes sign rapidly in the three jet regions. From LaCasce and Isachsen (2007).

a constant mean velocity, U.

b) Let $U = 0$ and $\beta = 1$. Consider the following wave:

$$\psi = Acos(5.1x + 2y - \omega_1 t) \tag{4.164}$$

What is the frequency ω_1? What is the phase speed in the $x-$direction, c_x? What is the group velocity in the x-direction, c_{gx}?

c) Now let the wave be the sum of two waves:

$$\psi = Acos(5.1x + 2y - \omega_1 t) + Acos(4.9x + 2y - \omega_2 t) \tag{4.165}$$

What is the group velocity in the x-direction of this wave?

4.2. Topographic Rossby waves

Bottom topography, like the β-effect, can support Rossby-like waves, called *topographic waves*. To see this, use the linearized version of

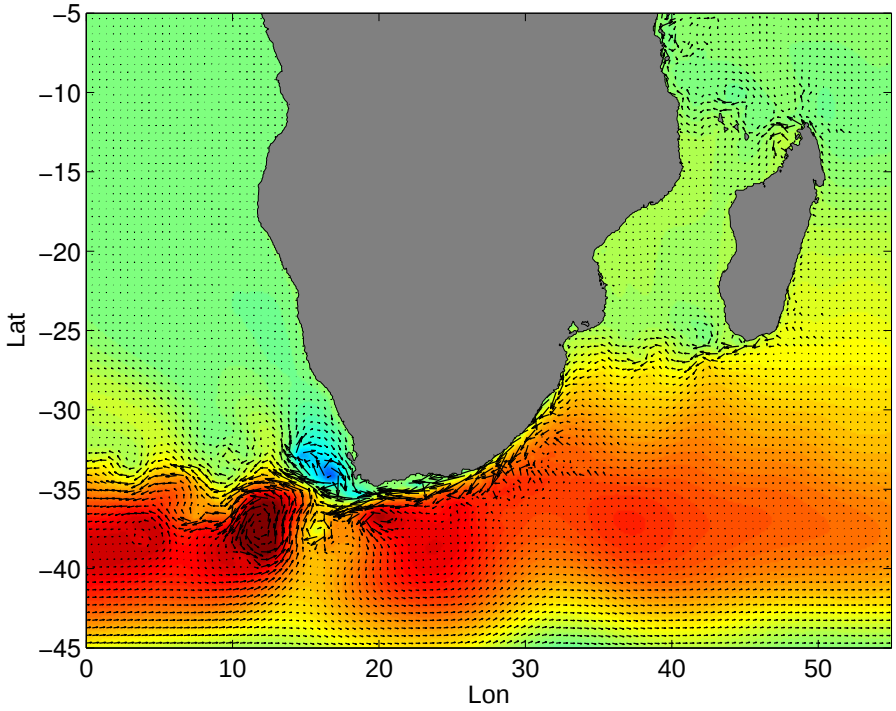

Figure 4.26: The sea surface height from a barotropic numerical simulation of the southern Indian and Atlantic Oceans. From LaCasce and Isachsen (2007).

the barotropic PV equation (4.9) with β=0 (a constant Coriolis parameter). Assume the depth is given by:

$$H = H_0 - \alpha x \tag{4.166}$$

Derive the phase speed (in the y-direction) for the waves, assuming no background flow ($U = V = 0$). Which way do the waves propagate, relative to the shallower water? What if $\alpha < 0$? What about in the southern hemisphere?

4.3. Mixed planetary-topographic waves (optional)

Now consider what happens when you have both a bottom slope and β. Say the depth is again given by:

$$H = H_0 - \alpha x$$

and that there is no forcing.

a) Simplify the barotropic PV equation, assuming no mean flow ($U = 0$).

b) Propose a wave solution.

c) Solve the equation and derive the dispersion relation.

d) What is the phase speed in the x-direction? What about in the y-direction? Which way are they going?

e) (Hard): How would you *rotate the coordinate system*, so that the new x-direction is parallel to the q_s contours?

f) Which way will the waves propagate in the new coordinate system? If you don't have the solution to (e), use your intuition.

4.4. Basin Rossby waves

We solved the Rossby wave problem on an infinite plane. Now consider what happens if there are solid walls. Start with the linear vorticity equation, with no mean flow ($U = 0$). Assume the variations in y are weak, so that you can approximate the vorticity by $\frac{\partial}{\partial x}v$. For the boundary conditions, let $\psi = 0$ at $x = 0$ and $x = L$—this ensures that there is no flow into the walls. What are the solutions for ω and k?

Hint 1: Assume $\psi = A(x)cos(kx - \omega t)$

Hint 2: Impose the boundary conditions on A.

Hint 3: The coefficients of the sine and cosine terms should both be zero.

Hint 4: The solutions are *quantized* (have discrete values).

4.5. Rossby wave reflection

Consider Rossby waves incident on a northern wall, i.e. oriented east-west, located at $y = 0$. Proceed as before, with one incident and one reflected wave. What can you say about the reflected wave?

Hint: there are two possibilities, depending on the sign of l_r.

4.6. Stress in the bottom Ekman layer

Derive the stress in the bottom Ekman layer. Show that it is 45° to the left of the geostrophic velocity. As such it is 90° to the *right* of the Ekman transport. Note that this contrasts with the surface, where the transport is to the right of the surface stress.

Note: having the stress in the same direction as the flow seems paradoxical. However, the depth-integrated, linear x-momentum equation is:

$$\frac{\partial}{\partial t}U - fV = -\frac{1}{\rho_c}\int_0^\delta \frac{\partial}{\partial x}p - \frac{\tau^x}{\rho_c}$$

if U and V are the transports in the Ekman layer. So a positive bottom stress acts to decelerate U.

4.7. Mountain waves (optional)

Consider Rossby waves with an isolated mountain range. A purely sinusoidal mountain range is not very realistic. A more typical case

is one where the mountain is localized. Consider a mountain "range" centered at $x = 0$ with:

$$h(x, y) = h_0 \, e^{-x^2/L^2} \tag{4.167}$$

Because the range doesn't vary in y, we can write $\psi = \psi(x)$.

Write the wave equation, without friction. Transform the streamfunction and the mountain using the Fourier cosine transform. Then solve for the transform of ψ, and write the expression for $\psi(x)$ using the inverse transform (it's not necessary to evaluate the inverse transform).

Where do you expect the largest contribution to the integral to occur (which values of k)?

4.8. Sverdrup transport

Consider the following wind profiles. For each one, calculate a) the associated Ekman transport, b) the vertical velocity at the base of the Ekman layer and c) the Sverdrup transport in the underlying ocean.

- $\vec{\tau}^w = T_0 \, \hat{i}$
- $\vec{\tau}^w = T_0 \, cos(\frac{\pi y}{L}) \, \hat{i}$ (assuming a domain with $y = [0, L]$.
- $\vec{\tau}^w = T_0 \, exp(-\frac{(y-L/2)^2}{D^2}) \, \hat{i}$ (where $D = L/10$).

4.9. Is there really western intensification?

To convince ourselves of this, we can solve the Stommel problem in 1-D, as follows. Let the wind stress be given by:

$$\vec{\tau} = y\hat{i} \tag{4.168}$$

Write the vorticity equation following Stommel (linear, U=V=0, steady). Ignore variations in y, leaving a 1-D equation. Assume the domain goes from $x = 0$ to $x = L$, as before. Solve it.

Note that you should have two constants of integration. This will allow you to satisfy the boundary conditions $\psi = 0$ at $x = 0$ and $x = L$. Plot the meridional velocity $v(x)$. Assume that $(\beta\rho_c D_0)^{-1} = 1$ and $L(r\rho_c D)^{-1} = 10$. Where is the jet?

4.10. Barotropic instability.

We have a region with $0 \leq x < 1$ and $-1 \leq y < 1$. Consider the following velocity profiles:

a) $U = 1 - y^2$

b) $U = exp(-y^2)$

c) $U = sin(\pi y)$

d) $U = \frac{1}{6}y^3 + \frac{5}{6}y$

Which profiles are unstable by the Rayleigh-Kuo criterion if $\beta = 0$? How large must β be to stabilize *all* the profiles? Note that the terms here have been non-dimensionalized, so that β can be any number (e.g. an integer).

4.11. Instability over a slope (optional)

Consider a barotropic flow over the continental slope in the ocean. There is no forcing and no Ekman layer, and $\beta = 0$. The water depth is given by:

$$H = D - \alpha x \tag{4.169}$$

The flow is confined to a channel, with walls at $x = 0$ and $x = L$ (Fig. 4.27). There are no walls at the northern and southern ends; assume that the flow is periodic in the y-direction.

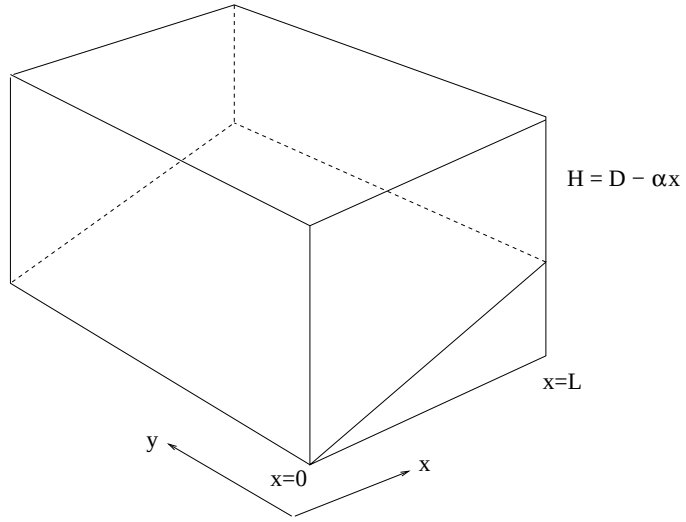

Figure 4.27: A channel with a bottom slope.

a) What is the PV equation governing the dynamics in this case? What are the boundary conditions?

b) Linearize the equation, assuming no mean flow. What is an appropriate wave solution? Substitute the wave solution to find a dispersion relation.

c) Now assume there is a mean flow, $V = V(x)\,\hat{j}$ (which follows the bottom topgraphy). Linearize the equation in (a) assuming this mean flow. What are the q_s contours?

d) Write down an appropriate wave solution for this case. Note that $V(x)$ can be any function of x. Substitute this into the PV equation. Then multiply the equation by the complex conjugate of the wave amplitude, and derive a condition for the stability of V.

Chapter 5

Synoptic scale baroclinic flows

We will now examine what happens with vertical shear. In this case the winds at higher levels need not be parallel to or of equal strength with those at lower levels, and surface currents in the ocean can be quite different from those near the bottom. Baroclinic flows are inherently more three dimensional than barotropic ones. Nevertheless, we will see that we get the same type of solutions with baroclinic flows as with barotropic ones. We have baroclinic Rossby waves, mountain waves and baroclinic instability. These phenomena involve some modifications though.

5.1 Vorticity equation

Consider the vorticity equation (4.2):

$$(\frac{\partial}{\partial t} - \frac{\partial \psi}{\partial y}\frac{\partial}{\partial x} + \frac{\partial \psi}{\partial y}\frac{\partial}{\partial x})(\nabla^2\psi + f) = f_0\frac{\partial}{\partial z}w \tag{5.1}$$

This equation was derived from the shallow water equations. However, at synoptic scales, the vertical advection of momentum is much weaker than horizontal advection. As such, the horizontal momentum equations are *quasi-horizontal*, meaning we can neglect the terms with w in them. Cross-differentiating the momentum equations and then invoking incompressibil-

ity produces the same vorticity equation above. This works equally well with baroclinic flows as barotropic ones at synoptic scales.

For atmospheric flows, we use the pressure coordinate version of the vorticity equation. This is nearly the same:

$$(\frac{\partial}{\partial t} - \frac{\partial \psi}{\partial y}\frac{\partial}{\partial x} + \frac{\partial \psi}{\partial y}\frac{\partial}{\partial x})(\nabla^2\psi + f) = f_0\frac{\partial}{\partial p}\omega \tag{5.2}$$

These equations have two unknowns, ψ, and w or ω. With a barotropic flow, one can eliminate w or ω by integrating over the depth of the fluid. Then the vertical velocity only enters at the upper and lower boundaries. But for baroclinic flows, in which u and v vary with height, we require a second equation to close the system.

5.2 Density Equation

For this, we use the equation for the fluid density (temperature). In the atmosphere, we have the thermodynamic equation (1.64):

$$c_p\frac{d(ln\theta)}{dt} = \frac{J}{T} \tag{5.3}$$

With zero heating, $J = 0$, implying:

$$\frac{d\theta}{dt} = 0 \tag{5.4}$$

i.e. the potential temperature is conserved. This equation can be rewritten in terms of ψ and ω and then combined with the pressure coordinate version of the vorticity equation (Appendix 6.6).

To illustrate this, we'll use the thermodynamic equation for the ocean:

$$\frac{d\rho}{dt} = \frac{\partial}{\partial t}\rho + \vec{u}\cdot\nabla\rho = 0 \tag{5.5}$$

Here the velocity here is the full velocity, not just the geostrophic one.

As in sec. (2.1), we can decompose the pressure and density into static and moving parts:

$$p = p_0(z) + p'(x, y, z, t), \quad \rho = \rho_0(z) + \rho'(x, y, z, t)$$

where the dynamic terms are much smaller:

$$|\rho'| \ll \rho_0, \quad |p'| \ll p_0 \tag{5.6}$$

Both the static and dynamic parts are separately in hydrostatic balance:

$$\frac{\partial}{\partial z} p_0 = -\rho_0 g, \quad \frac{\partial}{\partial z} p' = -\rho' g \tag{5.7}$$

Inserting these into the density equation yields:

$$\left(\frac{\partial}{\partial t} + u\frac{\partial}{\partial x} + v\frac{\partial}{\partial y} + w\frac{\partial}{\partial z}\right)\rho' + w\,\frac{\partial}{\partial z}\rho_0 = 0 \tag{5.8}$$

Now we simplify this by replacing the horizontal velocities with the geostrophic ones, and neglecting the vertical advection of the perturbation density gradient compared to that of the background density gradient:

$$\left(\frac{\partial}{\partial t} + u_g\frac{\partial}{\partial x} + v_g\frac{\partial}{\partial y}\right)\rho' + w\,\frac{\partial}{\partial z}\rho_0 = 0 \tag{5.9}$$

Using hydrostatic balance, we can re-write this as:

$$\left(\frac{\partial}{\partial t} + u_g\frac{\partial}{\partial x} + v_g\frac{\partial}{\partial y}\right)\frac{\partial p'}{\partial z} - gw\,\frac{\partial}{\partial z}\rho_0 = 0 \tag{5.10}$$

after multiplying through by $-g$. Lastly, we use the geostrophic stream-function (4.15) to get:

$$\left(\frac{\partial}{\partial t} - \frac{\partial\psi}{\partial y}\frac{\partial}{\partial x} + \frac{\partial\psi}{\partial x}\frac{\partial}{\partial y}\right)\frac{\partial\psi}{\partial z} + \frac{N^2}{f_0}w = 0 \tag{5.11}$$

This is the quasi-geostrophic density equation. Here N^2 is the *buoyancy frequency*:

$$N^2 = -\frac{g}{\rho_c}\frac{d\rho_0}{dz} \tag{5.12}$$

The buoyancy frequency is a measure of the stratification in z-coordinates. It reflect the frequency of oscillation of parcels in a stably stratified fluid which are displaced up or down (see problem 3.1).

Consider what the density equation means. If there is vertical motion in the presence of background stratification, the perturbation density will change. For example, if the background density decreases going up (as it must for a stably stratified fluid), a rising parcel has:

$$w\frac{\partial}{\partial z}\rho_0 < 0$$

This implies that the pertubation density must increase in time. So as the parcel rises, it becomes heavier relative to the background density.

There is an interesting parallel here. The vorticity equation implies that *meridional* motion changes the parcels *vorticity*. Here we see that *vertical* motion affects its *density*. The two effects are intimately linked when you have baroclinic instability (sec. 5.8).

5.3 QG Potential vorticity

We now have two equations with two unknowns. It is straightforward to combine them to produce a single equation with only one unknown, by eliminating w from (5.1) and (5.11). First we multiply (5.11) by f_0^2/N^2 and take the derivative with respect to z:

$$\frac{\partial}{\partial z}\left(\frac{f_0^2}{N^2}\frac{\partial}{\partial t}\frac{\partial \psi}{\partial z}\right) + \frac{\partial}{\partial z}\left[\vec{u}_g \cdot \nabla\left(\frac{f_0^2}{N^2}\frac{\partial \psi}{\partial z}\right)\right] = -f_0\frac{\partial}{\partial z}w \tag{5.13}$$

The second term can be expanded thus:

$$(\frac{\partial}{\partial z}\vec{u}_g)\cdot\nabla(\frac{f_0^2}{N^2}\frac{\partial\psi}{\partial z})+\vec{u}_g\cdot\nabla(\frac{\partial}{\partial z}(\frac{f_0^2}{N^2}\frac{\partial\psi}{\partial z}))$$

The first term vanishes. You can see this by writing the velocity in terms of the streamfunction:

$$\frac{f_0^2}{N^2}[-\frac{\partial}{\partial z}(\frac{\partial\psi}{\partial y})\frac{\partial}{\partial x}(\frac{\partial\psi}{\partial z})+\frac{\partial}{\partial z}(\frac{\partial\psi}{\partial x})\frac{\partial}{\partial y}(\frac{\partial\psi}{\partial z})]=0 \tag{5.14}$$

The physical reason for this is that the the geostrophic velocity is parallel to the pressure; thus the dot product between $(\frac{\partial}{\partial z}\vec{u}_g)$ and the gradient of $\frac{\partial}{\partial z}\psi$ must be zero. So (5.13) reduces to:

$$(\frac{\partial}{\partial t}+\vec{u}_g\cdot\nabla)\,[\frac{\partial}{\partial z}(\frac{f_0^2}{N^2}\frac{\partial\psi}{\partial z})]=-f_0\frac{\partial}{\partial z}w$$

If we combine this with (5.1), we get:

$$(\frac{\partial}{\partial t}+\vec{u}_g\cdot\nabla)\,[\nabla^2\psi+\frac{\partial}{\partial z}(\frac{f_0^2}{N^2}\frac{\partial\psi}{\partial z})+\beta y]=0 \tag{5.15}$$

This is the *quasi-geostrophic potential vorticity* (QGPV) equation. It has only one unknown, ψ. The equation implies that the potential vorticity:

$$q=\nabla^2\psi+\frac{\partial}{\partial z}(\frac{f_0^2}{N^2}\frac{\partial\psi}{\partial z})+\beta y \tag{5.16}$$

is *conserved following a parcel moving with the geostrophic flow*. This is a powerful constraint. Without forcing, the flow evolves such that q is only redistributed, not changed.

The first term in the QGPV is the QG relative vorticity and the third term is the planetary vorticity, as seen before. The second term is new

though; this is the *stretching vorticity*. This is related to vertical gradients in the density.

The QGPV equation can be used to model synoptic scale flows. If one to solve this numerically, it would require several steps. First, the QGPV equation is advanced in time to obtain the PV at the next time step. Then the PV is *inverted* to obtain the streamfunction. From this, we can obtain the velocities and then advance the QGPV equation again. But doing this requires *boundary conditions*.

5.4 Boundary conditions

Notice the QGPV equation (5.15) doesn't contain any Ekman or topographic terms. This is because the PV equation pertains to the interior. In the barotropic case, we introduced those terms by integrating between the lower and upper boundaries, but here, we must treat the boundary conditions separately.

For these, we use the density equation (5.11), rewritten thus:

$$\frac{f_0}{N^2}\frac{d_g}{dt}\frac{\partial \psi}{\partial z} = -w \tag{5.17}$$

The vertical velocity at the boundary can come from either pumping from an Ekman layer or flow over topography. Thus for the lower boundary, we have:

$$\frac{f_0}{N^2}\frac{d_g}{dt}\frac{\partial \psi}{\partial z}\,|_{zb} = -u_g \cdot \nabla h - \frac{\delta}{2}\nabla^2 \psi \tag{5.18}$$

where the velocities and streamfunction are evaluated at the bottom boundary, which we take to be at $z = z_b$.

The upper boundary condition is similar. For the ocean, with the ocean

surface at $z = z_u$, we have:

$$\frac{f_0}{N^2}\frac{d_g}{dt}\frac{\partial\psi}{\partial z}\,|_{zu} = -\frac{1}{\rho_c f_0}\nabla\times\vec{\tau}_w \tag{5.19}$$

The upper boundary condition for the atmosphere depends on the application. If we are considering the entire atmosphere, we could demand that the amplitude of the motion decay as $z \to \infty$, or that the energy flux is directed upwards. However, we will primarily be interested in motion in the troposphere. Then we can treat the tropopause as a surface, either rigid or freely moving. If it is a rigid surface, we would have simply:

$$\frac{1}{N^2}\frac{d_g}{dt}\frac{\partial\psi}{\partial z^*}\,|_{zu} = 0 \tag{5.20}$$

at $z = z_u$. A free surface is only slightly more complicated, but the rigid upper surface will suffice for what follows.

5.5 Baroclinic Rossby waves

Now we'll look at some specific solutions. We begin with seeing how stratification alters the Rossby wave solutions.

First we linearize the PV equation (5.15) assuming a constant background flow:

$$(\frac{\partial}{\partial t} + U\frac{\partial}{\partial x})\,[\nabla^2\psi + \frac{\partial}{\partial z}(\frac{f_0^2}{N^2}\frac{\partial\psi}{\partial z})] + \beta\frac{\partial}{\partial x}\psi = 0 \tag{5.21}$$

Assume for simplicity that the domain lies between two rigid, flat surfaces. With the ocean in mind, we'll take the boundaries at $z = 0$ and $z = -D$ (the result is the same with positive z). We'll also neglect Ekman layers on those surfaces. So the linearized boundary condition on each surface is:

$$(\frac{\partial}{\partial t} + U\frac{\partial}{\partial x})\frac{\partial\psi}{\partial z} = 0 \tag{5.22}$$

This implies that the density (or temperature) doesn't change on parcels advected by the mean flow along the boundary. So the density is constant on the boundaries, and we take the constant to be zero:

$$\frac{\partial \psi}{\partial z} = 0 \tag{5.23}$$

The coefficients in the PV equation do not vary with time or in (x, y), but the buoyancy frequency, N, can vary in z. So an appropriate choice of wave solution would be:

$$\psi = Re\{\hat{\psi}(z)e^{i(kx+ly-\omega t)}\} \tag{5.24}$$

Substituting this into the PV equation, we get:

$$(-i\omega + ikU)[-(k^2+l^2)\hat{\psi} + \frac{d}{dz}(\frac{f_0^2}{N^2}\frac{d\hat{\psi}}{dz})] + i\beta k\hat{\psi} = 0 \tag{5.25}$$

or:

$$\frac{d}{dz}(\frac{f_0^2}{N^2}\frac{d\hat{\psi}}{dz}) + \lambda^2\hat{\psi} = 0 \tag{5.26}$$

where:

$$\lambda^2 \equiv \frac{\beta k}{Uk-\omega} - k^2 - l^2 \tag{5.27}$$

Equation (5.26) determines the vertical structure, $\hat{\psi}(z)$, of the Rossby waves. With the boundary conditions (5.23), this constitutes an *eigenvalue* or "Sturm-Liouville" problem. Only specific values of λ will be permitted. In order to find the dispersion relation for the waves, we must first solve for the vertical structure.

5.5.1 Baroclinic modes with constant stratification

To illustrate, consider the simplest case, with $N^2 = const.$ Then we have:

$$\frac{d^2\hat{\psi}}{dz^2} + \frac{N^2\lambda^2}{f_0^2}\hat{\psi} = 0 \tag{5.28}$$

This has a general solution:

$$\hat{\psi} = Acos(\frac{N\lambda z}{f_0}) + Bsin(\frac{N\lambda z}{f_0}) \tag{5.29}$$

In order to satisfy $\frac{\partial}{\partial z}\hat{\psi} = 0$ on the upper boundary (at $z = 0$), we require that $B = 0$. But in addition, it must work on the lower boundary, at $z = -D$. So either $A = 0$ (so that we have no wave at all) or:

$$sin(\frac{N\lambda D}{f_0}) = 0 \tag{5.30}$$

For this to be true:

$$\frac{N\lambda D}{f_0} = n\pi \tag{5.31}$$

where $n = 0, 1, 2...$ is an integer. In other words, only specific combinations of of the parameters will work. Solving for λ, we get:

$$\lambda^2 = \frac{n^2\pi^2 f_0^2}{N^2 D^2} \equiv \frac{n^2}{L_D^2} \tag{5.32}$$

Here,

$$L_D = \frac{ND}{\pi f_0}$$

is the baroclinic *deformation radius*. Combining this with the definition of λ^2, we get:

$$\frac{n^2}{L_D^2} \equiv \frac{\beta k}{Uk - \omega} - k^2 - l^2 \tag{5.33}$$

Solving for ω, we obtain:

$$\omega \equiv \omega_n = Uk - \frac{\beta k}{k^2 + l^2 + n^2/L_D^2} \tag{5.34}$$

This is the *dispersion relation for baroclinic Rossby waves*.

In fact, there are an infinite number of relations here, one for each value of n, each with a different vertical structure. The wave structure corresponding to each is given by:

$$\psi = Acos(kx + ly - \omega_n t)\, cos(\frac{n\pi z}{D}) \tag{5.35}$$

Consider first the case with $n = 0$. The dispersion relation is:

$$\omega_0 = Uk - \frac{\beta k}{k^2 + l^2} \tag{5.36}$$

This is just the dispersion relation for the barotropic Rossby wave obtained earlier (sec. 4.4). The wave solution with $n = 0$ is

$$\psi_0 = Acos(kx + ly - \omega_n t) \tag{5.37}$$

This doesn't vary in the vertical, exactly as we would expect for a barotropic wave. So the *barotropic mode* exists, even though there is stratification. All the properties that we derived before apply to this wave as well.

Why does the barotropic mode exist? The mode has no vertical shear, so the stretching vorticity is zero, and as such, equation (5.21) is exactly the same as the barotropic Rossby wave equation (4.26). Also–and equally importantly–the boundary conditions at the top and bottom permit solutions with no vertical shear.

With $n = 1$, the streamfunction is:

$$\psi_1 = Acos(kx + ly - \omega_n t)cos(\frac{\pi z}{D}) \tag{5.38}$$

This is the *first baroclinic mode*, shown as the red curve in Fig. (5.1). The streamfunction (and thus the velocities) change sign in the vertical. Thus if the velocity is eastward near the upper boundary, it is westward near the bottom. There is also a "zero-crossing" at $z = -D/2$, where the velocities vanish. The waves have an associated density perturbation as well:

$$\rho_1 \propto \frac{\partial}{\partial z}\psi_1 = -\frac{n\pi}{D}Acos(kx + ly - \omega_n t)sin(\frac{\pi z}{D}) \tag{5.39}$$

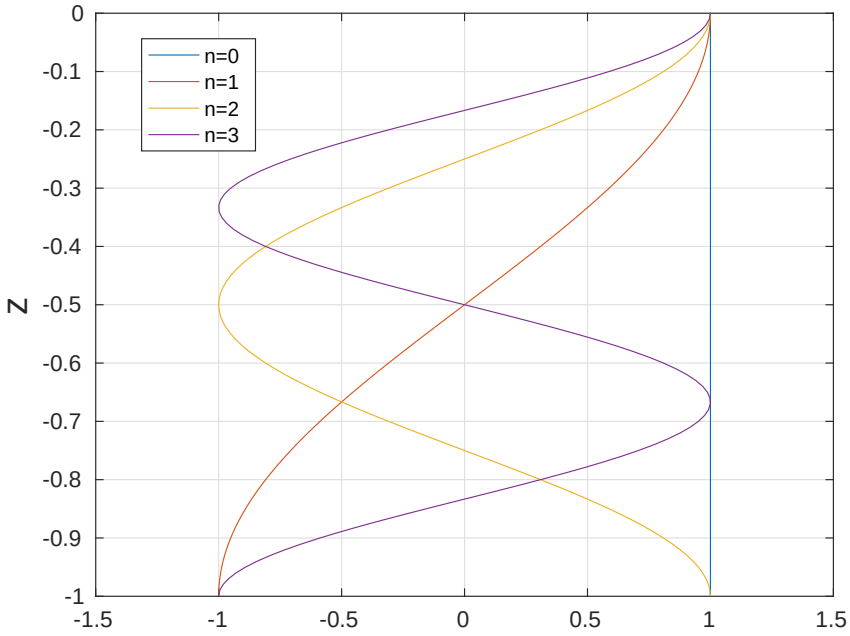

Figure 5.1: The baroclinic modes with constant stratification.

So the density perturbation is largest at the mid-depth, where the horizontal velocities vanish. In the ocean, first mode baroclinic Rossby waves cause large deviations in the *thermocline*, which is the subsurface maximum in the density gradient.

We have assumed the surface and bottom are flat, and our solution has no density perturbations on those surfaces. However, if we had allowed the upper surface to move, we would have found that the first baroclinic mode has an associated surface deflection. Moreover, this deflection is of the opposite in sign to the density perturbation at mid-depth. If the density contours are pressed down at mid-depth, the surface rises. This means one can observe baroclinic Rossby waves by satellite.

The dispersion relation for the first mode is:

$$\omega_1 = Uk - \frac{\beta k}{k^2 + l^2 + 1/L_D^2} \tag{5.40}$$

The corresponding zonal phase speed is:

$$c_1 = \frac{\omega_1}{k} = U - \frac{\beta}{k^2 + l^2 + 1/L_D^2} \tag{5.41}$$

So the first mode wave also propagates westward relative to the mean flow. But the phase speed is *slower* than that of the barotropic Rossby wave. However, if the wavelength is much smaller than the deformation radius (so that $k^2 + l^2 \gg 1/L_d^2$), then:

$$c_1 \approx U - \frac{\beta}{k^2 + l^2} \tag{5.42}$$

So small scale baroclinic waves have a phase speed like that of a barotropic wave of the same size.

If on the other hand the wave is much larger than the deformation radius, then:

$$c_1 \approx U - \beta L_D^2 = U - \frac{\beta N^2 D^2}{\pi^2 f_0^2} \tag{5.43}$$

This means the large waves are *non-dispersive*, because the phase speed is independent of the wavenumber. This phase speed, known as the "long wave speed", is a strong function of latitude, varying inversely with the square of the Coriolis parameter. Where f_0 is small—at low latitudes—the long baroclinic waves move faster.

The phase speeds from the first four modes are plotted as a function of wavenumber in Fig. (5.2). Here we plot the function:

$$c_n = \frac{1}{2k^2 + n^2} \tag{5.44}$$

(note that the actual c is the negative of this). We have set $\beta = L_D = 1$ and $k = l$ and assumed the mean flow is zero. The barotropic mode ($n = 0$) has a phase speed which increases without bound as the wavenumber goes to zero. This is actually a consequence of having a rigid lid at the surface;

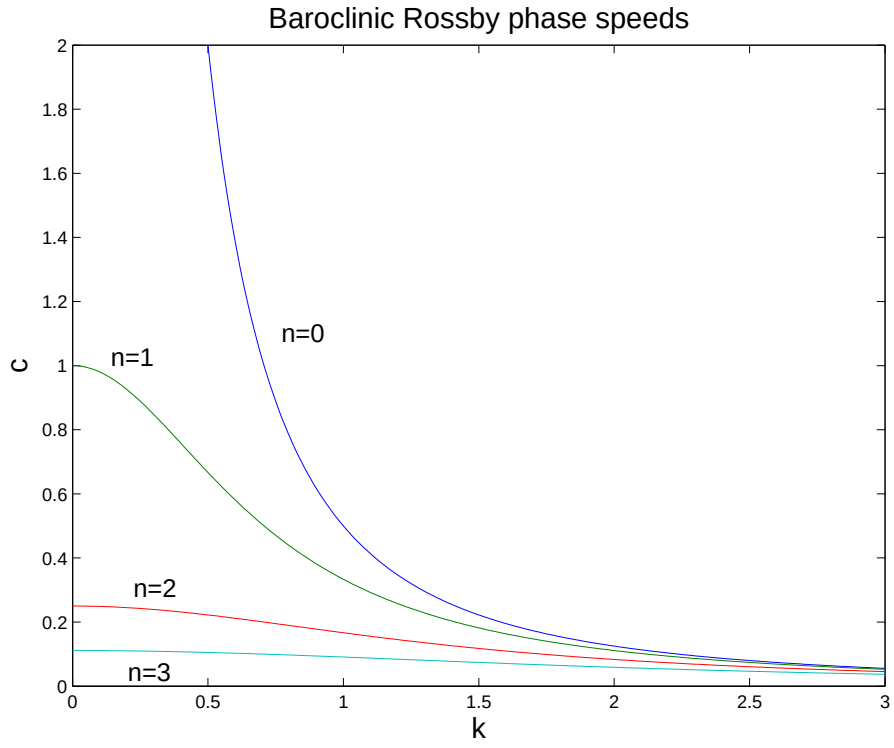

Figure 5.2: Rossby phase speeds as a function of wavenumber for the first four modes.

if we had a free (moving) surface, the wave would have a finite phase speed at $k = 0$. The first baroclinic mode ($n = 1$) has a constant phase speed at low k, equal to $c = 1$. This is the long wave speed with $L_D = 1$. The second and third baroclinic modes ($n = 2, 3$) also have long wave speeds, but these are four and nine times smaller than the first baroclinic long wave speed.

5.5.2 Baroclinic modes with exponential stratification

In the preceding section, we assumed a constant buoyancy frequency, N. This implies the density has linear profile in the vertical. In reality, the oceanic density varies strongly with z. In many locations, the buoyancy frequency exhibits a nearly exponential dependence on depth, with larger

values near the surface and smaller ones at depth.

An exponential profile can also be solved analytically. Assume:

$$N = N_0 e^{\alpha z} \tag{5.45}$$

Substituting (5.45) into (5.26) yields:

$$\frac{d^2\hat{\psi}}{dz^2} - \alpha\frac{d\hat{\psi}}{dz} + \frac{N_0^2\lambda^2}{f_0^2}e^{2\alpha z}\hat{\psi} = 0 \tag{5.46}$$

Making the substitution $\zeta = e^{\alpha z}$, we obtain:

$$\zeta^2\frac{d^2\hat{\psi}}{d\zeta^2} - \zeta\frac{d\hat{\psi}}{d\zeta} + \frac{4N_0^2\lambda^2}{\alpha^2 f_0^2}\zeta^2\hat{\psi} = 0 \tag{5.47}$$

This is a Bessel-type equation. The solution which satisfies the upper boundary condition (at $z = 0$) is:

$$\hat{\psi} = Ae^{\alpha z}[Y_0(\gamma)J_1(\gamma e^{\alpha z}) - J_0(\gamma)Y_1(\gamma e^{\alpha z})] \tag{5.48}$$

where $\gamma = N_0\lambda/(\alpha f_0)$. If we then impose the bottom boundary condition, we get:

$$J_0(\gamma)Y_0(\gamma e^{-\alpha H}) - Y_0(\gamma)J_0(\gamma e^{-\alpha H}) = 0 \tag{5.49}$$

Equation (5.49), a *transcendental equation*, admits only certain discrete values, γ_n. As before, γ_n is quantized. Once γ_n is found, the wave frequencies can be determined from the dispersion relation as before. Equation (5.49) is more difficult to solve than with constant stratification, but it's possible to do this numerically. Notice though that $\gamma = 0$ is also a solution of (5.49)—so there is also a barotropic mode in this case as well.

The baroclinic modes, $\hat{\psi}(z)$, with one value of α are shown in Fig. (5.3). Again there is the depth-independent barotropic mode, and depth-varying baroclinic modes. The first baroclinic mode again has one zero crossing, the second mode has two, and so forth. But unlike the cosine modes, the

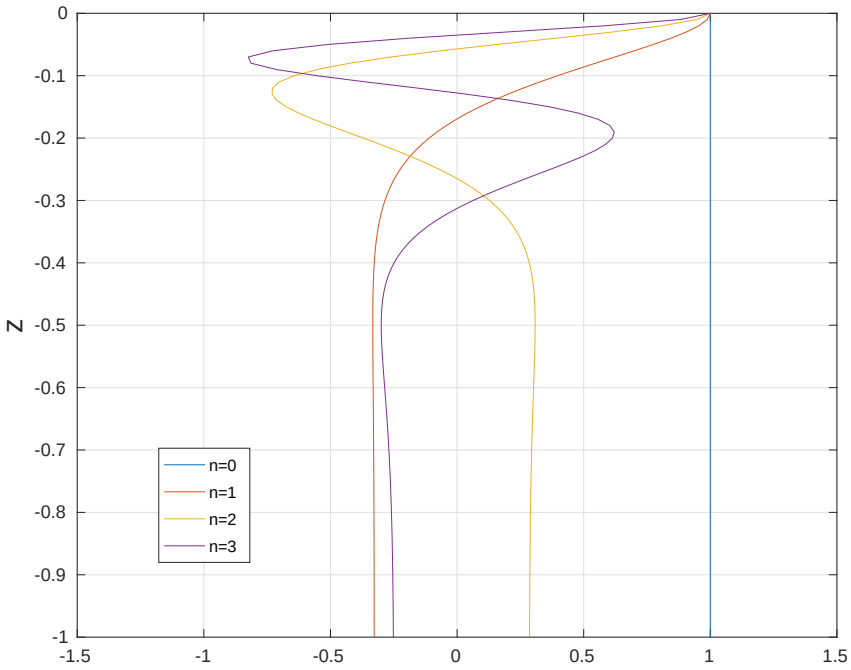

Figure 5.3: The baroclinic modes with exponential stratification. The e-folding rate for the stratification, α, is 2.5.

exponential modes have their largest amplitudes near the surface. This implies that the Rossby wave velocities and density perturbations are likewise surface-intensified.

5.5.3 Baroclinic modes with actual stratification

In most cases though, the stratification has a more complicated dependence on depth. An example is shown in the left panel of Fig. (5.4), from a location in the ocean off the west coast of Oregon in the U.S (Kundu et al., 1974). Below about 10 m depth N^2 decreases approximately exponentially. But above that it also decreases, toward the surface. We refer to this weakly stratified upper region as the *mixed layer*. It is here that surface cooling and wind-induced turbulent mixing stir the waters, making the stratification more homogeneous. This is a common phenomenon in

the world ocean.

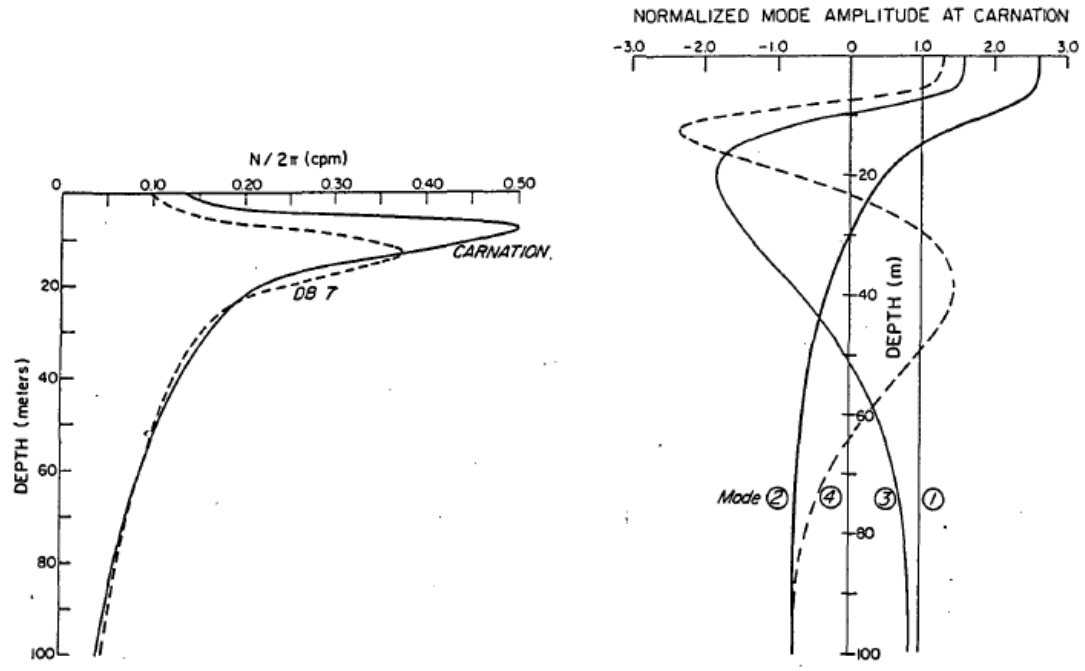

Figure 5.4: The buoyancy frequency (left panel) and the corresponding vertical modes (right panel) from a location on the continental shelf off Oregon. From Kundu et al. (1974).

With profiles of N^2 like this, it is necessary to solve equation (5.26) numerically. The authors did this, and the result is shown in the right panel of Fig. (5.4). Below 10 m, the modes resemble those obtained with exponential stratification. The baroclinic modes have larger amplitudes near the surface, and the zero crossings are also higher up in the water column. Where they differ though is in the upper 10 m. Here the modes flatten out, indicating weaker vertical shear. So the flow in the mixed layer is more barotropic than below. Note though that there is still a barotropic mode. This is always present under the condition of a vanishing density perturbation on the boundaries.

It can be shown that the the eigenfunctions obtained from the Sturm-

Liouville problem form a *complete basis*. That means that we can express an arbitrary function in terms of them, if that function is continuous. So oceanic currents can be decomposed into vertical modes. Wunsch (1997) studied currents using a large collection of current meters deployed all over the world. He found that the variability projects largely onto the barotropic and first baroclinic modes. So these two modes are the most important for time-varying motion.

5.5.4 Observations of oceanic Rossby waves

As noted in sec. (4.4.3), baroclinic Rossby waves can be seen by satellite-derived measurements of sea surface height (SSH). The SSH fields in Fig. (4.8) were from two different times in 1993. There are large scale anomalies and these migrate westward in time. The speed of propagation moreover increases towards the equator, which is evident from a bending of the leading wave front (indicated by the white contours).

Chelton and Schlax (1996) took cuts in the fields at various latitudes to construct time-longitude plots or "Hovmuller" diagrams (Fig. 5.5). Time is increasing on the y-axis, so the tilt towards the upper left is consistent with westward phase propagation. The tilt can be used to deduce the phase speeds, which are on the order of cm/sec. Interestingly the speeds are strongly dependent on latitude, being fastest at 21N and slowest at 39N.

Shown in Fig. (5.6) are the calculated phase speeds plotted against latitude. A curve showing the long wave speed for the first baroclinic mode is also shown. We see there is reasonable agreement at most latitudes. The agreement is very good below about 20 degrees of latitude; at higher latitudes there is a systematic discrepancy, with the observed waves moving perhaps twice as fast as predicted. There are a number of theories which

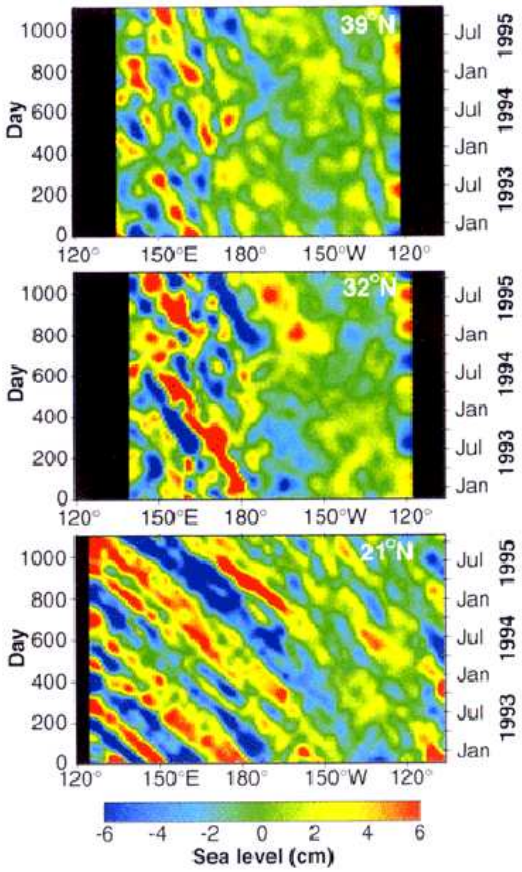

Figure 5.5: Three Hovmuller diagrams constructed from sea surface height in the North Pacific. From Chelton and Schlax (1996).

have tried to explain this.[1] For our purposes though, we see that the simple theory does surprisingly well at predicting the observed sea surface height propagation.

This is still an active area of research. For example, the reason why the waves are more pronounced west of 150-180 W in Fig. (4.8) is still unknown.

[1] See for example LaCasce and Pedlosky (2004) and Isachsen et al. (2007).

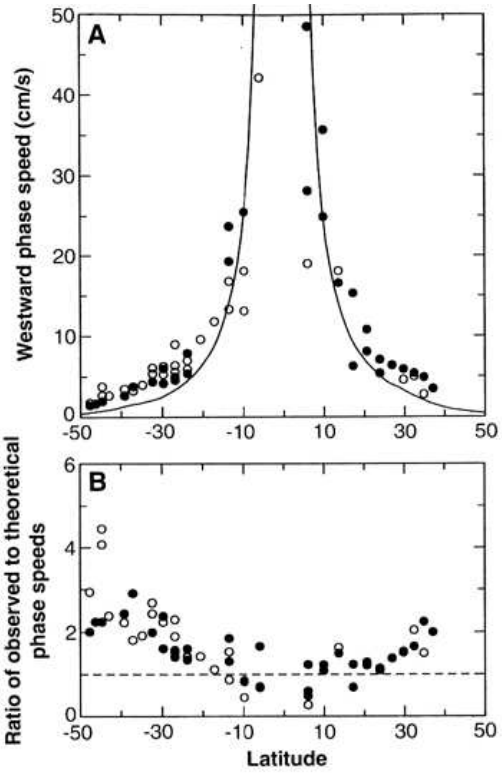

Figure 5.6: Westward phase speeds deduced from the motion of sea surface height anomalies, compared with the value predicted by the long wave phase speed given in (5.43). The lower panel shows the ratio of observed to predicted phase speed. Note the observed speeds are roughly twice as fast at high latitudes. From Chelton and Schlax (1996).

5.6 Mountain waves

In sec. (4.8), we saw how a mean wind blowing over mountains could excite standing Rossby waves. Now we will consider what happens in the baroclinic case.

We consider the potential vorticity equation (5.15), without forcing:

$$\frac{d_g}{dt}[\nabla^2\psi + \frac{\partial}{\partial z}(\frac{f_0^2}{N^2}\frac{\partial\psi}{\partial z}) + \beta y] = 0 \tag{5.50}$$

As before, we consider a steady flow forced by a mean zonal wind:

$$U\frac{\partial}{\partial x}[\nabla^2\psi + \frac{\partial}{\partial z}(\frac{f_0^2}{N^2}\frac{\partial\psi}{\partial z})] + \beta\frac{\partial}{\partial x}\psi = 0 \tag{5.51}$$

Note that even though the Rossby waves will be baroclinic, the mean flow is assumed to be barotropic (otherwise there would be an additional term involving the mean shear). We will again assume that the stratification parameter, N^2, is constant, for simplicity.

With a constant N^2, all the coefficients in the vorticity equation are constant. But given that we have a boundary in z, it's still wise to leave the z-dependence undetermined. So our wave solution is:

$$\psi = \hat{\psi}(z)e^{ikx+ily} \tag{5.52}$$

Substituting this into (5.51) yields:

$$ikU[-(k^2+l^2)\hat{\psi} - \frac{f_0^2}{N^2}\frac{d^2\hat{\psi}}{dz^2}] + ik\beta\hat{\psi} = 0 \tag{5.53}$$

Rearranging, we get:

$$\frac{d^2\hat{\psi}}{dz^2} + m^2\hat{\psi} = 0 \tag{5.54}$$

where:

$$m = \pm\frac{N}{f_0}\sqrt{\frac{\beta}{U} - k^2 - l^2} \tag{5.55}$$

There are actually four possibilites for the vertical structure; m can be positive or negative, and real or imaginary. This in turn depends on the term in the square root; if positive, m is real and has wave-like solutions. But if it is negative, m is imaginary and the vertical dependence is *exponential* in the vertical.

Consider the second case first. Then we can write:

$$m = \pm im_i \equiv \pm i\frac{N}{f_0}\sqrt{k^2 + l^2 - \frac{\beta}{U}} \tag{5.56}$$

as the term in the root is positive. The streamfunction is thus:

$$\psi = (Ae^{m_i z} + Be^{-m_i z})e^{ikx+ily} \tag{5.57}$$

The first term in the parentheses grows with height. This is not realistic, as the velocities would become extremely large at great heights in the atmosphere. So we conclude that $A = 0$ and that all wave solutions are trapped at the surface. Thus the pressure field excited by the mountains is basically trapped over the mountains.

When the term in the root in (5.55) is positive on the other hand, we have:

$$\psi = (Ae^{imz} + Be^{-imz})e^{ikx+ily} \tag{5.58}$$

Then the solution is wave-like in the vertical, meaning the waves can effectively propagate upward to infinity, leaving the troposphere and entering the stratosphere and beyond. In such situations, the mountain waves can disturb the atmospheric flow well above them.

Which term do we take though, the positive or the negative exponent? To find out, we examine the group velocity in the vertical direction. The dispersion relation for baroclinic Rossby waves with a mean flow and a wave-like structure in the vertical is:

$$\omega = Uk - \frac{\beta k}{k^2 + l^2 + m^2 f_0^2/N^2} \tag{5.59}$$

(sec. 5.5). The corresponding vertical group velocity is:

$$c_{gz} = \frac{\partial \omega}{\partial m} = \frac{2\beta k m f_0^2}{N^2(k^2 + l^2 + m^2 f_0^2/N^2)^2} \tag{5.60}$$

This is positive if the product km is positive. Thus if k is positive, we require that m also be positive. So we could write:

$$\psi = Ae^{ikx+ily+imz} \tag{5.61}$$

where:

$$m = sgn(k)\frac{N}{f_0}\sqrt{\frac{\beta}{U} - k^2 - l^2} \tag{5.62}$$

Here $sgn(k)$ is +1 if k is positive and -1 if it is negative.

Thus the character of the solution in the vertical depends on the sign of the argument of the root in (5.55). This is positive when:

$$\frac{\beta}{U} > k^2 + l^2 \tag{5.63}$$

This implies that the mean flow, U, must be *positive*, or eastward. Rewriting the relation, we have:

$$0 < U < \frac{\beta}{k^2 + l^2} \equiv U_s \tag{5.64}$$

So while U must be positive, neither can it be too strong. It must, in particular, be less than U_s, the speed at which the barotropic Rossby wave is stationary (sec. 4.4.1).

Why is the mean flow limited by speed of the barotropic wave? As we saw in the previous section, the barotropic mode is the *fastest* of all the Rossby modes. So standing waves are possible only when the mean speed is slow enough so that one of the baroclinic Rossby modes is *stationary*.

Notice that we have not said anything about the lower boundary, where the waves are forced. In fact, the form of the mountains determines the structure of the stationary waves. But the general condition above applies to all types of mountain. If the mean flow is eastward and not too strong, the waves generated over the mountains can extend upward indefinitely.

Upward propagating Rossby waves are important in the stratosphere, and can greatly disturb the flow there. They can even change the usual equator-to-pole temperature difference, a *stratospheric warming* event.

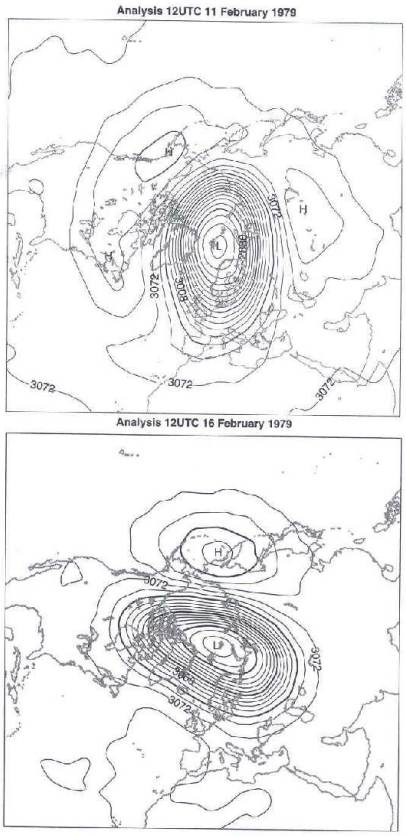

Fig. 12.10 *(continued)*

Figure 5.7: The geopotential height at 10 hPa on February 11 and 16, 1979. The polar vortex is being perturbed by a disturbance over the Pacific. From Holton, *An Introduction to Dynamic Meteorology*.

Consider Figs. (5.7) and (5.8). In the first panel of Fig. (5.7), we see the *polar vortex* over the Arctic. This is a region of persistent low pressure (with a correspondingly low tropopause height). In the second panel, a high pressure is developing over the North Pacific. This high intensifies, eventually causing the polar vortex to split in two, making a mode 2 planetary wave (Fig. 5.8). The wave has a corresponding temperature perturbation, and in some regions the air actually *warms* moving from south to north.

Stratospheric warming events occur only in the wintertime. Charney

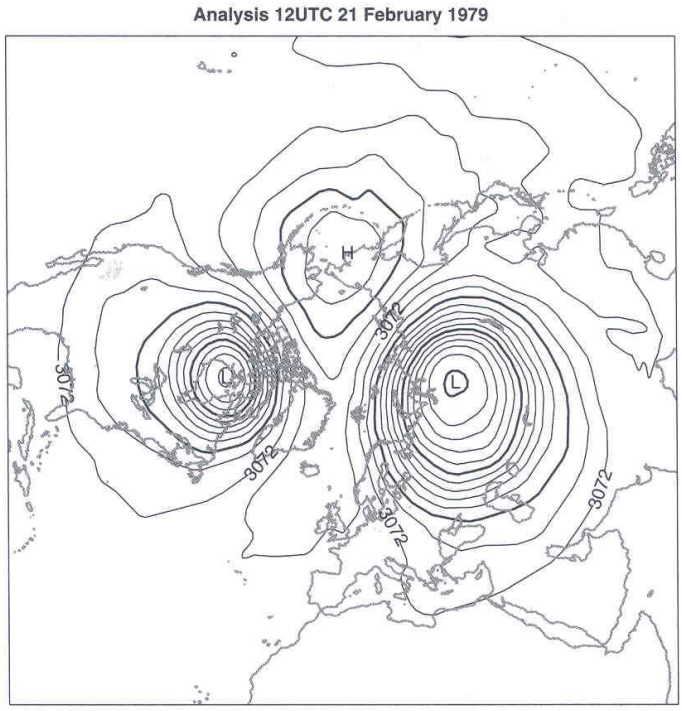

Fig. 12.10 10 hPa geopotential height analyses for February 11, 16, and 21, 1979 at 12UTC showing breakdown of the polar vortex associated with a wave number 2 sudden stratospheric warming. Contour interval: 16 dam. Analysis from ERA-40 reanalysis courtesy of the European Centre for Medium-Range Weather Forecasts (ECMWF).

Figure 5.8: The geopotential height at 10 hPa on February 21, 1979 (following Fig. 5.7). The polar vortex has split in two, appearing now as a mode 2 Rossby wave. From Holton, *An Introduction to Dynamic Meteorology*.

and Drazin (1961) used the above theory to explain which this happens. In the wintertime, the winds are eastward, so that upward propagation is possible. But in the summertime, the stratospheric winds are westward, preventing upward propagation. So Rossby waves only alter the stratospheric circulation in the wintertime.

5.7 Topographic waves

In an earlier problem, we found that a sloping bottom can support Rossby waves, just like the β-effect. The waves propagate with shallow water to

their right (or "west", when facing "north" up the slope). Topographic waves exist with stratification too, and it is useful to examine their structure.

We'll use the potential vorticity equation, linearized with zero mean flow ($U = 0$) and on the f-plane ($\beta = 0$). We'll also assume that the buoyancy frequency, N, is constant. Then we have:

$$\frac{\partial}{\partial t}(\nabla^2\psi + \frac{f_0^2}{N^2}\frac{\partial^2}{\partial z^2}\psi) = 0 \tag{5.65}$$

Thus the potential vorticity in the interior of the fluid *does not change in time*; it is simply constant. We can take this constant to be zero.

For the bottom boundary condition, we will assume a linear topographic slope. This can be in any direction, but we will say the depth is decreasing toward the north:

$$D = D_0 - \alpha y \tag{5.66}$$

so that $h = \alpha y$. In fact, this is a general choice because with f=const., the system is rotationally invariant (why?). With this topography, the bottom boundary condition (5.18) becomes:

$$\begin{aligned} \frac{d_g}{dt}\frac{\partial\psi}{\partial z} + \frac{N^2}{f_0}w &= \\ \frac{d_g}{dt}\frac{\partial\psi}{\partial z} + \frac{N^2}{f_0}u_g \cdot \nabla h &= \\ \frac{d_g}{dt}\frac{\partial\psi}{\partial z} + \frac{N^2}{f_0}\alpha v &= 0 \end{aligned} \tag{5.67}$$

We'll take the bottom to be at $z = 0$. Also we won't worry about the upper boundary, as the waves will be trapped near the lower one.

To see that, assume a solution which is wave-like in x and y:

$$\psi = Re\{\hat{\psi}(z)e^{ikx+ily-i\omega t}\} \tag{5.68}$$

Under the condition that the PV is zero, we have:

$$(-k^2 - l^2)\hat{\psi} + \frac{f_0^2}{N^2}\frac{d^2\hat{\psi}}{dz^2} = 0 \tag{5.69}$$

or

$$\frac{d^2\hat{\psi}}{dz^2} - \frac{N^2\kappa^2}{f_0^2}\hat{\psi} = 0 \tag{5.70}$$

where $\kappa = (k^2 + l^2)^{1/2}$ is again the total wavenumber. This equation only has exponential solutions. The one that decays going up from the bottom boundary has:

$$\hat{\psi}(z) = Ae^{-N\kappa z/|f_0|} \tag{5.71}$$

This is the vertical structure of the topographic waves. It implies the waves have a vertical e-folding scale of:

$$H \propto \frac{|f_0|}{N\kappa} = \frac{|f_0|\lambda}{2\pi N}$$

if λ is the wavelength of the wave. Thus the vertical scale of the wave *depends on its horizontal scale*. Larger waves extend further into the interior. Also, we have a *continuum* of waves, not a discrete set like we did with the baroclinic modes (sec. 5.5).

Notice that we would have obtained the same result with the mountain waves in the previous section. If we take (5.55) and set $\beta = 0$, we get:

$$m = \pm\frac{N}{f_0}(-k^2 - l^2)^{1/2} = \pm\frac{iN\kappa}{f_0} \tag{5.72}$$

So with $\beta = 0$, we obtain *only* exponential solutions in the vertical. The wave-like solutions require an interior PV gradient.

To obtain the dispersion relation, we apply the bottom boundary condition. We linearize (5.67) with zero mean flow and write v in terms of the streamfunction:

$$\frac{\partial}{\partial t}\frac{\partial}{\partial z}\psi + \frac{N^2\alpha}{f_0}\frac{\partial \psi}{\partial x} = 0 \tag{5.73}$$

Substituting into the wave expression for ψ, we get:

$$-\frac{\omega N\kappa}{|f_0|}A - \frac{N^2\alpha k}{f_0}A = 0 \tag{5.74}$$

so that:

$$\omega = -\frac{N\alpha k}{\kappa}sgn(f_0) \tag{5.75}$$

where $sgn(f_0)$ is +1 if $f > 0$ (Northern Hemisphere) and -1 if $f < 0$ (Southern).

This is the dispersion relation for stratified topographic waves. The phase speed in the x-direction (along the isobaths, the lines of constant depth) is:

$$c_x = -\frac{N\alpha}{\kappa}sgn(f_0) \tag{5.76}$$

This then is "westward" in the Northern Hemisphere, i.e. with the shallow water on the right. As with planetary waves, the fastest waves are the largest ones (with small κ). These are also the waves the penetrate the highest into the water column. Thus the waves which are closest to barotropic are the fastest.

Topographic waves are often observed in the ocean, particularly over the continental slope. Observations suggest that disturbances originating at the equator propagate north (with shallow water on the right) past California towards Canada. Topographic waves have also been observed off the east coast of the United States, propagating towards the south. The waves have also been found propagating south (with the shallow water on the left) past Peru.

5.8 Baroclinic instability

Now we return to instability. As discussed before, solar heating of the earth's surface causes a temperature gradient, with a warmer equator and colder poles. This north-south temperature gradient is accompanied by a vertically sheared flow in the east-west direction. The flow is weak near the surface and increases moving upward in the troposphere.

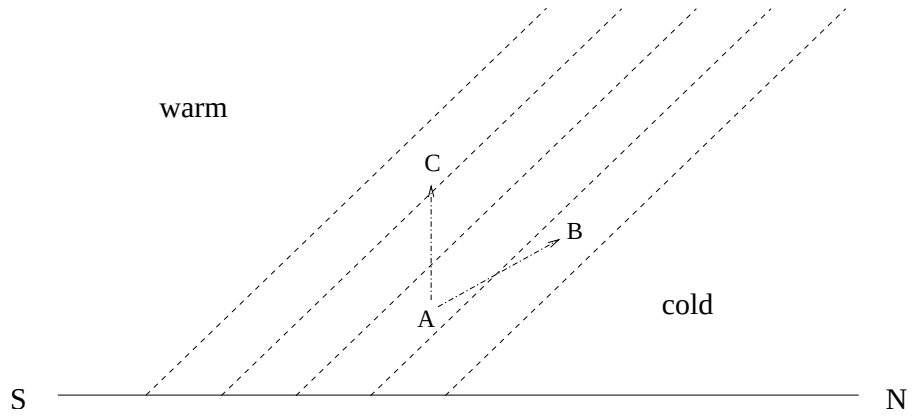

Figure 5.9: Slantwise convection. The slanted isotherms are accompanied by a thermal wind shear. The parcel A is colder, and thus heavier, than parcel C, implying static stability. But A is lighter than B. So A and B can be interchanged, releasing potential energy.

5.8.1 Basic mechanism

The isotherms look (crudely) as sketched in Fig. (5.9). The temperature decreases to the north, and also increases going up. Thus the parcel A is colder (and heavier) than parcel C, which is directly above it. The air is stably stratified, because exchanging A and C would *increase* the potential energy.

However, because the isotherms tilt, there is a parcel B which is above A and heavier. So A and B can be exchanged, *releasing* potential energy. This is often referred to as "slantwise" convection, and it is the basis for baroclinic instability. Baroclinic instability simultaneously *reduces the vertical shear* while *decreasing the north-south temperature gradient*. In effect, it causes the temperature contours to slump back to a more horizontal configuration, which reduces the thermal wind shear while decreasing the meridional temperature difference.

Baroclinic instability is extremely important. For one, it allows us to live at high latitudes—without it, the poles would be much colder than the equator.

5.8.2 Charney-Stern criterion

We can derive conditions for baroclinic instability, just as we did to obtain the Rayleigh-Kuo criterion for barotropic instability. We begin, as always, with the PV equation (5.15):

$$\frac{d_g}{dt}[\nabla^2\psi + \frac{\partial}{\partial z}(\frac{f_0^2}{N^2}\frac{\partial\psi}{\partial z}) + \beta y] = 0 \tag{5.77}$$

We linearize this about a mean flow, U, which varies in *both* the y and z-directions. Doing this is the same thing if we had writen the streamfunction

as:

$$\psi = \Psi(y,z) + \psi'(x,y,z,t) \tag{5.78}$$

where the primed streamfunction is much smaller than the mean streamfunction. The mean streamfunction has an associated zonal flow:

$$U(y,z) = -\frac{\partial}{\partial y}\Psi \tag{5.79}$$

Note it has no meridional flow (V) because Ψ is independent of x. Using this, we see the mean PV is:

$$q_s = \frac{\partial^2}{\partial y^2}\Psi + \frac{\partial}{\partial z}(\frac{f_0^2}{N^2}\frac{\partial \Psi}{\partial z}) + \beta y \tag{5.80}$$

So the full linearized PV equation is:

$$(\frac{\partial}{\partial t} + U\frac{\partial}{\partial x})[\nabla^2\psi + \frac{\partial}{\partial z}(\frac{f_0^2}{N^2}\frac{\partial \psi}{\partial z})] + (\frac{\partial}{\partial y}q_s)\frac{\partial}{\partial x}\psi = 0 \tag{5.81}$$

with:

$$\frac{\partial}{\partial y}q_s = \beta - \frac{\partial^2}{\partial y^2}U - \frac{\partial}{\partial z}(\frac{f_0^2}{N^2}\frac{\partial U}{\partial z}) \tag{5.82}$$

We saw the first two terms before, in the barotropic case, but the third term is new. This comes about because the mean velocity (and hence the mean streamfunction) varies in z.

In addition, we need the boundary conditions. We'll assume flat boundaries and no Ekman layers, to make this as simple as possible. Thus we use (5.20), linearized about the mean flow:

$$\frac{d_g}{dt}\frac{\partial \psi}{\partial z} = (\frac{\partial}{\partial t} + U\frac{\partial}{\partial x})\frac{\partial \psi}{\partial z} + v\frac{\partial}{\partial y}\frac{\partial \Psi}{\partial z}$$

$$= (\frac{\partial}{\partial t} + U\frac{\partial}{\partial x})\frac{\partial \psi}{\partial z} - v\frac{\partial U}{\partial z} = 0 \tag{5.83}$$

The boundaries are at the ground, at $z = 0$, and an upper level, $z = D$. The latter could be the tropopause. Alternatively, we could have no upper boundary at all, as with the mountain waves. We'll use an upper boundary in the Eady model in the next section, so it's useful to include that now.

Because U is potentially a function of both y and z, we can only assume a wave structure in (x, t). So we use a Fourier solution with the following form:

$$\psi = \hat{\psi}(y, z)e^{ik(x-ct)} \tag{5.84}$$

Substituting into the PV equation (5.81), we get:

$$(U - c)[-k^2\hat{\psi} + \frac{\partial^2}{\partial y^2}\hat{\psi} + \frac{\partial}{\partial z}(\frac{f_0^2}{N^2}\frac{\partial \hat{\psi}}{\partial z})] + (\frac{\partial}{\partial y}q_s)\hat{\psi} = 0 \tag{5.85}$$

after canceling the factor of k. Similarly, the boundary conditions are:

$$(U - c)\frac{\partial}{\partial z}\hat{\psi} - (\frac{\partial}{\partial z}U)\hat{\psi} = 0 \tag{5.86}$$

We now do as we did in sec. (4.11.1): we divide (5.85) by $U - c$ and then multiply by the complex conjugate of $\hat{\psi}$:

$$\hat{\psi}^*[\frac{\partial^2}{\partial y^2}\hat{\psi} + \frac{\partial}{\partial z}(\frac{f_0^2}{N^2}\frac{\partial \hat{\psi}}{\partial z})] - k^2|\hat{\psi}|^2 + \frac{1}{U - c}(\frac{\partial}{\partial y}q_s)|\hat{\psi}|^2 = 0 \tag{5.87}$$

We then separate real and imaginary parts. The imaginary part of the equation is:

$$\hat{\psi}_r\frac{\partial^2}{\partial y^2}\hat{\psi}_i - \hat{\psi}_i\frac{\partial^2}{\partial y^2}\hat{\psi}_r + \hat{\psi}_r\frac{\partial}{\partial z}(\frac{f_0^2}{N^2}\frac{\partial \hat{\psi}_i}{\partial z}) - \hat{\psi}_i\frac{\partial}{\partial z}(\frac{f_0^2}{N^2}\frac{\partial \hat{\psi}_r}{\partial z})$$

$$+\frac{c_i}{|U-c|^2}(\frac{\partial}{\partial y}q_s)|\hat{\psi}|^2 = 0 \tag{5.88}$$

We have again used:

$$\frac{1}{U-c} = \frac{1}{U-c_r-ic_i} = \frac{U-c_r+ic_i}{|U-c|^2}$$

The flow will be confined to a zonal channel, with $\hat{\psi} = 0$ at the north and south walls (at $y = 0$ and $y = L$). Integrating the PV equation in y and then using integration by parts yields, for the first two terms on the LHS:

$$\int_0^L (\hat{\psi}_i \frac{\partial^2}{\partial y^2}\hat{\psi}_r - \hat{\psi}_r \frac{\partial^2}{\partial y^2}\hat{\psi}_i)\, dy = \hat{\psi}_i \frac{\partial}{\partial y}\hat{\psi}_r|_0^L - \int_0^L \frac{\partial}{\partial y}\hat{\psi}_i \frac{\partial}{\partial y}\hat{\psi}_r\, dy$$
$$-\hat{\psi}_r \frac{\partial}{\partial y}\hat{\psi}_i|_0^L + \int_0^L \frac{\partial}{\partial y}\hat{\psi}_r \frac{\partial}{\partial y}\hat{\psi}_i\, dy = 0 \tag{5.89}$$

We can similarly integrate the PV equation in the vertical, from $z = 0$ to $z = D$, and again integrate by parts. This leaves:

$$\hat{\psi}_r \frac{f_0^2}{N^2}\frac{\partial \hat{\psi}_i}{\partial z}|_0^D - \hat{\psi}_i \frac{f_0^2}{N^2}\frac{\partial \hat{\psi}_r}{\partial z}|_0^D \tag{5.90}$$

(the leftover integrals are the same and cancel each other). We then evaluate these two terms using the boundary condition. We rewrite that as:

$$\frac{\partial}{\partial z}\hat{\psi} = (\frac{\partial}{\partial z}U)\frac{\hat{\psi}}{U-c} \tag{5.91}$$

The real part of this is:

$$\frac{\partial}{\partial z}\hat{\psi}_r = (\frac{\partial}{\partial z}U)[\frac{(U-c_r)\hat{\psi}_r}{|U-c|^2} - \frac{c_i\hat{\psi}_i}{|U-c|^2}] \tag{5.92}$$

and the imaginary part is:

$$\frac{\partial}{\partial z}\hat{\psi}_i = (\frac{\partial}{\partial z}U)[\frac{(U-c_r)\hat{\psi}_i}{|U-c|^2} + \frac{c_i\hat{\psi}_r}{|U-c|^2}] \tag{5.93}$$

If we substitute these into (5.90), we get:

$$\frac{f_0^2}{N^2}(\frac{\partial}{\partial z}U)\frac{c_i\hat{\psi}_i^2}{(U-c_r)^2+c_i^2}|_0^D + \frac{f_0^2}{N^2}(\frac{\partial}{\partial z}U)\frac{c_i\hat{\psi}_r^2}{(U-c_r)^2+c_i^2}|_0^D = \frac{f_0^2}{N^2}(\frac{\partial}{\partial z}U)\frac{c_i\hat{|\psi|}^2}{(U-c_r)^2+c_i^2}|_0^D \tag{5.94}$$

So the doubly-integrated (5.90) reduces to:

$$c_i[\int_0^L\int_0^D \frac{|\hat{\psi}|^2}{|U-c|^2}(\frac{\partial}{\partial y}q_s)\,dz\,dy + \int_0^L \frac{f_0^2}{N^2}\frac{\hat{|\psi|}^2}{|U-c|^2}(\frac{\partial}{\partial z}U)\;|_0^D\,dy\,] = 0 \tag{5.95}$$

This is the *Charney-Stern criterion* for instability. In order to have instability, $c_i > 0$ and that requires that the term in brackets vanish.

Note that the first term is identical to the one we got for the Rayleigh-Kuo criterion (4.156). In that case we had:

$$\frac{\partial}{\partial y}q_s = \beta - \frac{\partial^2}{\partial y^2}U \tag{5.96}$$

For instability, we required that $\frac{\partial}{\partial y}q_s$ had to be zero somewhere in the domain.

The baroclinic condition is similar, except that now the background PV is given by (5.82), so:

$$\frac{\partial}{\partial y}q_s = \beta - \frac{\partial^2}{\partial y^2}U - \frac{\partial}{\partial z}(\frac{f_0^2}{N^2}\frac{\partial U}{\partial z}) = 0$$

Thus the vertical shear can also cause the PV gradient to vanish.

In addition, the boundary contributions also come into play. In fact we have *four* possibilities:

- $\frac{\partial}{\partial y}q_s$ vanishes in the interior, with $\frac{\partial}{\partial z}U = 0$ on the boundaries
- $\frac{\partial}{\partial z}U$ at the upper boundary has the opposite sign as $\frac{\partial}{\partial y}q_s$
- $\frac{\partial}{\partial z}U$ at the lower boundary has the same sign as $\frac{\partial}{\partial y}q_s$
- $\frac{\partial}{\partial z}U$ has the same sign on the boundaries, with $\frac{\partial}{\partial y}q_s = 0$ in the interior

The first condition is the Rayleigh-Kuo criterion. This is the only condition in the baroclinic case too if the vertical shear vanishes at the boundaries. Note that from the thermal wind balance:

$$\frac{\partial}{\partial z}U \propto \frac{\partial}{\partial y}T$$

So having zero vertical shear at the boundaries implies the temperature is *constant* on them. The boundaries are important only if there is a temperature gradient on them.

The fourth condition applies when the PV (and hence the gradient) is zero in the interior. Then the two boundaries can interact to produce instability. This is Eady's (1949) model of baroclinic instability, which we consider in the next section.

In the atmosphere, the mean relative vorticity is generally smaller than the β-effect. So the interior gradient is positive (and approximately equal to β) and the main effect is for the lower boundary to cancel the interior term. This is what happens in Charney's (1947) model of baroclinic instability.

It is also possible to construct a model with zero shear at the boundaries and where the gradient of the interior PV vanishes because of the vertical term. This is what happens in Phillip's (1954) model. This has two fluid

layers, with the flow in each layer being barotropic. Because ot the barotropic flow, the shear at the upper and lower boundaries is zero. But the PV in each layer can be different. If the PV in the layers is of opposite sign, then they can potentially sum to zero, leading to instability.

As with the Rayleigh-Kuo criterion, the Charney-Stern criteria represent a necessary condition for instability, but not a sufficient one. Satisfying one of the conditions above indicates instability *may* occur. Furthermore, only one needs to be satisfied. But if none of the conditions are satisfied, the flow is unconditionally stable.

5.9 The Eady model

The simplest model of baroclinic instability with continuous stratification is that of Eady (1949). This came out two years after Charney's (1947) model, which also has continuous stratification *and* the β-effect (something not included in the Eady model). But the Eady model is comparatively simple, and illustrates the major aspects.

The configuration for the Eady model is shown in Fig. (5.10). The flow is confined to a channel, with no normal flow at the meridional walls (at $y = 0, L$) and at the upper and lower flat plates (at $z = 0, D$). We also make the following key assumptions:

- A constant Coriolis parameter ($\beta = 0$)
- Uniform stratification ($N = const.$)
- The mean velocity has constant vertical shear but no lateral shear ($U = \Lambda z$)

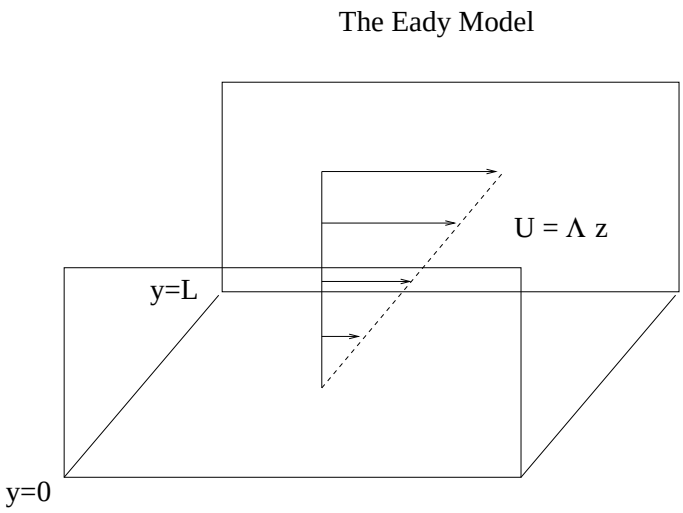

Figure 5.10: The configuration for the Eady model.

The uniform stratification assumption is reasonable for the troposphere but less so for the ocean (where the stratification is greater near the surface). The flat boundaries are also unrealistic, but simplify the boundary conditions.

From the Charney-Stern criteria, we see that the model can be unstable because U_z is the same on the two boundaries. The interior PV on the other hand is zero, so this cannot contribute to the instability. We will see that the interior in the Eady model is basically passive. It is the interaction between anomalies on the boundaries which are important.

We will use a wave solution with the following form:

$$\psi = \hat{\psi}(z) sin(\frac{n\pi y}{L}) e^{ik(x-ct)}$$

The sin term satisfies the boundary conditions on the channel walls because:

$$v = \frac{\partial}{\partial x}\psi = 0 \quad \rightarrow \quad ik\hat{\psi} = 0 \tag{5.97}$$

which implies that $\hat{\psi} = 0$. (Note too that $k = m\pi/L_x$; it is quantized to satisfy periodicity in x.)

The linearized PV equation for the Eady model is:

$$(\frac{\partial}{\partial t} + U\frac{\partial}{\partial x})(\nabla^2\psi + \frac{f_0^2}{N^2}\frac{\partial^2}{\partial z^2}\psi) = 0 \tag{5.98}$$

Because there is no β term, the PV is constant on air parcels advected by the mean flow. Inserting the wave solution in yields:

$$(U-c)[(-(k^2 + \frac{n^2\pi^2}{L^2})\hat{\psi} + \frac{f_0^2}{N^2}\frac{d^2\psi}{dz^2}] = 0 \tag{5.99}$$

Either the phase speed equals the mean velocity or the PV itself is zero. This defines what is known as a *critical layer*. This is not an issue for an unstable wave, which a non-zero value of c_i. Thus we assume instead the PV is zero. This implies:

$$\frac{d^2\psi}{dz^2} = \alpha^2\hat{\psi} \tag{5.100}$$

where

$$\alpha \equiv \frac{N\kappa}{f_0}$$

and where $\kappa = (k^2 + (n\pi/L)^2)^{1/2}$ is the total horizontal wavenumber. This is exactly the same as in the topographic wave problem in (5.7). Equation (5.100) determines the vertical structure of the waves.

For a wave solution, we'll use the following:

$$\hat{\psi} = Ae^{\alpha z} + Be^{-\alpha z} \tag{5.101}$$

Note that this applies over the whole interior, including both boundaries.

Next, we impose the boundary conditions, which involve the linearized density equation:

$$(\frac{\partial}{\partial t} + U\frac{\partial}{\partial x})\frac{\partial \psi}{\partial z} - \frac{\partial \psi}{\partial x}\frac{dU}{dz} = 0 \tag{5.102}$$

(see eq. (5.83)). With the mean velocity and using the wave dependence in x and t, this reduces to:

$$(\Lambda z - c)\frac{\partial \psi}{\partial z} - \Lambda\hat{\psi} = 0 \tag{5.103}$$

after cancelling the factor of ik. Plugging the wave solution into (5.103) we get, at $z = 0$:

$$(-c\alpha - \Lambda)A + (\alpha c - \Lambda)B = 0 \tag{5.104}$$

while at the upper boundary, at $z = D$, we get:

$$(\alpha(\Lambda D - c) - \Lambda)e^{\alpha D}A + (-\alpha(\Lambda D - c) - \Lambda)e^{-\alpha D}B = 0 \tag{5.105}$$

We can rewrite these equations in matrix form as follows:

$$\begin{pmatrix} c\alpha + \Lambda & -c\alpha + \Lambda \\ (-\alpha c + \Lambda(\alpha D - 1))e^{\alpha D} & (\alpha c - \Lambda(\alpha D + 1))e^{-\alpha D} \end{pmatrix} \begin{pmatrix} A \\ B \end{pmatrix} = \begin{pmatrix} 0 \\ 0 \end{pmatrix} \tag{5.106}$$

Note we multiplied the first equation through by -1. Because this system is homogeneous, solutions exist *only* if the determinant of the coefficients vanishes. Multiplying this out, we get:

$$c^2\alpha^2(-e^{\alpha D} + e^{-\alpha D}) + c\alpha(\Lambda - \Lambda\alpha D - \Lambda)e^{-\alpha D} + c\alpha(\Lambda\alpha D - \Lambda + \Lambda)e^{\alpha D} -$$

$$\Lambda^2(\alpha D+1)e^{-\alpha D}-\Lambda^2(\alpha D-1)e^{\alpha D}=0 \tag{5.107}$$

or:

$$-2c^2\alpha^2 sinh(\alpha D)+2c\alpha^2\Lambda D sinh(\alpha D)-2\Lambda^2\alpha D cosh(\alpha D)$$

$$+2\Lambda^2 sinh(\alpha D)=0 \tag{5.108}$$

Dividing through by $-2\alpha^2 sinh(\alpha D)$:

$$c^2-\Lambda Dc+\frac{\Lambda^2 D}{\alpha}coth(\alpha D)-\frac{\Lambda^2}{\alpha^2}=0 \tag{5.109}$$

This quadratic equation has the solutions:

$$c=\frac{\Lambda D}{2}\pm\frac{\Lambda D}{2}[1-\frac{4}{\alpha D}coth(\alpha D)+\frac{4}{\alpha^2 D^2}]^{1/2} \tag{5.110}$$

We can rewrite the part in the square root using the identity:

$$cothx=\frac{1}{2}[tanh\frac{x}{2}+coth\frac{x}{2}]$$

Then, pulling in a factor of $\alpha D/2$, the solution is:

$$c=\frac{\Lambda D}{2}\pm\frac{\Lambda}{\alpha}[\frac{\alpha^2 D^2}{4}-\frac{\alpha D}{2}coth(\frac{\alpha D}{2})-\frac{\alpha D}{2}tanh(\frac{\alpha D}{2})+1]^{1/2}$$

$$=\frac{\Lambda D}{2}\pm\frac{\Lambda}{\alpha}[(\frac{\alpha D}{2}-coth[\frac{\alpha D}{2}])(\frac{\alpha D}{2}-tanh[\frac{\alpha D}{2}])]^{1/2} \tag{5.111}$$

You can show that for all x, $x > tanh(x)$, so the second factor in the root is always positive. So the sign of the product in the square root is determined by the sign of the other term. In particular, if:

$$\frac{\alpha D}{2}>coth[\frac{\alpha D}{2}] \tag{5.112}$$

the term inside the root is positive. Then c has two roots, both of which real; hence the flow is *stable*.

The stable solutions occur when α is large. Since:

$$\alpha = \frac{N}{f_0}(k^2 + \frac{n^2\pi^2}{L^2})^{1/2}$$

this occurs when the wavenumbers, k and n, are large. Thus short waves are more likely to be stable. Furthermore, a large α implies the waves have limited vertical extent (which is proportional to α^{-1}). For large arguments:

$$coth(x) \to 1$$

So small waves have $\alpha D/2 \gg 1$, so that:

$$\alpha^{-1} \ll \frac{D}{2}$$

Thus the wave's vertical extent is *much less than half the height of the domain*. As such, the waves on the upper and lower boundaries aren't in contact with each other, and hence not interacting. An example is shown in Fig. (5.11).

Furthermore, in this limit the phase speeds are approximately:

$$c = 0, \quad \Lambda D \tag{5.113}$$

Thus the phase speeds are nearly equal to the mean velocities on the boundaries. To first order, the waves are just being swept along by the background flow.

If, on the other hand:

$$\frac{\alpha D}{2} < coth[\frac{\alpha D}{2}] \tag{5.114}$$

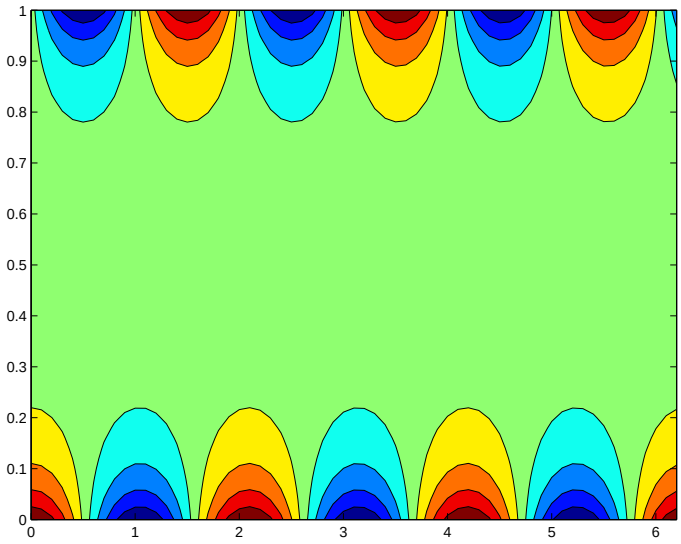

Figure 5.11: The Eady streamfunction in the limit of large α.

the term inside the root of (5.111) is negative. Then c has an imaginary part, and instability is possible.

In Fig. (5.12), we plot x and $coth(x)$. You can see that x is less for small values of x, so the condition for instability is met when α is small—large waves are more unstable.

When this condition is met, we can write the phase speed as:

$$c = \frac{\Lambda D}{2} \pm ic_i \tag{5.115}$$

where:

$$c_i = \frac{\Lambda}{\alpha}[(coth[\frac{\alpha D}{2}] - \frac{\alpha D}{2})(\frac{\alpha D}{2} - tanh[\frac{\alpha D}{2}])]^{1/2}$$

Putting this into the wave expression, we have that:

$$\psi \propto e^{ik(x-ct)} = e^{ik(x-\Lambda Dt/2)\pm kc_i t} \tag{5.116}$$

Thus at each wavenumber there is a growing wave and a decaying wave,

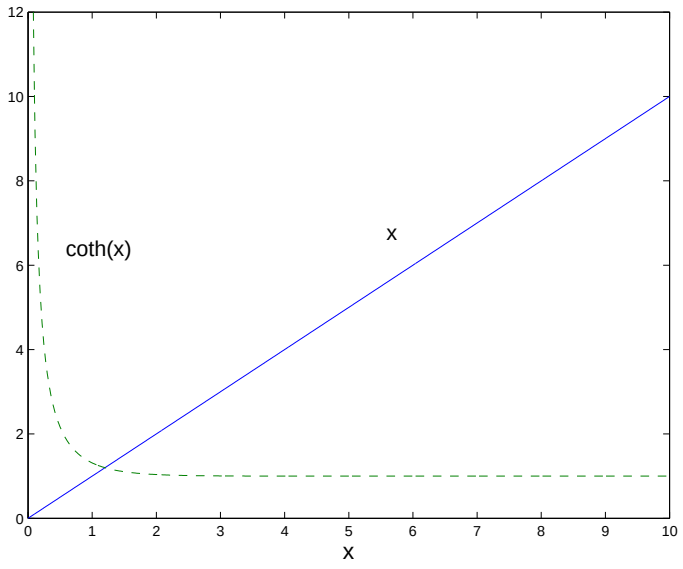

Figure 5.12: x and $coth(x)$.

with growth rates of $\pm kc_i$.

The real part of the phase speed is:

$$c_r = \frac{\Lambda D}{2} \tag{5.117}$$

Thus the waves are propagating at a speed equal to the mean flow speed at the midpoint in the vertical. As such, the waves are moving slower than the mean flow speed at the upper boundary and faster than that at the lower boundary. We call the midpoint, where the speeds are equal, the *steering level*.

The growth rate, kc_i, is plotted in Fig. (5.13) for the meridional $n = 1$ mode (which is the fastest growing). We use the following parameters:

$$N = 0.01\, sec^{-1}, \quad f_0 = 10^{-4}\, sec^{-1}, \quad \Lambda = 0.005\, sec^{-1},$$
$$D = 10^4\, m, \quad L = 2 \times 10^6\, m$$

This shear parameter yields a velocity of 50 m/sec at the tropopause height

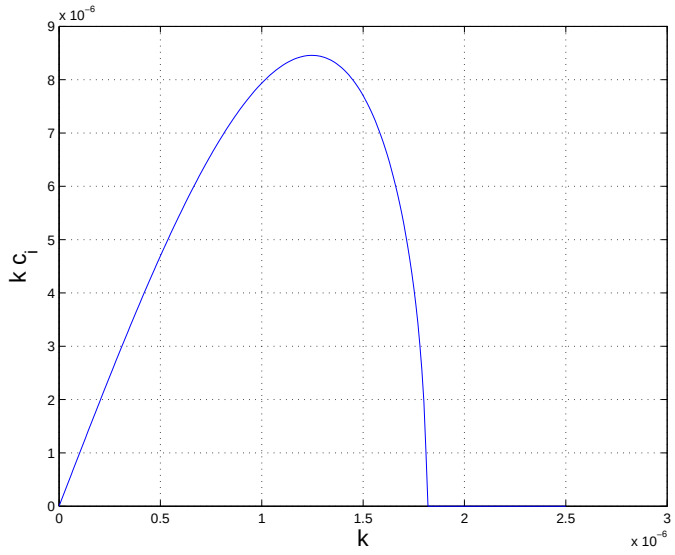

Figure 5.13: The Eady growth rate as a function of the wavenumber, k.

(10 km), similar to the peak velocity in the Jet Stream. For these values, the Eady model yields complex phase speeds, indicating the jet is baroclinically unstable.

The growth rate increases from zero as k increases, reaches a maximum value and then goes to zero. For k larger than a critical value, the waves are stable, as argued above. Thus there is a short wave cut-off for the instability, as we also saw for the barotropic jet in sec. (4.11.2).

The growth rate is a maximum at $k = 1.25 \times 10^{-6}\, m$, corresponding to a wavelength of $2\pi/k = 5027$ km. The "storm scale" (i.e. the size of a low pressure region) is one half of a wavelength, or roughly 2500 km here. A wave of this size will grow faster than any other. If we begin with a random collection of waves, this will dominate after a period of time.

Furthermore, the maximum value of kc_i is 8.46 $\times 10^{-6}$ sec^{-1}, or equivalently $1/1.4\ day^{-1}$. Thus both the length and time scales in the Eady model are consistent with observations of storm development in the troposphere.

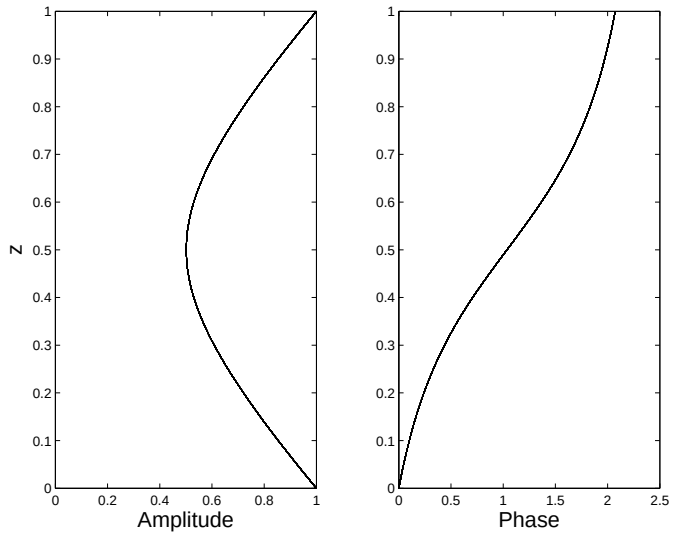

Figure 5.14: The amplitude (left) and phase (right) of the Eady streamfunction vs. height.

The ocean is quite different geometrically from the atmosphere, as noted before. But it's useful to compare the results anyway. Using values typical of oceanic conditions:

$$N = 0.0005\, sec^{-1}, \quad f_0 = 10^{-4}\, sec^{-1}, \quad \Lambda = 0.0001\, sec^{-1},$$

$$D = 5 \times 10^3\, m, \quad L = 2 \times 10^6\, m$$

we get a maximum wavelength of about 100 km, or a half wavelength of $50\, km$. Because the deformation radius is so much less in the ocean, the "storms" are correspondingly smaller. The growth times are also roughly ten times longer than in the troposphere. But these values should be taken as very approximate, because N in the ocean varies greatly between the surface and bottom.

Let's see what the unstable waves look like. To plot them, we rewrite the solution slightly. From the condition at the lower boundary, we have:

$$(c\alpha + \Lambda)A + (-c\alpha + \Lambda)B = 0$$

So the wave solution can be written:

$$\psi = A[e^{\alpha z} + \frac{c\alpha + \Lambda}{c\alpha - \Lambda}e^{-\alpha z}]sin(\frac{n\pi y}{L})e^{ik(x-ct)}$$

Rearranging slightly, we get:

$$\psi = A[cosh(\alpha z) - \frac{\Lambda}{c\alpha}sinh(\alpha z)]sin(\frac{n\pi y}{L})e^{ik(x-ct)} \tag{5.118}$$

We have absorbed the αc into the unknown A. Because c is complex, the second term in the brackets will affect the phase of the wave. To take this into account, we rewrite the streamfunction thus:

$$\psi = A\Phi(z)sin(\frac{n\pi y}{L})cos[k(x - c_r t) + \gamma(z)]e^{kc_i t} \tag{5.119}$$

where

$$\Phi(z) = [(cosh(\alpha z) - \frac{c_r\Lambda}{|c|^2\alpha}sinh(\alpha z))^2 + (\frac{c_i\Lambda}{|c|^2\alpha}sinh(\alpha z))^2]^{1/2}$$

is the magnitude of the amplitude and

$$\gamma = tan^{-1}[\frac{c_i\Lambda sinh(\alpha z)}{|c|^2\alpha cosh(\alpha z) - c_r\Lambda sinh(\alpha z)}]$$

is its phase. These are plotted in Fig. (5.14). The amplitude is greatest near the boundaries. But it is not negligible in the interior, falling to only about 0.5 at the mid-level. Rather than two separate waves, we have one which spans the depth of the fluid. Also, the phase changes with height. So the streamlines *tilt* in the vertical.

We see this in Fig. (5.15), which shows the streamfunction, temperature, meridional and vertical velocity for the most unstable wave. The streamfunction extends between the upper and lower boundaries, and the streamlines tilt to the west going upward. This means the wave is tilted *against* the mean shear. You get the impression the wave is working against the mean flow, trying to reduce its shear (which it is).

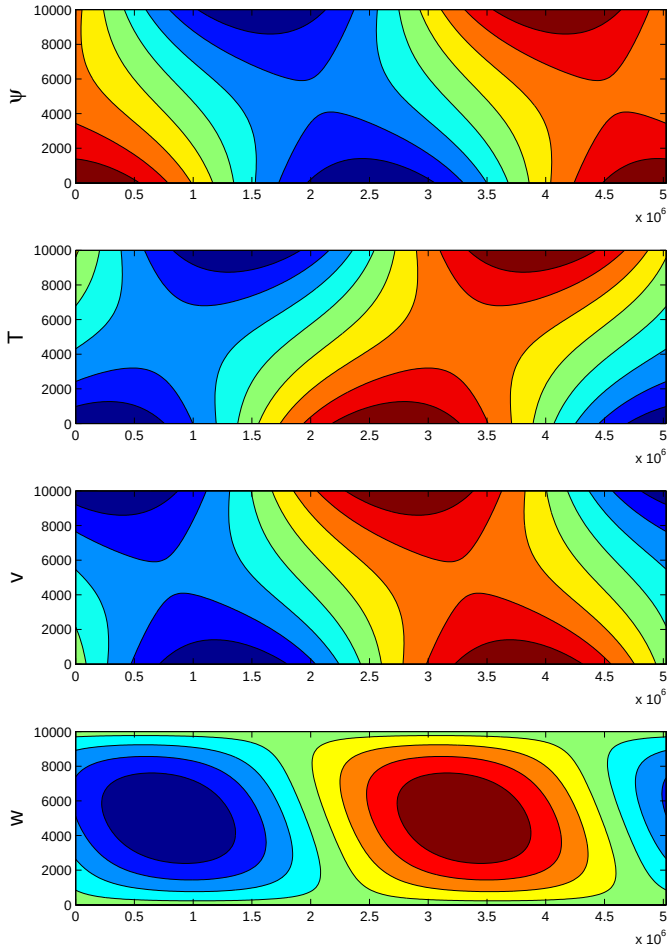

Figure 5.15: The streamfunction (upper), temperature (second), meridional velocity (third) and vertical velocity for the most unstable wave in the Eady problem.

This westward tilt with height is a well-known feature of developing storm systems. To understand it, consider Fig. (5.16). This shows the wave on the upper surface (thick contours) superimposed over the wave

on the lower surface (dashed contours). The velocities associated with the upper anomaly are indicated by the arrows. You see that the upper anomaly has northward flow above a warm anomaly, which will cause it to amplify. Likewise there is southward flow over a cold anomaly, which has the same effect

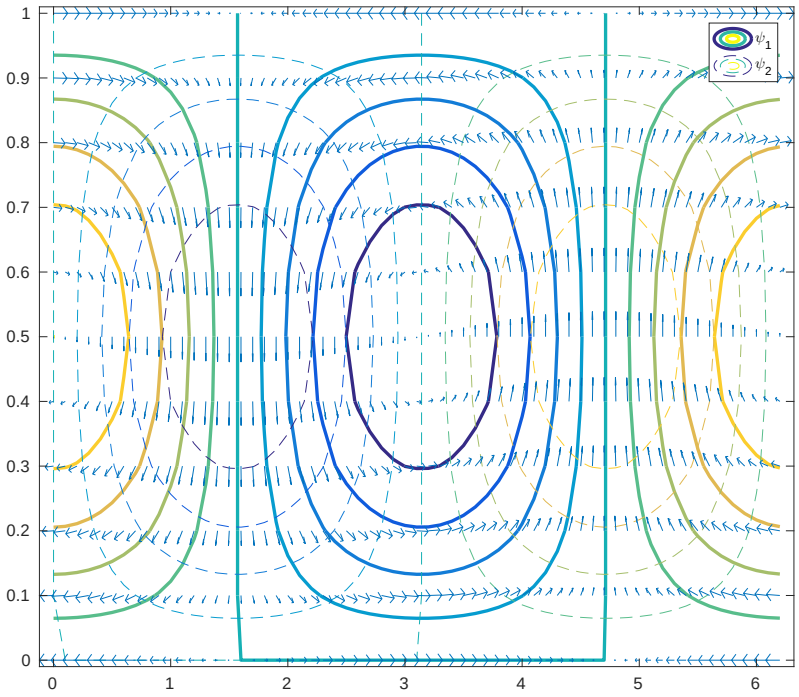

Figure 5.16: A schematic illustrating the interaction of the upper surface wave (thick contours) with that on the lower surface (dashed contours) for the fastest growing Eady wave. The arrows show the velocity associated with the upper anomaly.

The meridional velocity actually varies with height as well for the Eady wave. This is shown in the third panel of Fig. (5.16). The velocity tilts like the streamfunction, but is shifted by 90 degrees. The temperature on the other hand (second panel) tilts toward the *east* with height. The result is that the cold anomalies tend to align with regions of southward (equatorward) flow, and the warm anomalies align with northward (poleward) flow.

We can also derive the vertical velocity for the Eady wave. Inverting the linearized temperature equation, we have:

$$w = -\frac{f_0}{N^2}(\frac{\partial}{\partial t} + \Lambda z \frac{\partial}{\partial x})\frac{\partial \psi}{\partial z} + \frac{f_0}{N^2}\Lambda \frac{\partial \psi}{\partial x} \tag{5.120}$$

This is shown in the bottom panel for the most unstable wave. There is generally downward motion when the flow is toward the south and upward motion when toward the north. This fits exactly with our expectations for slantwise convection, illustrated in Fig. (5.9). Fluid parcels which are higher up and to the north are being exchanged with parcels lower down to the south. So the Eady model captures most of the important elements of baroclinic instability.

However, the Eady model lacks an interior PV gradient (it has no β-effect). Though this greatly simplifies the derivation, the atmosphere possesses such gradients, and it is reasonable to ask how they alter the instability. Interior gradients are considered in both the the Charney (1947) and Phillips (1954) models. Details are given by Pedlosky (1987) and by Vallis (2006).

5.10 *Exercises*

5.1. Consider a fluid parcel which is displaced from its initial vertical position, z_0, a distance δz. Assume we have a mean background stratification for which:

$$\frac{\partial}{\partial z} p = -\rho_0 g$$

Substitute this into the vertical momentum equation to find:

$$\frac{dw}{dt} = g(\frac{\rho_0 - \rho}{\rho})$$

Estimate ρ_0 at $z_0 + \delta z$ by Taylor-expanding about z_0. Assume the parcel conserves its density from z_0. Then use the vertical momentum equation to show that:

$$\frac{d^2(\delta z)}{dt^2} = -N^2 \delta z$$

and define N^2. This is known as the buoyancy frequency. What happens if $N^2 > 0$? What if it is negative?

5.2. Baroclinic Rossby waves.

a) What is the phase velocity for a long first baroclinic Rossby wave in the ocean at 10N? Assume that $N = 0.001\ sec^{-1}$ and that the ocean depth is 5 km.

b) What about at 30N?

c) What is the group velocity for long first baroclinic Rossby waves?

d) What do you think would happen to a long wave if it encountered a western wall?

5.3. Topographic waves vs. Eady waves

Consider a wave which exists at the lower boundary of a fluid, at $z = 0$. Assume the region is small enough to neglect β and let N and ρ_c be constant. Also let the upper boundary be at $z = \infty$.

a) Write the expression for the PV. Substitute in a wave solution of the form:

$$\psi = A(z) e^{ikx + ily - i\omega t} \tag{5.121}$$

Assuming the PV is zero in the interior, solve for the vertical dependence of $A(z)$.

b) Assume there is a topographic slope, such that $h = \alpha y$. Find the phase speed of the wave, assuming no mean flow ($U = 0$).

c) Now assume the bottom is flat and that there is a sheared mean velocity, $U = \Lambda z$. Find the phase speed for the wave.

d) Compare the two results. In particular, what does the shear have to be in (c) so that the phase speed is the same as in (b)?

5.4. A rough bottom.

We solved for the baroclinic modes assuming the the upper and lower boundaries were flat surfaces, with $w = 0$. As a result, the waves have non-zero flow at the bottom. But if the lower boundary is *rough*, a better condition is to assume that the horizontal velocity vanishes, i.e. $u = v = 0$.

Find the modes with this boundary condition, assuming no mean flow ($U = V = 0$). Compare the solutions to those with a flat bottom. What happens to the barotropic mode? The derivation is slightly simpler if you have the bottom at $z = 0$ and the surface at $z = D$.

5.5. Mountain waves (optional)

Suppose that a stationary linear Rossby wave is forced by flow over sinusoidal topography with height $h(x) = h_0\, cos(kx)$. Show that the lower boundary condition on the streamfunction can be expressed as:

$$\frac{\partial}{\partial z}\psi = -\frac{hN^2}{f_0} \tag{5.122}$$

Using this, and assuming that the energy flux is upward, solve for $\psi(x, z)$. What is the position of the crests relative to the mountain tops?

5.6. Topographic waves.

Say we are in a region where there is a steep topographic slope rising to the east, as off the west coast of Norway. The bottom decreases by 1 km over a distance of about 20 km. Say there is a southward flow of 10 cm/sec over the slope (which is constant with depth). Several fishermen have seen topographic waves which span the entire slope. But they disagree about which way they are propagating—north or south. Solve the problem for them, given that $N \approx 10 f_0$ and that we are at 60N.

5.7. Instability and the Charney-Stern relation.

Consider a region with $-1 \leq y < 1$ and $0 \leq z \leq D$. We have the following velocity profiles:

a) $U = Acos(\frac{\pi z}{D})$

b) $U = Az + B$

c) $U = z(1 - y^2)$

Which profiles are stable or unstable if $\beta = 0$ and $N^2 = const.$? What if $\beta \neq 0$?

(Note the terms have been non-dimensionalized, so β can be any number, e.g. 1, 3.423, .5, etc.).

5.8. Eady waves

a) Consider a mean flow $U = -Bz$ over a flat surface at $z = 0$ with no Ekman layer and no upper surface. Assume that $\beta = 0$ and that

$N = const.$. Find the phase speed of a perturbation wave on the lower surface.

b) Consider a mean flow with $U = Bz^2$. What is the phase speed of the wave at $z = 0$ now? Assume that $\beta = 2Bf_0^2/N^2$, so that there still is no PV gradient in the interior. What is the mean temperature gradient on the surface?

c) Now imagine a sloping bottom with zero mean flow. How is the slope oriented and how steep is it so that the topographic waves are propagating at the same speed as the waves in (a) and (b)?

5.9. Eady heat fluxes (optional)

Eady waves can flux heat. To see this, we calculate the correlation between the northward velocity and the temperature:

$$\overline{vT} \propto \overline{\frac{\partial\psi}{\partial x}\frac{\partial\psi}{\partial z}} \equiv \frac{1}{L}\int_0^L \frac{\partial\psi}{\partial x}\frac{\partial\psi}{\partial z}dx$$

where L is the wavelength of the wave. Calculate this for the Eady wave and show that it is positive; this implies that the Eady waves transport warm air northward. You will also find that the heat flux is *independent of height*.

• Hint: use the form of the streamfunction given in (5.119).

• Hint:

$$\int_0^L sin(k(x-ct))\, cos(k(x-ct))\, dx = 0$$

• Hint:

$$\frac{d}{dz}tan^{-1}\frac{y}{x} = \frac{x^2}{x^2+y^2}(\frac{xdy/dz - ydx/dz}{x^2}) = \frac{xdy/dz - ydx/dz}{x^2+y^2}$$

• Hint: The final result will be proportional to c_i. Note that c_i is *positive* for a growing wave.

5.10. Eady momentum fluxes (optional)

Unstable waves can flux momentum. The zonal *momentum flux* is defined as:

$$\overline{uv} \propto -\overline{\frac{\partial\psi}{\partial y}\frac{\partial\psi}{\partial x}} \equiv -\frac{1}{L}\int_0^L \frac{\partial\psi}{\partial y}\frac{\partial\psi}{\partial x}dx$$

Calculate this for the Eady model. Why do you think you get the answer you do?

5.11. An Eady model with β (optional)

Consider a mean flow in a channel $0 \leq y \leq L$ and $0 \leq z \leq 1$ with:

$$U = \frac{\beta N^2}{2f_0^2}z(z-1)$$

Assume $N^2 = const.$ and that $\beta \neq 0$.

a) What is the mean PV (q_s)?

b) Is the flow stable or unstable by the Charney-Stern criterion?

c) Linearize the PV equation for this mean flow.

d) Propose a wave solution and solve for the vertical structure of the waves.

e) Linearize the temperature equation for this mean flow.

f) Use the temperature equation to find two equations for the two unknown wave amplitudes.

g) Solve for phase speed, c. Does this agree with your result in (a)?

Chapter 6

Appendices

6.1 Kelvin's theorem

The vorticity equation can be derived in an elegant way. This is based on the *circulation*, which is the integral of the vorticity over a closed area:

$$\Gamma \equiv \iint \vec{\zeta} \cdot \hat{n}\, dA \tag{6.1}$$

where $\hat{n}$ is the normal vector to the area. From Stoke's theorem, the circulation is equivalent to the integral of the velocity around the circumference:

$$\Gamma = \iint (\nabla \times \vec{u}) \cdot \hat{n}\, dA = \oint \vec{u} \cdot\ d\vec{l} \tag{6.2}$$

Thus we can derive an equation for the circulation if we integrate the momentum equations around a closed circuit. For this, we will use the momentum equations in vector form. The derivation is somewhat easier if we work with the fixed frame velocity:

$$\frac{d}{dt}\vec{u}_F = -\frac{1}{\rho}\nabla p + \vec{g} + \vec{F} \tag{6.3}$$

If we integrate around a closed area, we get:

$$\frac{d}{dt}\Gamma_F = -\oint \frac{\nabla p}{\rho}\cdot\vec{dl} + \oint \vec{g}\cdot\vec{dl} + \oint \vec{F}\cdot\vec{dl} \tag{6.4}$$

The gravity term vanishes because it can be written in terms of a potential (the geopotential):

$$\vec{g} = -g\hat{k} = \frac{\partial}{\partial z}(-gz) \equiv \nabla\Phi \tag{6.5}$$

and because the closed integral of a potential vanishes:

$$\oint \nabla\Phi\cdot\vec{dl} = \oint d\Phi = 0 \tag{6.6}$$

So:

$$\frac{d}{dt}\Gamma_F = -\oint \frac{dp}{\rho} + \oint \vec{F}\cdot\vec{dl} \tag{6.7}$$

Now the circulation, Γ_F, has two components:

$$\Gamma_F = \oint \vec{u}_F\cdot\vec{dl} = \iint \nabla\times\vec{u}_F\cdot\hat{n}\,dA = \iint(\vec{\zeta}+2\vec{\Omega})\cdot\hat{n}\,dA \tag{6.8}$$

As noted above, the most important components of the vorticity are in the vertical. So a natural choice is to take an area which is in the horizontal, with $\hat{n} = \hat{k}$. Then:

$$\Gamma_F = \iint(\zeta + f)\,dA \tag{6.9}$$

Putting this back in the circulation equation, we get:

$$\frac{d}{dt}\iint(\zeta+f)\,dA = -\oint\frac{dp}{\rho} + \oint\vec{F}\cdot\vec{dl} \tag{6.10}$$

Now, the first term on the RHS of (6.10) is zero under the Boussinesq approximation because:

$$\oint \frac{dp}{\rho} = \frac{1}{\rho_c} \oint dp = 0$$

It is also zero if we use pressure coordinates because:

$$\oint \frac{dp}{\rho}|_z \rightarrow \oint d\Phi|_p = 0$$

Thus, in both cases, we have:

$$\frac{d}{dt}\Gamma_a = \oint \vec{F} \cdot \vec{dl} \tag{6.11}$$

So the absolute circulation can only change under the action of friction. If $\vec{F} = 0$, the absolute circulation is conserved on the parcel. This is Kelvin's theorem.

6.2 The linear shallow water wave equation

It's possible to reduce the three shallow water equations to one equation with a single unknown. It's relatively easy to do this if we take the Coriolis parameter, f, to be constant. As noted in sec. (2.3), this is the "f-plane approximation" and it applies if the area under consideration is small.

Under the f-plane approximation, we can reduce (3.37-3.39) to a single equation. First we rewrite the equations in terms of the *transports* $(U, V) \equiv (Hu, Hv)$:

$$\frac{\partial}{\partial t}U - fV = -gH\frac{\partial}{\partial x}\eta \tag{6.12}$$

$$\frac{\partial}{\partial t}V + fU = -gH\frac{\partial}{\partial y}\eta \tag{6.13}$$

$$\frac{\partial}{\partial t}\eta + \frac{\partial}{\partial x}U + \frac{\partial}{\partial y}V = 0 \tag{6.14}$$

Then we derive equations for the divergence and vorticity:

$$\frac{\partial}{\partial t}\chi - f\zeta = -g\nabla \cdot (H\nabla\eta) \tag{6.15}$$

$$\frac{\partial}{\partial t}\zeta + f\chi = -gJ(H,\eta) \tag{6.16}$$

where $\chi \equiv (\frac{\partial}{\partial x}U + \frac{\partial}{\partial y}V)$ is the transport divergence, $\zeta \equiv (\frac{\partial}{\partial x}V - \frac{\partial}{\partial y}U)$ is the transport vorticity. We use the Jacobian function:

$$J(a,b) \equiv \frac{\partial}{\partial x}a\frac{\partial}{\partial y}b - \frac{\partial}{\partial x}b\frac{\partial}{\partial y}a \tag{6.17}$$

to simplify the expression. We can eliminate the vorticity by taking the time derivative of (6.15) and substituting in from (6.16). The result is:

$$(\frac{\partial^2}{\partial t^2} + f^2)\,\chi = -g\frac{\partial}{\partial t}\nabla \cdot (H\,\nabla\eta) - f\,g\,J(H,\eta) \tag{6.18}$$

From (6.14) we have:

$$\frac{\partial}{\partial t}\eta + \chi = 0 \tag{6.19}$$

which we can use to eliminate the divergence from (6.18). This leaves a single equation for the sea surface height:

$$\frac{\partial}{\partial t}\{(\frac{\partial^2}{\partial t^2} + f^2)\,\eta - \nabla \cdot (c_0^2\,\nabla\eta)\} - f\,g\,J(H,\eta) = 0 \tag{6.20}$$

The term $c_0 = \sqrt{gH}$ has the units of a velocity, and we will see later this is related to the speed of free gravity waves. If the fluid depth is 4000 m, $c_0 = 200$ m/sec.

So we have one equation with a single unknown: η. The problem is that if the topography, H, is complex, the solutions may be very hard to obtain analytically.

If we assume the bottom is flat however, the Jacobian term vanishes, leaving:

$$\frac{\partial}{\partial t}\{(\frac{\partial^2}{\partial t^2} + f_0^2)\,\eta - c_0^2\nabla^2\eta\} = 0 \tag{6.21}$$

6.3 Fourier wave modes

In many of the examples in the text, we use solutions derived from the Fourier transform. The Fourier transform is very useful; we can represent any continuous function $f(x)$ in this way. More details are given in any one of a number of different texts.[1]

Say we have a function, $f(x)$. We can write this as a sum of Fourier components thus:

$$f(x) = \int_{-\infty}^{\infty} \hat{f}(k)\, e^{ikx}\, dk \tag{6.22}$$

where:

$$e^{ikx} = cos(kx) + isin(kx) \tag{6.23}$$

is a complex number. The Fourier amplitude, $\hat{f}(k)$, is also typically complex:

$$\hat{f}(k) = \hat{f}_r + i\hat{f}_i \tag{6.24}$$

We can obtain the amplitude by taking the inverse relation of the above:

$$\hat{f}(k) = \frac{1}{2\pi}\int_{-\infty}^{\infty} \hat{f}(k)\, e^{-ikx}\, dx \tag{6.25}$$

[1] See, for example, Arfken, *Mathematical Methods for Physicists* or Boas, *Mathematical Methods in the Physical Sciences*.

In all the examples in the text, the equations we will solve are *linear*. A linear equation can be solved via a *superposition of solutions*: if $f_1(x)$ is a solution to the equation and $f_2(x)$ is another solution, then $f_1(x) + f_2(x)$ is also a solution. In practice, this means we can examine a single Fourier mode. Then in effect we find solutions which apply to all Fourier modes. Moreover, since we can represent general continuous functions in terms of Fourier modes, we are solving the equation at once for almost any solution.

Thus we will use solutions like:

$$\psi = Re\{\hat{\psi}(k, l, \omega)e^{ikx+ily-i\omega t}\} \tag{6.26}$$

Note we have implicitly performed *three* transformations—in x, y and in t. But we only write one wave component (we don't carry the infinite integrals along). Notice too that we use negative ω instead of positive—this is frequently done to distinguish the transform in time (but is not actually necessary). Here k and l are the *wavenumbers* in the x and y directions, and ω is the wave *frequency*.

As noted in sec. (3.5), the wave solution has an associated wavelength and phase speed. The wave above is two-dimensional, so its wavelength is defined:

$$\lambda = \frac{2\pi}{\kappa} \tag{6.27}$$

where:

$$\kappa = (k^2 + l^2)^{1/2} \tag{6.28}$$

is the total wavenumber. Note that the wavelength is always a positive number, while the wavenumbers k and l can be positive or negative. The

phase speed is velocity of the crests of the wave. This is defined as:

$$\vec{c} = \frac{\omega \vec{\kappa}}{\kappa^2} \tag{6.29}$$

In most of the examples in the text, we're interested in the motion of crests in the x-direction (parallel to latitude lines). This velocity is given by:

$$c_x = \frac{\omega}{k} \tag{6.30}$$

The exact choice of Fourier component depends on the application. The form written above is appropriate for an infinite plane, where there are no specific boundary conditions. We will use this one frequently.

However, there are other possibilities. A typical choice for the atmosphere is a periodic channel, because the mid-latitude atmosphere is re-entrant in the x-direction but limited in the y-direction. So we would have solid walls, say at $y = 0$ and at $y = L_y$, and periodic conditions in x. The boundary condition at the walls is $v = 0$. This implies that $\frac{\partial}{\partial x}\psi = 0$, so that ψ must be constant on the wall. In most of the subsequent examples, we'll take the constant to be zero. The periodic condition on the other hand demands that ψ be the same at the two limits, for instance at $x = 0$ and $x = L_x$.

So a good choice of wave solution would be:

$$\psi = Re\{\hat{\psi}(n, m, \omega)\, e^{in\pi x/L_x - i\omega t}\, sin(\frac{m\pi y}{L_y})\} \tag{6.31}$$

This has an integral number of waves in both the x and y directions. But the streamfunction vanishes at $y = 0$ and $y = L_y$, whereas the streamfunction is merely *the same* at $x = 0$ and $x = L_x$—it is not zero. We will use a

channel solution for example in the Eady problem in sec. (5.9).

Another possibility is to have solid wall boundaries in both directions, as in an ocean basin. An example of this is a Rossby wave in a basin, which has the form:

$$\psi \propto A(x,t)sin(\frac{n\pi x}{L_x})sin(\frac{m\pi y}{L_y}) \tag{6.32}$$

The two last factors guarantee that the streamfunction vanish at the lateral walls.

In general, the choice of wave solution is dictated both by the equation and the boundary conditions. If, for example, the equation has coefficients which vary only in z, or if there are boundaries in the vertical direction, we would use something like:

$$\psi = Re\{\hat{\psi}(z)e^{ikx+ily-i\omega t}\} \tag{6.33}$$

6.4 Rossby wave energetics

Another way to derive the group velocity is via the energy equation for the waves. For this, we first need the energy equation for the wave. As the wave is barotropic, it has only kinetic energy. This is:

$$E = \frac{1}{2}(u^2+v^2) = \frac{1}{2}[(-\frac{\partial\psi}{\partial y})^2 + (\frac{\partial\psi}{\partial x})^2] = \frac{1}{2}|\nabla\psi|^2$$

To derive an energy equation, we multiply the wave equation (4.26) by ψ. The result, after some rearranging, is:

$$\frac{\partial}{\partial t}(\frac{1}{2}|\nabla\psi|^2) + \nabla\cdot[-\psi\nabla\frac{\partial}{\partial t}\psi - \hat{i}\beta\frac{1}{2}\psi^2] = 0 \tag{6.34}$$

We can also write this as:

$$\frac{\partial}{\partial t}E + \nabla \cdot \vec{S} = 0 \tag{6.35}$$

So the kinetic energy changes in response to the divergence of an energy *flux*, given by:

$$\vec{S} \equiv -\psi \nabla \frac{\partial}{\partial t}\psi - \hat{i}\beta\frac{1}{2}\psi^2$$

The energy equation is thus like the continuity equation, as the density also changes in response to a divergence in the velocity. Here the kinetic energy changes if there is a divergence in $\vec{S}$.

Let's apply this to the wave. We have

$$E = \frac{k^2 + l^2}{2} A^2 sin^2(kx + ly - \omega t) \tag{6.36}$$

So the energy varies sinusoidally in time. Let's average this over one wave period:

$$< E > \equiv \int_0^{2\pi/\omega} E\, dt = \frac{1}{4}\left(k^2 + l^2\right) A^2 \tag{6.37}$$

The flux, $\vec{S}$, on the other hand is:

$$\vec{S} = -(k\hat{i} + l\hat{j})\, \omega\, A^2 cos^2(kx + ly - \omega t) - \hat{i}\beta\, \frac{A^2}{2} cos^2(kx + ly - \omega t) \tag{6.38}$$

which has a time average:

$$< S > = \frac{A^2}{2}[-\omega(k\hat{i} + l\hat{j}) - \frac{\beta}{2}\hat{i}] = \frac{A^2}{4}[\beta\frac{k^2 - l^2}{k^2 + l^2}\,\hat{i} + \frac{2\beta kl}{k^2 + l^2}\,\hat{j}] \tag{6.39}$$

Rewriting this slightly:

$$< S >= [\beta \frac{k^2 - l^2}{(k^2 + l^2)^2} \hat{i} + \frac{2\beta kl}{(k^2 + l^2)^2} \hat{j}] \; E \equiv \vec{c}_g < E > \tag{6.40}$$

So the mean flux is the product of the mean energy and the group velocity, $\vec{c}_g$. It is straightforward to show that the latter is the same as:

$$c_g = \frac{\partial \omega}{\partial k} \hat{i} + \frac{\partial \omega}{\partial l} \hat{j} \tag{6.41}$$

Since c_g only depends on the wavenumbers, we can write:

$$\frac{\partial}{\partial t} < E > + \vec{c}_g \cdot \nabla < E >= 0 \tag{6.42}$$

We could write this in Lagrangian form then:

$$\frac{d_c}{dt} < E >= 0 \tag{6.43}$$

where:

$$\frac{d_c}{dt} = \frac{\partial}{\partial t} + \vec{c}_g \cdot \nabla \tag{6.44}$$

In words, this means that the energy is conserved when moving at the group velocity. The group velocity then is the relevant velocity to consider when talking about the energy of the wave.

6.5 Fjørtoft's criterion

This is an alternate condition for barotropic instability, derived by Fjørtoft (1950). This follows from taking the real part of (4.151):

$$(\hat{\psi}_r \frac{\partial^2}{\partial y^2} \hat{\psi}_r + \hat{\psi}_i \frac{\partial^2}{\partial y^2} \hat{\psi}_i) - k^2 |\hat{\psi}|^2 + (U - c_r) \frac{|\hat{\psi}|^2}{|U - c|^2} \frac{\partial}{\partial y} q_s = 0 \tag{6.45}$$

If we again integrate in y and rearrange, we get:

$$\int_0^L (U - c_r)\frac{|\hat{\psi}|^2}{|U-c|^2}\frac{\partial}{\partial y}q_s = \\ -\int_0^L (\hat{\psi}_r\frac{\partial^2}{\partial y^2}\hat{\psi}_r + \hat{\psi}_i\frac{\partial^2}{\partial y^2}\hat{\psi}_i)dy + \int_0^L k^2|\hat{\psi}|^2 dy \tag{6.46}$$

We can use integration by parts again, on the first term on the RHS. For instance,

$$\int_0^L \hat{\psi}_r\frac{\partial^2}{\partial y^2}\hat{\psi}_r\, dy = \hat{\psi}_r\frac{\partial}{\partial y}\hat{\psi}_r|_0^L - \int_0^L (\frac{\partial}{\partial y}\hat{\psi}_r)^2\, dy \tag{6.47}$$

The first term on the RHS vanishes because of the boundary condition. So (6.45) can be written:

$$\int_0^L (U - c_r)\frac{|\hat{\psi}|^2}{|U-c|^2}\frac{\partial}{\partial y}q_s\, dy = \int_0^L (\frac{\partial}{\partial y}\hat{\psi}_r)^2 + (\frac{\partial}{\partial y}\hat{\psi}_i)^2 + k^2|\hat{\psi}|^2\, dy \tag{6.48}$$

The RHS is always *positive*. Now from the Rayleigh-Kuo criterion, we know that if $c_i \neq 0$:

$$\int_0^L \frac{|\hat{\psi}|^2}{|U-c|^2}\frac{\partial}{\partial y}q_s\, dy = 0 \tag{6.49}$$

So we conclude that:

$$\int_0^L U(y)\frac{|\hat{\psi}|^2}{|U-c|^2}\frac{\partial}{\partial y}q_s > 0 \tag{6.50}$$

Thus we must have:

$$U(y)\frac{\partial}{\partial y}q_s > 0 \tag{6.51}$$

somewhere in the domain. If this fails, the flow is stable ($c_i = 0$).

This represents an additional constraint to the Rayleigh-Kuo criterion. Sometimes a flow will satisfy the Rayleigh-Kuo criterion but not Fjørtoft's—then the flow is stable. It's possible to show that Fjørtoft's criterion requires the flow have a relative vorticity maximum somewhere in the domain interior, not just on the boundaries.

6.6 QGPV in pressure coordinates

The PV equation in pressure coordinates is very similar to that in z-coordinates. First off, the vorticity equation is given by:

$$\frac{d_H}{dt}(\zeta + f) = -(\zeta + f)(\frac{\partial u}{\partial x} + \frac{\partial v}{\partial y}) \tag{6.52}$$

Using the incompressibility condition (2.40), we rewrite this as:

$$\frac{d_H}{dt}(\zeta + f) = (\zeta + f)\frac{\partial \omega}{\partial p} \tag{6.53}$$

The quasi-geostrophic version of this is:

$$\frac{d_g}{dt}(\zeta + f) = f_0\frac{\partial \omega}{\partial p} \tag{6.54}$$

where $\zeta = \nabla^2\Phi/f_0$.

To eliminate ω, we use the potential temperature equation (1.64). For simplicity we assume no heating, so the equation is simply:

$$\frac{d\theta}{dt} = 0 \tag{6.55}$$

We assume:

$$\theta_{tot}(x, y, p, t) = \theta_0(p) + \theta(x, y, p, t)\ , \quad |\theta| \ll |\theta_0|$$

where θ_{tot} is the full temperature, θ_0 is the "static" temperature and θ is the "dynamic" temperature. Substituting these in, we get:

$$\frac{\partial\theta}{\partial t} + u\frac{\partial\theta}{\partial x} + v\frac{\partial\theta}{\partial y} + w\frac{\partial}{\partial p}\theta_0 = 0 \tag{6.56}$$

We neglect the term $\omega\partial\theta/\partial p$ because it is much less than the term with θ_0.

The geopotential is also dominated by a static component:

$$\Phi_{tot} = \Phi_0(p) + \Phi(x, y, p, t)\,, \quad |\Phi| \ll |\Phi_0| \tag{6.57}$$

Then the hydrostatic relation (2.41) yields:

$$\frac{d\Phi_{tot}}{dp} = \frac{d\Phi_0}{dp} + \frac{d\Phi}{dp} = -\frac{RT_0}{p} - \frac{RT'}{p} \tag{6.58}$$

and where:

$$T_{tot} = T_0(p) + T(x, y, p, t)\,, \quad |T| \ll |T_0| \tag{6.59}$$

Equating the static and dynamic parts, we find:

$$\frac{d\Phi}{dp} = -\frac{RT'}{p} \tag{6.60}$$

Now we need to rewrite the hydrostatic relation in terms of the potential temperature. From the definition of potential temperature, we have:

$$\theta = T\,(\frac{p_s}{p})^{R/c_p}, \quad \theta_0 = T_0\,(\frac{p_s}{p})^{R/c_p}$$

where again we have equated the dynamic and static parts. Thus:

$$\frac{\theta}{\theta_0} = \frac{T}{T_0} \tag{6.61}$$

So:

$$\frac{1}{T_0}\frac{d\Phi}{dp} = -\frac{RT}{pT_0} = -\frac{R\theta}{p\theta_0} \tag{6.62}$$

So, dividing equation (6.56) by θ_0, we get:

$$(\frac{\partial}{\partial t} + u\frac{\partial}{\partial x} + v\frac{\partial}{\partial y})\,\frac{\theta'}{\theta_0} + \omega\,\frac{\partial}{\partial p} ln\theta_0 = 0 \tag{6.63}$$

Finally, using (6.62) and approximating the horizontal velocities by their geostrophic values, we obtain the QG temperature equation:

$$(\frac{\partial}{\partial t} + u_g\frac{\partial}{\partial x} + v_g\frac{\partial}{\partial y})\,\frac{\partial\Phi}{\partial p} + \sigma\omega = 0 \tag{6.64}$$

The parameter:

$$\sigma(p) = -\frac{RT_0}{p}\frac{\partial}{\partial p} ln(\theta_0)$$

reflects the static stratification and is proportional to the buoyancy frequency (sec. 5.2). We can write this entirely in terms of Φ and ω:

$$(\frac{\partial}{\partial t} - \frac{1}{f_0}\frac{\partial}{\partial y}\Phi\frac{\partial}{\partial x} + \frac{1}{f_0}\frac{\partial}{\partial x}\Phi\frac{\partial}{\partial y})\,\frac{\partial\Phi}{\partial p} + \omega\sigma = 0 \tag{6.65}$$

As in sec. (5.3), we can combine the vorticity equation (6.54) and the temperature equation (6.65) to yield a PV equation. In pressure coordinates, this is:

$$(\frac{\partial}{\partial t} - \frac{1}{f_0}\frac{\partial}{\partial y}\Phi\frac{\partial}{\partial x} + \frac{1}{f_0}\frac{\partial}{\partial x}\Phi\frac{\partial}{\partial y})\,[\frac{1}{f_0}\nabla^2\Phi + \frac{\partial}{\partial p}(\frac{f_0}{\sigma}\frac{\partial\Phi}{\partial p}) + \beta y] = 0 \tag{6.66}$$